RANGELANDS

CLUSTER REPORT

CLIMATE CHANGE IN AUSTRALIA

PROJECTIONS

FOR AUSTRALIA´S NRM REGIONS

CSIRO

Australian Government

Department of the Environment

Bureau of Meteorology


−20°
−10°
0°
10°
20°
30°
40°
50°

RANGELANDS

CLUSTER REPORT

PROJECTIONS

FOR AUSTRALIA´S NRM REGIONS

CLIMATE CHANGE IN AUSTRALIA PROJECTIONS
CLUSTER REPORT – RANGELANDS

ISBN
Print: 978-1-4863-0426-4
Online: 978-1-4863-0427-1

CITATION

Watterson, I. *et al.* 2015, *Rangelands Cluster Report,* Climate Change in Australia Projections for Australia's Natural Resource Management Regions: Cluster Reports, eds. Ekström, M. *et al.,* CSIRO and Bureau of Meteorology, Australia

CONTACTS

E: enquiries@csiro.au

T: 1300 363 400

ACKNOWLEDGEMENTS

Lead Author – Ian Watterson

Contributing Authors – Debbie Abbs, Jonas Bhend, Francis Chiew, John Church, Marie Ekström, Dewi Kirono, Andrew Lenton, Chris Lucas, Kathleen McInnes, Aurel Moise, Didier Monselesan, Freddie Mpelasoka, Leanne Webb and Penny Whetton

Editors – Marie Ekström, Penny Whetton, Chris Gerbing, Michael Grose, Leanne Webb and James Risbey

Additional acknowledgements – Janice Bathols, Tim Bedin, John Clarke, Clement Davis, Tim Erwin, Craig Heady, Peter Hoffman, Jack Katzfey, Julian O'Grady, Tony Rafter, Surendra Rauniyar, Rob Smalley, Bertrand Timbal, Yang Wang, Ian Watterson, and Louise Wilson

Project Coordinators – Kevin Hennessy, Paul Holper and Mandy Hopkins

Design and editorial support – Alicia Annable, Siobhan Duffy, Liz Butler, and Peter Van Der Merwe

We gratefully acknowledge the assistance of Andrew Tait, Michael Hutchinson and David Karoly

We acknowledge the World Climate Research Programme's Working Group on Coupled Modelling, which is responsible for CMIP, and we thank the climate modelling groups for producing and making available their model output. For CMIP the U.S. Department of Energy's Program for Climate Model Diagnosis and Intercomparison provides coordinating support and led development of software infrastructure in partnership with the Global Organization for Earth System Science Portals.

This report has been printed on ecoStar, a recycled paper made from 100% post-consumer waste.

TABLE OF CONTENTS

PREFACE

Australia's changing climate represents a significant challenge to individuals, communities, governments, businesses and the environment. Australia has already experienced increasing temperatures, shifting rainfall patterns and rising oceans.

The Intergovernmental Panel on Climate Change (IPCC) *Fifth Assessment Report* (IPCC 2013) rigorously assessed the current state and future of the global climate system. The report concluded that:

- greenhouse gas emissions have markedly increased as a result of human activities
- human influence has been detected in warming of the atmosphere and the ocean, in changes in the global water cycle, in reductions in snow and ice, in global mean sea level rise, and in changes in some climate extremes
- it is extremely likely that human influence has been the dominant cause of the observed warming since the mid-20th century
- continued emissions of greenhouse gases will cause further warming and changes in all components of the climate system.

In recognition of the impact of climate change on the management of Australia's natural resources, the Australian Government developed the Regional Natural Resource Management Planning for Climate Change Fund. This fund has enabled significant research into the impact of the future climate on Australia's natural resources, as well as adaptation opportunities for protecting and managing our land, soil, water, plants and animals.

Australia has 54 natural resource management (NRM) regions, which are defined by catchments and bioregions. Many activities of organisations and ecosystem services within the NRM regions are vulnerable to impacts of climate change.

For this report, these NRM regions are grouped into 'clusters', which largely correspond to the broad-scale climate and biophysical regions of Australia (Figure A). The clusters are diverse in their history, population, resource base, geography and climate. Therefore, each cluster has a unique set of priorities for responding to climate change.

CSIRO and the Australian Bureau of Meteorology have prepared tailored climate change projection reports for each NRM cluster. These projections provide guidance on the changes in climate that need to be considered in planning.

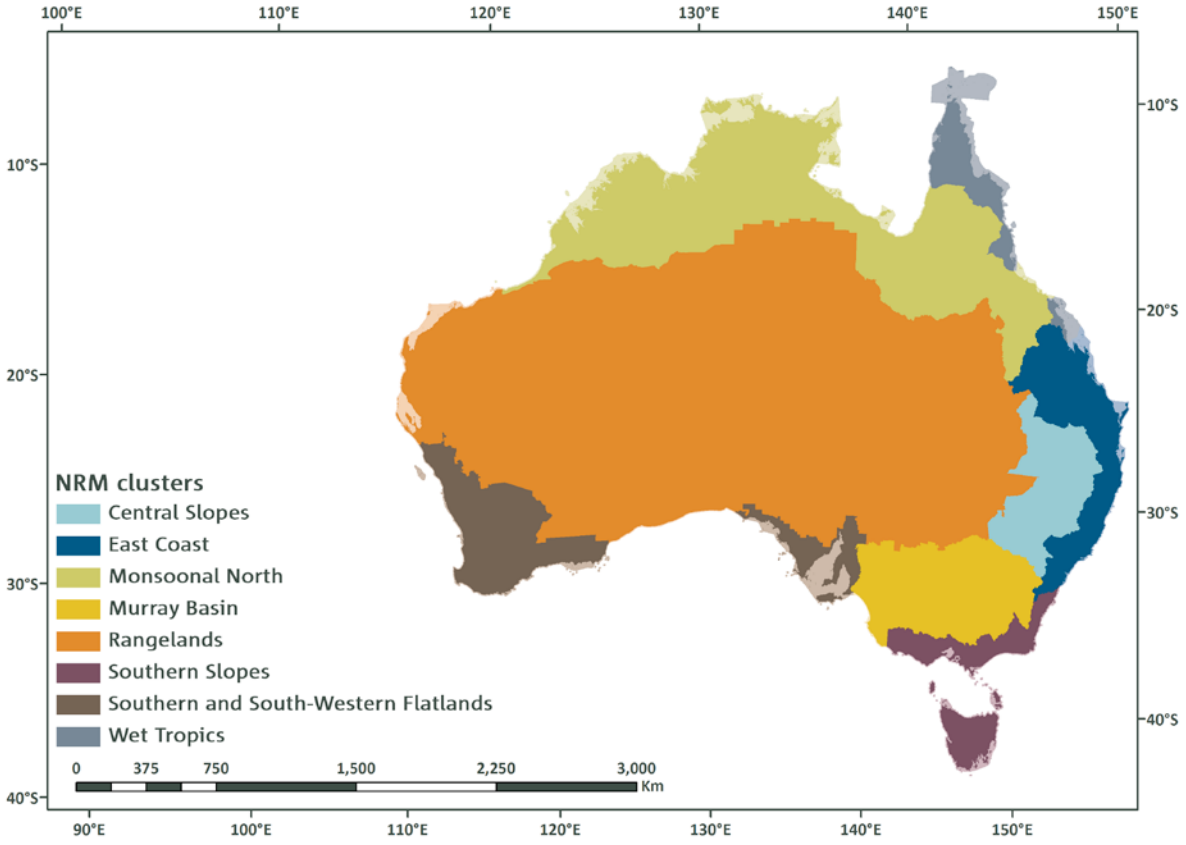

FIGURE A: THE EIGHT NATURAL RESOURCE MANAGEMENT (NRM) CLUSTERS.

This is the regional projections report for the Rangelands cluster. This document provides projections in a straightforward and concise format with information about the cluster as a whole, as well as additional information at finer scales where appropriate.

This cluster report is part of a suite of products. These include a brochure for each cluster that provides the key projection statements in a brief format. There is also the Australian climate change projections Technical Report, which describes the underlying scientific basis for the climate change projections. Box 1 describes all supporting products.

This report provides the most up to date, comprehensive and robust information available for this part of Australia, and draws on both international and national data resources and published peer-reviewed literature.

The projections in this report are based on the outputs of sophisticated global climate models (GCMs). GCMs are based on the laws of physics, and have been developed over many years in numerous centres around the world. These models are rigorously tested for their ability to reproduce past climate. The projections in this report primarily use output from the ensemble of model simulations brought together for the Coupled Model Inter-comparison Project phase 5 (CMIP5) (Taylor *et al*., 2012), where phase 5 is the most recent comparison of model simulations addressing, amongst other things, projections of future climates. In this report, outputs from GCMs in the CMIP5 archive are complemented by regional climate modelling and statistical downscaling.

BOX 1: CLIMATE CHANGE IN AUSTRALIA – PRODUCTS

This report is part of a suite of Climate Change in Australia (CCIA) products prepared with support from the Australian Government's Regional Natural Resource Management Planning for Climate Change Fund. These products provide information on climate change projections and their application.

CLUSTER BROCHURES

Purpose: key regional messages for everyone

A set of brochures that summarise key climate change projections for each of the eight clusters. The brochures are a useful tool for community engagement.

CLUSTER REPORTS

Purpose: regional detail for planners and decision-makers

The cluster reports are to assist regional decision-makers in understanding the important messages deduced from climate change projection modelling. The cluster reports present a range of emissions scenarios across multiple variables and years. They also include relevant sub-cluster level information in cases where distinct messages are evident in the projections.

TECHNICAL REPORT

Purpose: technical information for researchers and decision-makers

A comprehensive report outlining the key climate change projection messages for Australia across a range of variables. The report underpins all information found in other products. It contains an extensive set of figures and descriptions on recent Australian climate trends, global climate change science, climate model evaluation processes, modelling methodologies and downscaling approaches. The report includes a chapter describing how to use climate change data in risk assessment and adaptation planning.

WEBSITE

URL: www.climatechangeinaustralia.gov.au

Purpose: one stop shop for products, data and learning

The CCIA website is for Australians to find comprehensive information about the future climate. This includes some information on the impacts of climate change that communities, including the natural resource management sector, can use as a basis for future adaptation planning. Users can interactively explore a range of variables and their changes to the end of the 21st century. A 'Climate Campus' educational section is also available. This explains the science of climate change and how climate change projections are created.

Information about climate observations can be found on the Bureau of Meteorology website (www.bom.gov.au/climate). Observations of past climate are used as a baseline for climate projections, and also in evaluating model performance.

EXECUTIVE SUMMARY

INTRODUCTION

This report presents projections of future climate for the Rangelands based on our current understanding of the climate system, historical trends and model simulations of the climate response to changing greenhouse gas and aerosol emissions. Sub-clusters will also be reported on when their climate differs from the cluster mean, namely: Rangelands North (RN) and Rangelands South (RS) (Figure 1.1). The simulated climate response is that of the CMIP5 model archive, which also underpins the science of the *Fifth Assessment Report* of the Intergovernmental Panel on Climate Change (IPCC, 2013).

The global climate model (GCM) simulations presented here represent the full range of emission scenarios, as defined by the Representative Concentration Pathways (RCPs) used by the IPCC, with a particular focus on RCP4.5 and RCP8.5. The former represents a pathway consistent with low-level emissions, which stabilise the carbon dioxide concentration at about 540 ppm by the end of the 21st century. The latter is representative of a high-emission scenario, for which the carbon dioxide concentration reaches about 940 ppm by the end of the 21st century.

Projections are generally given for two 20-year time periods: the near future 2020–2039 (herein referred to as 2030) and late in the century 2080–2099 (herein referred to as 2090). The spread of model results are presented as the range between the 10th and 90th percentile in the CMIP5 ensemble output. For each time period, the model spread can be attributed to three sources of uncertainty: the range of future emissions, the climate response of the models, and natural variability. Climate projections do not make a forecast of the exact sequence of natural variability, so they are not 'predictions'. They do however show a plausible range of climate system responses to a given emission scenario and also show the range of natural variability for a given climate. Greenhouse gas concentrations are similar amongst different RCPs for the near future, and for some variables, such as rainfall, the largest range in that period stems from natural variability. Later in the century, the differences between RCPs are more pronounced, and climate responses may be larger than natural variability.

For each variable, the projected change is accompanied by a confidence rating. This rating follows the method used by the IPCC in the *Fifth Assessment Report*, whereby the confidence in a projected change is assessed based on the type, amount, quality and consistency of evidence (which can be process understanding, theory, model output, or expert judgment) and the degree of agreement amongst the different lines of evidence (IPCC, 2013). The confidence ratings used here are set as *low*, *medium*, *high* or *very high*.

HIGHER TEMPERATURES

Temperatures in the Rangelands have been increasing since national records began in 1910, especially since 1960. From 1910–2013, mean surface air temperature has increased by 1.0 °C in the North and 0.9 °C in the South using a linear trend.

Continued substantial increases for the Rangelands for mean, maximum and minimum temperature are projected with *very high confidence*. This takes into consideration the robust understanding of the driving mechanisms of warming as well as the strong agreement on direction and magnitude of change amongst GCMs and downscaling results.

For the near future (2030), the mean warming is around 0.6 to 1.4 °C above the climate of 1986–2005, with only minor differences between RCPs. The projected temperature range for late in the century (2090) shows larger differences with 1.5 to 3.1 °C (North), 1.3 to 2.6 °C (South) and 1.5 to 2.9 °C (all) for RCP4.5; and 3.1 to 5.6 °C (North), 2.8 to 5.1 °C (South) and 2.9 to 5.3 °C (all) for RCP8.5.

HOTTER AND MORE FREQUENT HOT DAYS, LESS FROST

A substantial increase in the temperature reached on the hottest days, in the frequency of hot days and in the duration of warm spells is projected with *very high confidence*, based on model results and physical understanding. For example, in Alice Springs, the number of days above 35 °C increases by 40 % by 2090 under RCP4.5 and median projected warming. The number of days over 40 °C nearly triples. The number of frost risk days in Alice Springs is reduced by more than half.

LESS RAINFALL IN WINTER (IN THE SOUTH) AND IN SPRING (CLUSTER-WIDE). CHANGES IN OTHER SEASONS ARE UNCLEAR

There has been a long-term increase in summer rainfall in the northwest of the Rangelands. In the far south, there has been a small decline in winter rainfall since 1960. However, natural variability of rainfall has been high in both North and South, especially in recent decades.

We have *high confidence* that natural climate variability will remain the major driver of rainfall changes by 2030 (annual-mean changes of ± 10 %, and seasonal-mean changes of about ± 20 %).

By 2090, decreases in winter rainfall are projected for the South with *high confidence*. There is strong model agreement and good understanding of the physical mechanisms driving this change, including a southward shift of winter storm systems. The magnitude of the change in winter rainfall under RCP8.5 for the South ranges from −20 % to +10 % for 2030; and from −45 % to 0 % for 2090.

Decreases are also projected for spring in both North and South, but with *medium confidence* only. The range for spring for 2090 under RCP8.5 is −55 % to +25 % for North, and −55 % to +20 % for South.

Changes to rainfall in other seasons, and annually, by 2090 are possible, but the direction of change cannot be reliably projected given the spread of model results. Such contrasts highlight the need to consider the risk of both a drier and wetter climate in impact assessment in the Rangelands.

INCREASED INTENSITY OF HEAVY RAINFALL EVENTS, CHANGES TO DROUGHT LESS CLEAR

Understanding of physical processes and high model agreement gives us *high confidence* that the intensity of heavy rainfall events will increase. There is *low confidence* in the magnitude of change and the time when any change may be evident against natural variability.

We have *low confidence* in projecting how the frequency and duration of extreme meteorological drought may change, although there is *medium confidence* that under RCP8.5 the time spent in drought will increase by 2090.

LITTLE CHANGE IN WIND SPEED

The median for projections of seasonal mean surface wind speed indicate little or no change throughout the 21st century. In the South, there is *medium confidence* in a decrease in mean surface wind speed in winter.

Based on global and regional studies, tropical cyclones are projected to become less frequent, but with increases in the proportion of the most intense storms *(medium confidence*).

INCREASED SOLAR RADIATION IN WINTER AND REDUCED HUMIDITY THROUGHOUT THE YEAR

Little change is projected for solar radiation for 2030 (*high confidence*). For 2090, there is *medium confidence* in increased winter radiation in the South, which is related to decreases in cloudiness associated with reduced rainfall.

We have *medium confidence* in little change in relative humidity for 2030. For 2090, based on model results and physical understanding, there is *medium confidence* in a decrease in relative humidity in summer and autumn, and there is *high confidence* in a decrease in winter and spring (about −5 to 0 % under RCP4.5 and −10 to 0 % under RCP8.5), with changes similar in both the North and South sub-cluster regions.

INCREASED EVAPORATION RATES, AND REDUCED SOIL MOISTURE, CHANGES TO RUNOFF LESS CLEAR

Projections for potential evapotranspiration indicate increases in all seasons, with the largest absolute rates in summer by 2090 (*high confidence*). However, despite high model agreement, we have only *medium confidence* in the magnitude of the projected change due to shortcomings in simulation of observed historical changes.

Soil moisture projections suggest overall seasonal decreases by 2090, but predominately in winter, and more strongly in the South (*medium confidence*). These changes in soil moisture are strongly influenced by those in rainfall, but tend to be more negative due to the increase in potential evapotranspiration. For similar reasons, runoff is projected to decrease, but only with *low confidence*. Furthermore, these estimates are based only on large-scale considerations. More detailed hydrological and environmental modelling is needed to assess local changes to these variables.

A HARSHER FIRE WEATHER CLIMATE IN THE FUTURE

Bushfire in the Rangelands depends highly on fuel availability, which mainly depends on rainfall. For most of this cluster, extensive bushfire activity occurs after extended wet periods. These lead to vegetation growth that burns after the wet period ends. There is *high confidence* that climate change will result in a harsher fire-weather climate in the future, due to higher temperature and lower rainfall. But there is *low confidence* in the magnitude of fire weather projections. When bushfires occur, more extreme fire behaviour can be expected.

HIGHER SEA LEVELS AND MORE FREQUENT SEA LEVEL EXTREMES

Relative sea level has risen around Australia at an average rate of 1.4 mm per year between 1966 and 2009, and 1.6 mm per year after the influence of the El Niño Southern Oscillation (ENSO) on sea level is removed.

There is very *high confidence* that sea level will continue to rise during the 21st century for both west and south coasts of the Rangelands. By 2030, the projected range of sea-level rise at Port Hedland is 0.07 to 0.17 m above the 1986–2005 level, with only minor differences between emission scenarios. As the century progresses, projections are sensitive to emissions pathways. By 2090, the intermediate emissions case (RCP4.5) gives a rise of 0.28 to 0.64 m, and the high emissions case (RCP8.5) gives a rise of 0.40 to 0.84 m. These ranges of sea level rise are considered *likely* (at least 66 % probability). However, if a collapse in the marine based sectors of the Antarctic ice sheet were initiated, these projections could be several tenths of a metre higher by late in the century.

Taking into account the nature of extreme sea levels along the Rangelands coastlines and the uncertainty in the sea level rise projections, an indicative extreme sea level 'allowance' is provided. The allowance being the minimum distance required to raise an asset to maintain current frequency of breaches under projected sea level rise. In 2030, the vertical allowances along the cluster coastline are in the range of 12 to 14 cm for all RCPs, and by 2090, 52 to 63 cm for RCP4.5 and 70 to 86 cm for RCP8.5.

WARMER AND MORE ACIDIC OCEANS IN THE FUTURE

Sea surface temperature (SST) has increased significantly across the globe over recent decades and is projected to continue to rise with *very high confidence*. Across the coastal waters of the Rangelands cluster region in 2090, warming is projected in the range of 2.4 to 3.7 °C for RCP8.5.

About 30 % of the anthropogenic carbon dioxide emitted into the atmosphere over the past 200 years has been absorbed by the oceans. This has led to a 0.1 pH fall in the ocean's surface water pH (a 26 % rise in acidity). Continued acidification will compromise the ability of calcifying marine organisms such as corals, oysters and some plankton to form their shells or skeletons. There is *very high confidence* that around Australia the ocean will become more acidic and also *high confidence* that the rate of ocean acidification will be proportional to carbon dioxide emissions. By 2030, pH is projected to fall by an additional 0.07 units in the coastal waters of the Rangelands cluster. By 2090, a decrease of up to 0.14 pH units is projected under RCP4.5 and a decrease of up to 0.3 units under RCP8.5. These values would represent a 40 % and 100 % increase in acidity respectively.

MAKING USE OF THESE PROJECTIONS FOR CLIMATE ADAPTATION PLANNING

These regional projections provide the best available science to support impact assessment and adaptation planning in the Rangelands cluster. This report provides some guidance on how to use these projections, including the Australian Climate Futures web tool, available from the Climate Change in Australia website. The tool allows users to investigate the range of climate model outcomes for their region across timescales and RCPs of interest, and to select and use data from models that represents a particular change of interest (*e.g.* warmer and drier conditions).

1 THE RANGELANDS CLUSTER

This report describes climate change projections for the Rangelands cluster, which covers much of the Australian interior (Figure 1.1) and spans some 3100 km in the east-west direction and 1400 km north-south. It includes NRM regions in four states and the Northern Territory. These include Desert Channels (western Queensland), South-West Queensland, South Australian Arid Lands, Alinytjara Wilurara and the former Western region of NSW. Note that since January 2014 the NRM regions of NSW have been reorganised into new Local Land Services (LLS) regions, and Rangelands includes the Western and North-West LLS. The Northern Territory and Western Australian Rangelands NRMs form a large expanse of the cluster, but exclude their respective northern sub-regions (Top End, Gulf Savanna and Kimberley).

The vast Rangelands cluster extends across much of the iconic 'Outback'. It contains varied landscapes, including the Flinders and Pilbara Ranges, salt lakes that flood sporadically (Hope *et al.*, 2004), and the Centre. There is a wide range of vegetation, from tropical woodlands to shrublands, grasslands and saltbush, and it includes relatively intact ecosystems. The water features shown in Figure 1.1 are mostly intermittent, and aside from the coastal rivers of the west, most streams drain into salty lakes, in particular Lake Eyre.

The cluster is home to many of Australia's indigenous people. Important agricultural activity includes the grazing of cattle and sheep. Rainfall is important to the wellbeing of all communities and their economic productivity. Rainfall systems vary from seasonally reliable monsoonal influences in the far north through to very low and variable rainfall patterns in much of centre and south. Given this, the Rangelands cluster has been divided into North (N or RN) and South (S or RS) sub-clusters. Climate statistics and projections will be mostly given for both. The split is motivated by the bioregions that result from the seasonal rainfall distribution, but for simplicity it has been specified by a straight line, approximately from Exmouth in the north-west to Cobar in the south-east. A range of climate change impacts and adaptation challenges have been identified by the NRM regions throughout this cluster.

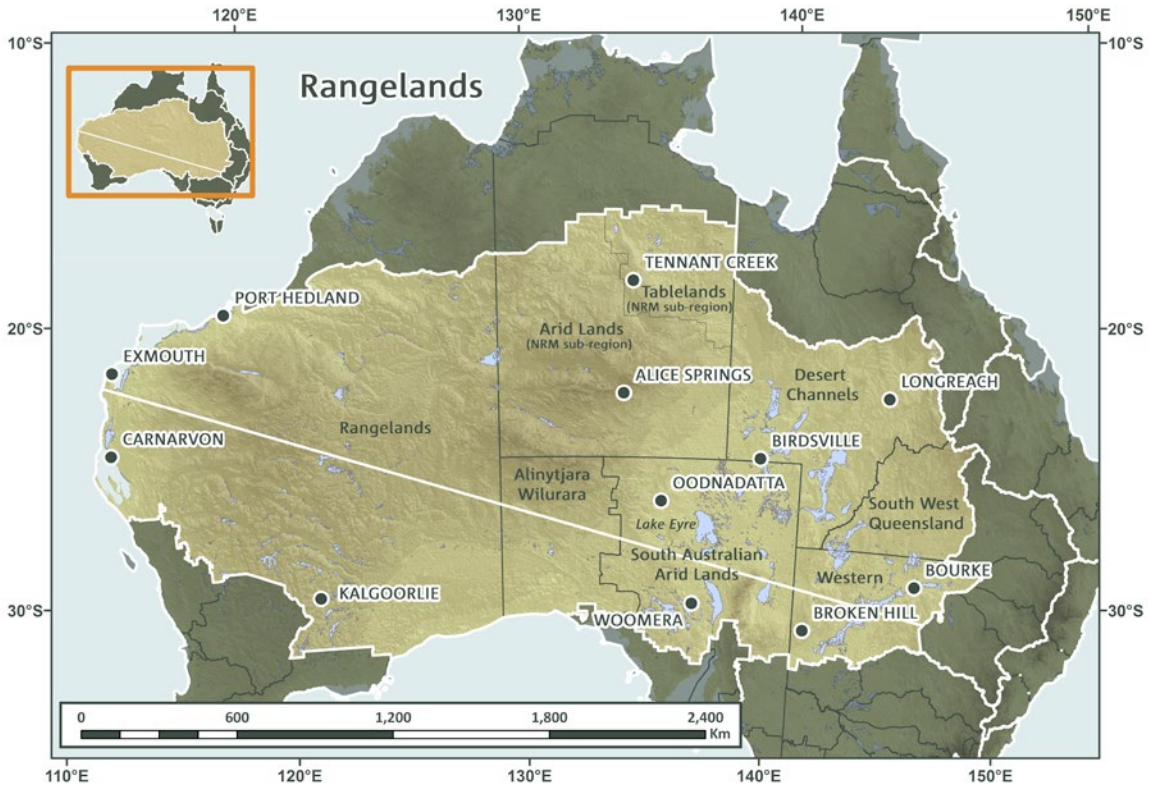

FIGURE 1.1: THE RANGELANDS CLUSTER, SHOWING NRM REGIONS AND SUB-REGIONS, TOWNS AND WATER FEATURES WITH RESPECT TO THE AUSTRALIAN CONTINENT. THE DIAGONAL WHITE LINE DEFINES THE PARTITION INTO NORTH AND SOUTH SUB-CLUSTERS.

2 CLIMATE OF RANGELANDS

This chapter gives an overview of the current climate of the Rangelands cluster for the period 1986–2005 (Box 3.1 presents the observational data sets used in this report).

For this period, seasonal mean temperatures range from below 12 °C in the south of Rangelands to over 30 °C in the north (Figure 2.1). In the cooler months the temperature gradient across latitudes is most pronounced in the north, particularly for daily minimum, on account of strong night-time cooling in the centre. In the warmer months, the gradient is stronger in the south. However, all parts of the cluster can experience very high daily maximum temperatures in summer. Averaged over the North or South (Figure 2.2), both parts are some 14 °C warmer in January than July, and have an average diurnal range of around 15 °C in each month.

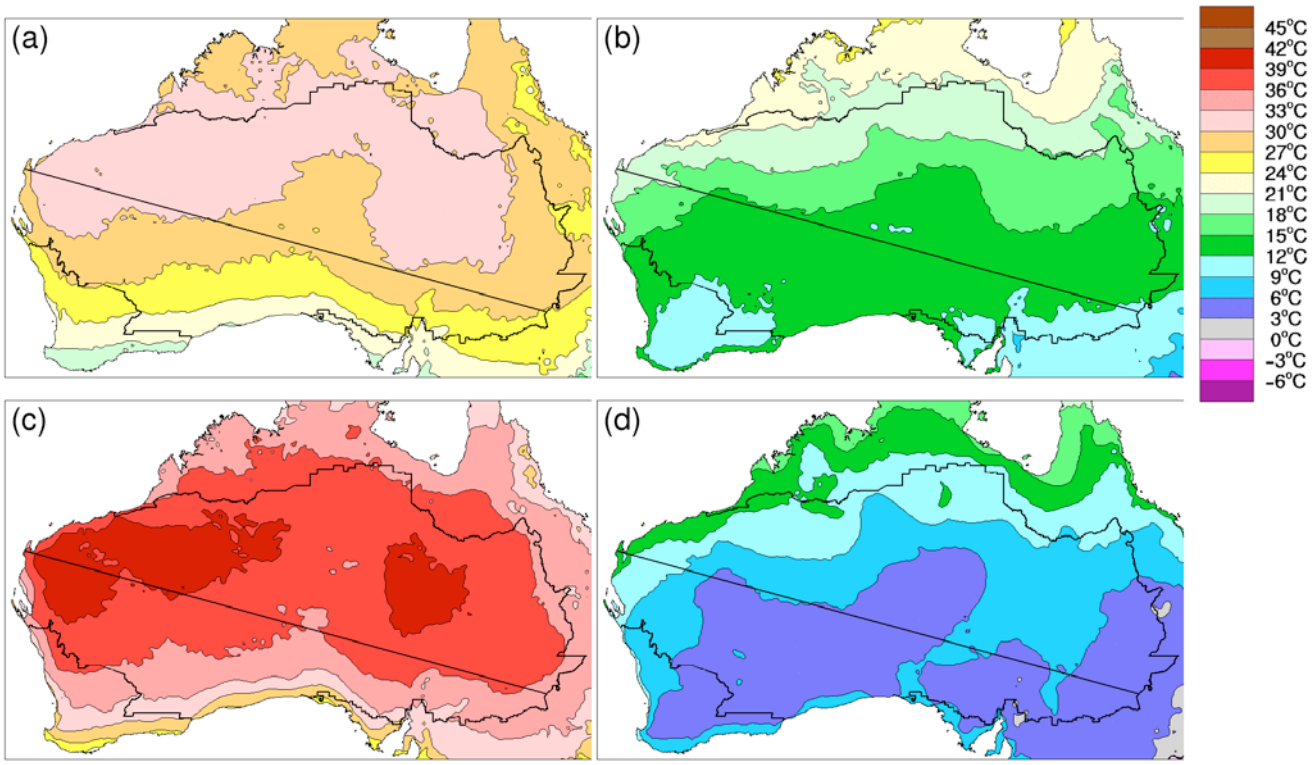

FIGURE 2.1: MAPS OF (A) AVERAGE SUMMER (DECEMBER TO FEBRUARY) DAILY MEAN TEMPERATURE, (B) AVERAGE WINTER (JUNE TO AUGUST) DAILY MEAN TEMPERATURE, (C) AVERAGE JANUARY MAXIMUM DAILY TEMPERATURE AND (D) AVERAGE JULY MINIMUM DAILY TEMPERATURE FOR THE PERIOD 1986–2005.

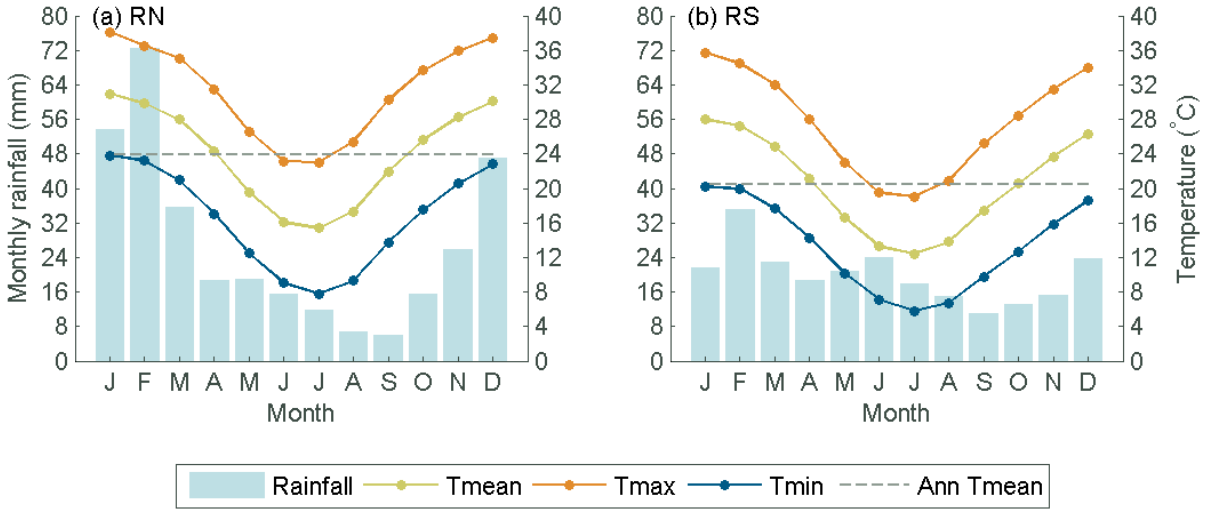

FIGURE 2.2: MONTHLY RAINFALL (BLUE BARS) AND TEMPERATURE CHARACTERISTICS FOR THE RANGELANDS CLUSTER NORTH (A) AND SOUTH (B) (1986–2005). *TMEAN* IS MONTHLY MEAN TEMPERATURE (GREEN LINE), *TMAX* IS MONTHLY MEAN MAXIMUM TEMPERATURE (ORANGE LINE), *TMIN* IS MONTHLY MEAN MINIMUM TEMPERATURE (BLUE LINE) AND *ANN TMEAN* IS THE ANNUAL AVERAGE OF MEAN TEMPERATURE (GREY LINE) (24.0 °C FOR THE NORTH AND 20.4 °C FOR THE SOUTH). TEMPERATURE AND RAINFALL DATA ARE FROM AWAP.

Most of the Rangelands cluster has relatively low annual rainfall, ranging from 500 mm along the northern and eastern fringes to less than 200 mm in the interior. Monsoonal winds and tropical cyclones bring rain to the north in the summer/warmer months, and most of the cluster can experience days of heavy rain. February has the highest average rainfall in both parts of the cluster, but with twice as much average rainfall in the North as compared to the South (Figure 2.2). Winter/cool season rain is rare in the north, but mid-latitude lows, fronts and the associated 'northwest cloud bands' can bring rain to the interior and the south, particularly in the far west and the east.

The wet-dry season partition of the rainfall is indicated by the percentage of annual rainfall that falls in the warmer six month period of November to April (Figure 2.3a; panel (b) is discussed in Chapter 3 and panel (c) in Chapter 4.3). This ranges from over 90 % in the north to below 50 % in the south and south-west. Corresponding maps of seasonal rainfall are shown in Figure 2.4. Apart from the far south, the heaviest rainfall events usually occur in summer, with monthly 90th percentile values around 50 to 200 mm in the north during the period 1900–2005. Summer thunderstorms can be hazardous due to accompanying winds, hail and flash floods and potentially damaging lightning strikes. The northern and western regions of Rangelands experience 20 to 40 thunder days a year, with the peak number in the central west (Kuleshov *et al.*, 2002).

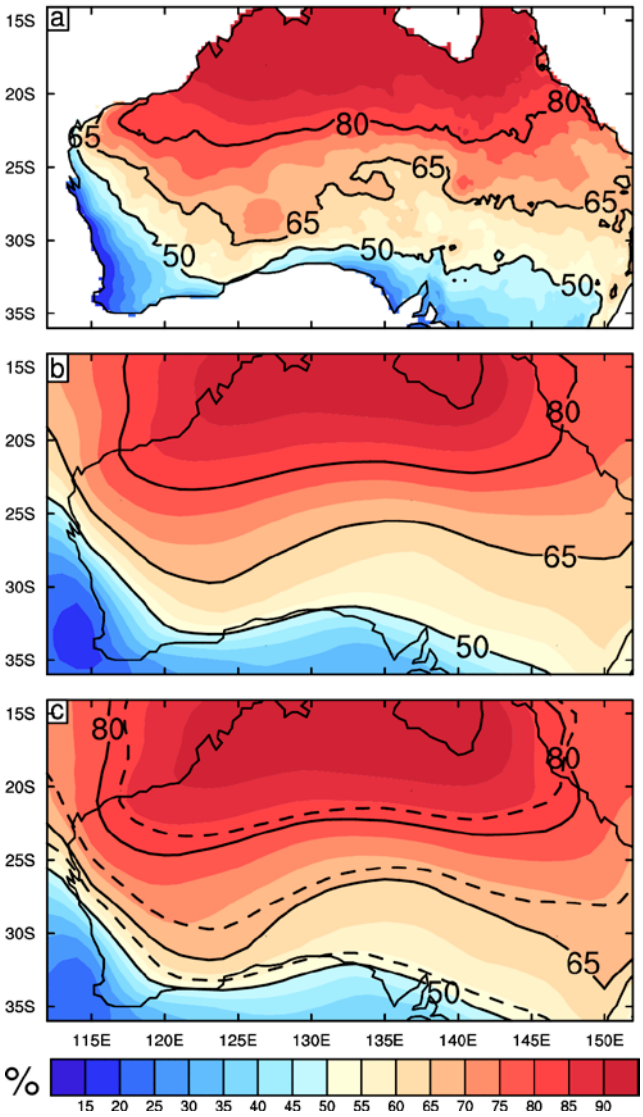

FIGURE 2.3: PERCENTAGE OF ANNUAL RAIN THAT FALLS IN THE WARMER SIX MONTHS (NOVEMBER TO APRIL): (A) OBSERVED 1986–2005 (AWAP); (B) FROM CMIP5 40 MODEL MEAN FOR 1986–2005; AND FOR (C) CMIP5 26 MODEL MEAN FOR 2080–2099. THE 50 % CONTOUR LINE INDICATES THE BOUNDARY BETWEEN THE SUMMER AND WINTER DOMINATED ZONES. THE DASHED LINES IN (C) REFER TO THE SOLID LINES IN THE MODEL SIMULATED CLIMATE IN (B).

The average values mask the inter-annual variability of rainfall, which is larger in most of the Rangelands than the rest of Australia, and within the Rangelands is highest in the seasonally drier regions (the north in winter, the south in summer). This variability can be influenced by variations in the tropical sea surface temperatures (SSTs) of adjacent ocean basins, and the associated variation in the regional pressure, reflected in the Southern Oscillation Index. Risbey *et al*. (2009) find a significant influence of Pacific SSTs (and El Niño or La Niña conditions) on rainfall in the centre and east, especially from September to November. The equatorial Indian Ocean influences rainfall in the far west and south, mostly in the cooler months. For further details of ENSO (El Niño Southern Oscillation) and other modes of variability see Chapter 4 in the Technical Report.

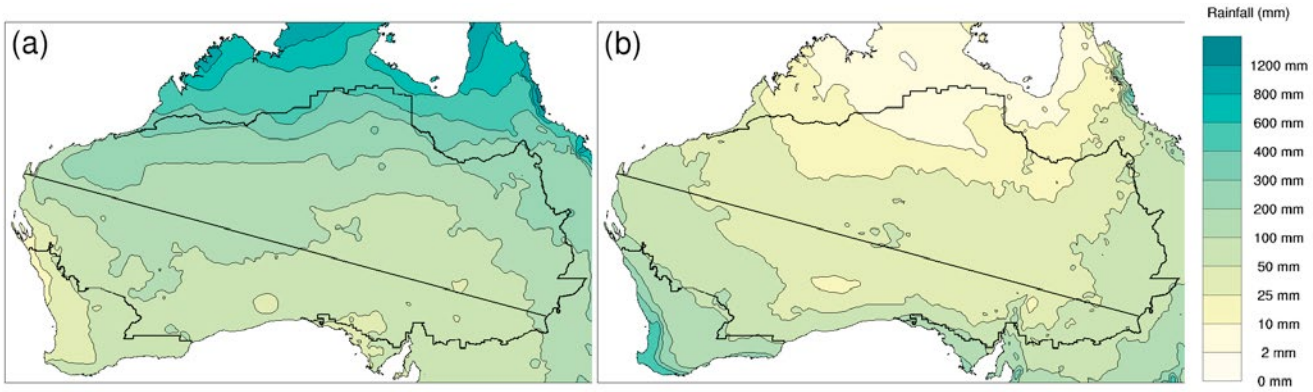

FIGURE 2.4: FOR THE 1986–2005 PERIOD, AVERAGE RAINFALL (MM) FOR THE (A) SUMMER (DECEMBER TO FEBRUARY) AND THE (B) WINTER (JUNE TO AUGUST).

3 SIMULATING REGIONAL CLIMATE

Researchers use climate models to examine future global and regional climate change. These models have a foundation in well-established physical principles and are closely related to the models used successfully in weather forecasting. Climate modelling groups from around the world produce their own simulations of the future climate, which may be analysed and compared to assess climate change in any region. For this report, projections are based on historical and future climate simulations from the CMIP5 model archive that holds the most recent simulations, as submitted by approximately 20 modelling groups (Taylor *et al.*, 2012). The number of models used in these projections varies by RCP and variable depending on availability, *e.g.* for monthly temperature and rainfall, data are available for 39 models for RCP8.5 but only 28 models for RCP2.6 (see Chapter 3 in the Technical Report.

The skill of a climate model is assessed by comparing model simulations of the current climate with observational data sets (see Box 3.1 for details on the observed data used for model evaluation for the Rangelands cluster). Accurate simulation of key aspects of the regional climate provides a basis for placing some confidence in the model's projections. However, models are not perfect representations of the real world. Some differences in model output relative to the observations are to be expected. The measure of model skill can also vary depending on the scoring measure used and regions being assessed.

For the Rangelands as a whole, CMIP5 models performed well in simulating the timing and magnitude of the seasonal cycle for temperature (Figure 3.1a). The majority of models adequately simulated the timing of the seasonal rainfall patterns (Figure 3.1b) and the geographical distribution of summer/winter dominated rainfall regions (Figure 2.3.b). In each month, the mean modelled rainfall is a little higher than observed rainfall. Nonetheless, given the large interannual and decadal variability of observations, the bias is not unexpected. To see how the models performed across different parts of Australia, refer to Chapter 5 in the Technical Report.

BOX 3.1: COMPARING MODELS AND OBSERVATIONS: EVALUATION PERIOD, DATA SETS, AND SPATIAL RESOLUTION

Model skill is assessed by running simulations over historical time periods and comparing simulations with observed climate data. Projections presented here are assessed using the 1986–2005 baseline period, which conforms to the *Fifth Assessment Report*, (IPCC, 2013). The period is also the baseline for projected changes, as presented in bar plots and tabled values in the Appendix. An exception is the time series projection plots, which use a baseline of 1950–2005, as explained in Section 6.2.2 of the Technical Report.

Several data sets are used to evaluate model simulations of the current climate. For assessment of rainfall and temperature, the observed data are derived from the Australian Water Availability Project (AWAP) (Jones *et al.*, 2009) and from the Australian Climate Observations Reference Network – Surface Air Temperature (ACORN-SAT), a data set developed for the study of long-term changes in monthly and seasonal climate (Fawcett *et al.*, 2012).

The spatial resolution of climate model data (around 200 km between the edges of grid cells) is much coarser than observations.

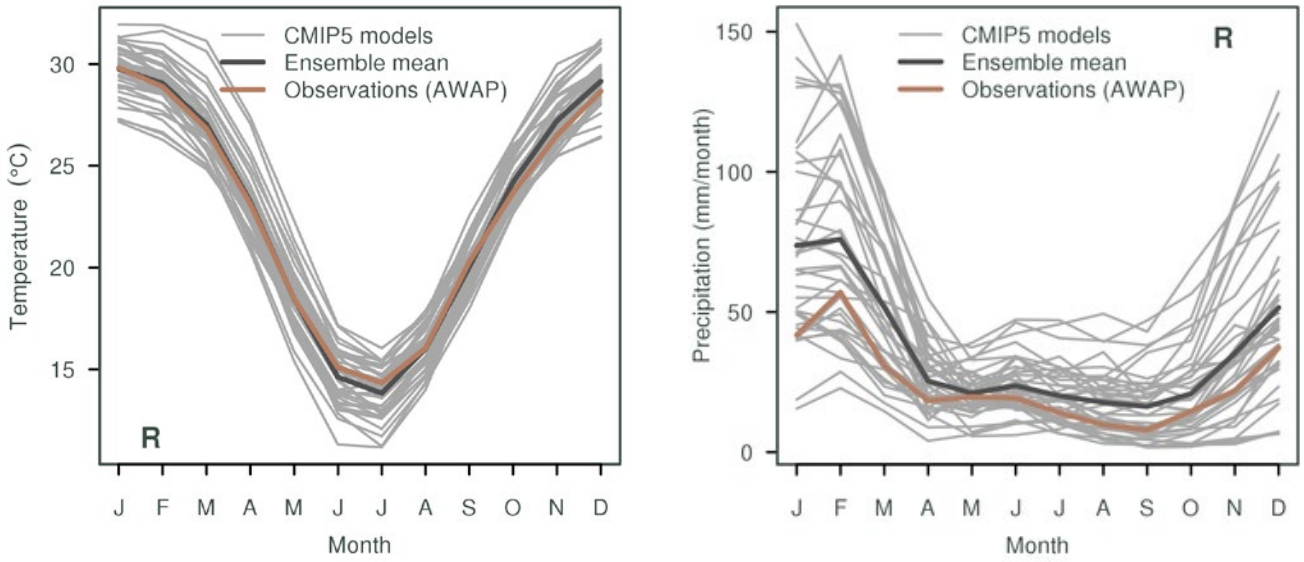

FIGURE 3.1: THE ANNUAL CYCLE OF TEMPERATURE (LEFT PANEL) AND RAINFALL (RIGHT PANEL) AVERAGED OVER RANGELANDS SIMULATED BY CMIP5 MODELS (GREY LINES) WITH MODEL ENSEMBLE MEAN (BLACK LINE) AND OBSERVED CLIMATOLOGY BASED ON AWAP (BROWN LINES) FOR THE BASELINE PERIOD 1986–2005.

The ability of CMIP5 models to simulate key modes of climatic variability affecting the cluster has also been assessed. Significantly, the connection between El Niño variations and rainfall is reasonably well simulated and improved over the previous generation of climate models. However, all models have at least some significant shortcomings across a range of tests (more details in Chapter 5 of the Technical Report). Some of these shortcomings are noted in the context of interpreting specific projection results in the Section that follows. No single or small number of models performed considerably better than others for the Rangelands cluster.

In addition to the CMIP5 model results, downscaling can be used to derive finer spatial information in the regional projections, thus potentially capturing processes occurring on a finer scale. It is advisable to consider more than one technique, as different downscaling techniques have different strengths and weaknesses. Whilst downscaling can provide added value on finer scale processes, it increases the uncertainty in the projections since there is no single best downscaling method, but a range of methods that are more or less appropriate depending on the application.

For the regional projections we consider downscaled projections from two techniques: outputs from a dynamical downscaling model, the Conformal Cubic Atmospheric Model, (CCAM; McGregor and Dix, 2008) using six CMIP5 GCMs as input and the Bureau of Meteorology analogue-based statistical downscaling model with 22 CMIP5 GCMs as input for rainfall and 21 CMIP5 GCMs as input for temperature (Timbal and McAvaney, 2001). As the largest cluster, downscaling has not been a focus of the analysis for Rangelands. Regional averages of changes in temperature and rainfall are not notably different in either downscaling technique to those from the full CMIP5 ensemble.

4 THE CHANGING CLIMATE OF RANGELANDS

This Section presents projections of climate change to the end of the 21st century for a range of climate variables, including average and extreme conditions, of relevance to the Rangelands cluster. Where there are relevant observational data available, the report shows historical trends.

As outlined in the *Fifth Assessment Report* (IPCC, 2013), greenhouse gases, such as carbon dioxide, have a warming effect on global climate. These gases absorb heat that would otherwise be lost to space, and re-radiate it back into the atmosphere and to the Earth's surface. The IPCC concluded that it was *extremely likely* that more than half of the observed increase in global average surface air temperature from 1951–2010 has been caused by the anthropogenic increase in greenhouse gas emissions and other anthropogenic forcings. Further increases in greenhouse gas concentrations resulting primarily from burning fossil fuel will lead to further warming, as well as other physical and chemical changes in the atmosphere, ocean and land surface.

The CMIP5 simulations give the climate response to a set of greenhouse gas, aerosol and land-use scenarios that are consistent with socio-economic assumptions of how the future may evolve. These scenarios are known as the Representative Concentration Pathways (RCPs) (Moss *et al.*, 2010; van Vuuren *et al.*, 2011). Box 4.1 presents a brief introduction to the RCPs.

In its *Fifth Assessment Report* (IPCC, 2013), the IPCC concluded that global mean surface air temperatures for 2081–2100 relative to 1986–2005 are likely to be in the following ranges: 0.3 to 1.7 °C warmer for RCP2.6 (representing low emissions); 1.1 to 2.6 °C and 1.4 to 3.1 °C warmer for RCP4.5 and RCP6.0 respectively (representing intermediate emissions); and 2.6 to 4.8 °C warmer for RCP8.5 (representing high emissions).

The projections for the climate of the Rangelands cluster consider model ranges of change as simulated by the CMIP5 ensemble. However, the projections should be viewed in the context of the confidence ratings that are provided, which consider a broader range of evidence than just the model outputs. The projected change is assessed for two 20-year periods: a near future 2020 to 2039 (herein referred to as 2030) and a period late in the 21st century, 2080 to 2099 (herein referred to as 2090) following RCPs 2.6, 4.5 and 8.5 (Box 4.1)[1].

The spread of model results is presented in graphical form (Box 4.2) and provided as tabulated percentiles in Table 1 (10th, 50th and 90th) and Table 3 (5th, 50th and 95th, for sea level rise) in the Appendix. CMIP5 results for additional time periods between 2030 and 2090 are provided through the Climate Change in Australia website (Box 1).

Unless otherwise stated, users of these projections should consider the projected change, as indicated by the different plots and tabulated values, as applicable to each location within the cluster.

1 For sea level rise and sea allowance, the future averaging periods are 2020–2040 and 2080–2100. In the report, these are referred to as 2030 and 2090 respectively.

BOX 4.1: REPRESENTATIVE CONCENTRATION PATHWAYS (RCPs)

The climate projections presented in this report are based on climate model simulations following a set of greenhouse gas, aerosol and land-use scenarios that are consistent with socio-economic assumptions of how the future may evolve. The well mixed concentrations of greenhouse gases and aerosols in the atmosphere are affected by emissions as well as absorption through land and ocean sinks.

There are four Representative Concentration Pathways (RCPs) underpinned by different emissions. They represent a plausible range of radiative forcing (in W/m^2) during the 21st century relative to pre-industrial levels. Radiative forcing is a measure of the energy absorbed and retained in the lower atmosphere. The RCPs are:

- RCP8.5: high radiative forcing (high emissions)
- RCP4.5 and 6.0: intermediate radiative forcing (intermediate emissions)
- RCP2.6: low radiative forcing (low emissions).

RCP8.5, represents a future with little curbing of emissions, with carbon dioxide concentrations reaching 940 ppm by 2100. The higher of the two intermediate concentration pathways (RCP6.0) assumes implementation of some mitigation strategies, with carbon dioxide reaching 670 ppm by 2100. RCP4.5 describes somewhat higher emissions than RCP6.0 in the early part of the century, with emissions peaking earlier then declining, and stabilisation of the carbon dioxide concentration at about 540 ppm by 2100. RCP2.6 describes emissions that peak around 2020 and then rapidly decline, with the carbon dioxide concentration at about 420 ppm by 2100. It is likely that later in the century active removal of carbon dioxide from the atmosphere would be required for this scenario to be achieved. For further details on all RCPs refer to Section 3.2 and Figure 3.2.2 in the Technical Report.

The previous generation of climate model experiments that underpins the science of the IPCC's *Fourth Assessment Report* used a different set of scenarios. These are described in the IPCC's Special Report on Emissions Scenarios (SRES) (Nakićenović and Swart, 2000). The RCPs and SRES scenarios do not correspond directly to each other, though carbon dioxide concentrations under RCP4.5 and RCP8.5 are similar to those of SRES scenarios B1 and A1FI respectively.

In the Technical and Cluster Reports, RCP6.0 is not included due to a smaller sample of model simulations available compared to the other RCPs. Remaining RCPs are included in most graphical and tabulated material of the Cluster Reports, with the text focusing foremost on results following RCP4.5 and RCP8.5.

4.1 RANGES OF PROJECTED CLIMATE CHANGE AND CONFIDENCE IN PROJECTIONS

Quantitative projections of future climate change in the Rangelands are presented as ranges. This allows for differences in how future climate may evolve for three factors – greenhouse gas and aerosol emissions, the climate response and natural variability – that are not known precisely:

- Future emissions cannot be known precisely and are dealt with here by examining several different RCPs described in Box 4.1. There is no 'correct' scenario, so the choice of how many and which scenarios to examine is dependent on the decision-making context.
- The response of the climate system to emissions is well known in some respects, but less well known in others. The thermodynamic response (direct warming) of the atmosphere to greenhouse gases is well understood, although the global climate sensitivity varies. However changes to atmospheric circulation in a warmer climate are one of the biggest uncertainties regarding the climate response. The range between different climate models (and downscaled models) gives some indication of the possible responses. However, the range of model results is not a systematic or quantitative assessment of the full range of possibilities, and models have some known regional biases that affect confidence.
- Natural variability (or natural 'internal variability' within the climate system) can dominate over the 'forced' climate change in some instances, particularly over shorter time frames and smaller geographic areas. The precise evolution of climate due to natural variability (*e.g.* the sequence of wet years and dry years) cannot be predicted (IPCC, 2013, see Chapter 11). However, the projections presented here allow for a range of outcomes due to natural variability, based on the different evolutions of natural climatic variability contained within each of the climate model simulations.

The projections presented are accompanied by a confidence rating that follows the system used by the IPCC in the *Fifth Assessment Report* (Mastrandrea *et al.*, 2010), whereby the confidence in a projected change is assessed based on the type, amount, quality and consistency of evidence (which can be process understanding, theory, model output, or expert judgment) and the extent of agreement amongst the different lines of evidence. Hence, this confidence rating does not equate precisely to probabilistic confidence. The levels of confidence used here are set as *low*, *medium*, *high* or *very high*. Note that although confidence may be high in the direction of change, in some cases confidence in magnitude of change may be medium or low (*e.g.* due to some known model deficiency). When confidence is low only qualitative assessments are given. More information on the method used to assess confidence in the projections is provided in Section 6.4 of the Technical Report.

4.2 TEMPERATURE

Surface air temperatures in the Rangelands have been increasing since national records began in 1910, especially since around 1960 (Figure 4.2.1, 4.2.2). From 1910–2013 mean temperature has risen by 1.0 °C in the North and 0.9 °C in the South using a linear trend. While several recent years were relatively cool in the North, 2013 was the warmest on record in South and second warmest in North. As can be seen in Figure 4.2.1, the warming trend and even some of the variation over the century is similar to that in global mean temperature.

Daytime maximum temperatures and overnight minimum temperatures have also increased since the mid 20th century (Figure 4.2.3), although variation from decade to decade is evident. From 1910–2013 maxima have risen by 0.9 °C and 0.8 °C in the North and South respectively, while minima have increased by 1.1 °C and 1.0 °C in the North and South respectively using a linear trend. The relatively high maxima in the early part of the 20th century, particularly in the South, are most likely explained by the drier than average conditions in this cluster during this period. The reason is that when the surface is dry, less energy is consumed by evaporation and proportionally more energy is felt as heat. There are also likely to be fewer clouds during dry conditions, allowing more sunlight to reach and warm the surface. This effect will be strongest during the day.

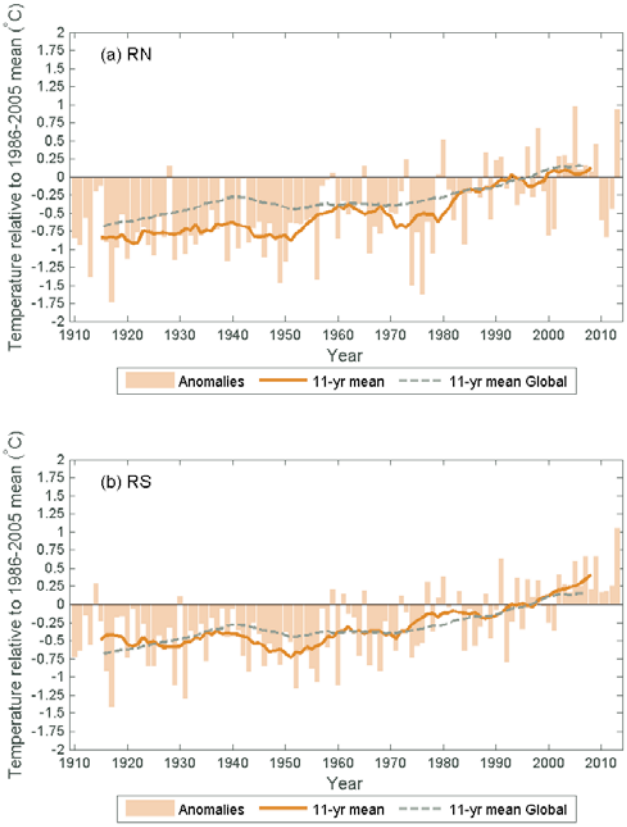

FIGURE 4.2.1: OBSERVED ANNUAL MEAN TEMPERATURE ANOMALIES (°C) FOR 1910–2013 COMPARED TO THE BASELINE 1986–2005 FOR RANGELANDS NORTH (A) AND SOUTH (B). CLUSTER AVERAGE DATA ARE FROM ACORN-SAT AND GLOBAL DATA ARE FROM HADCRUT3V (SEE BROHAN *ET AL.*, 2006).

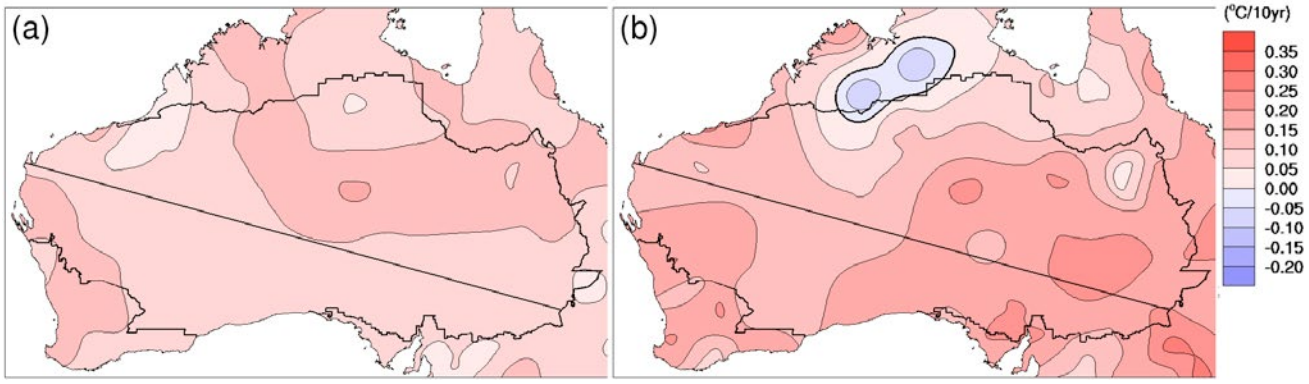

FIGURE 4.2.2: MAPS OF TREND IN MEAN TEMPERATURE (°C/10YEARS) FOR (A) 1910–2013 AND (B) 1960–2013 (ACORN-SAT).

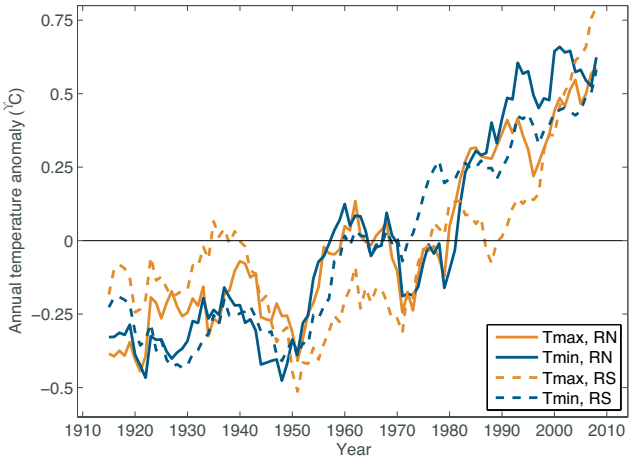

FIGURE 4.2.3: OBSERVED ANNUAL MEAN OF DAILY MAXIMUM (ORANGE LINE) AND MINIMUM (BLUE LINE) TEMPERATURE (°C, 11-YEAR RUNNING MEAN) FOR BOTH NORTH (SOLID) AND SOUTH (DASHED), PRESENTED AS ANOMALIES RELATIVE TO THEIR RESPECTIVE 1910–2013 MEAN VALUE (ACORN-SAT); RANGELANDS NORTH IS IN SOLID LINES AND RANGELANDS SOUTH IS IN DASHED LINES.

BOX 4.2: UNDERSTANDING PROJECTION PLOTS

Projections based on climate model results are illustrated using time series (a) and bar plots (b). The model data are expressed as anomalies from a reference climate. For the time series (a), anomalies are calculated as relative to 1950–2005, and for the bar plots (b) anomalies are calculated as the change between 1986–2005 and 2080–2099 (referred to elsewhere as '2090'). The graphs can be summarised as follows:

1. The middle (bold) line in both (a) and (b) is the median value of the model simulations (20-year moving average); half the model results fall above and half below this line.
2. The bars in (b) and dark shaded areas in (a) show the range (10th to 90th percentile) of model simulations of 20-year average climate.
3. Line segments in (b) and light shaded areas in (a) represent the projected range (10th to 90th percentile) of individual years taking into account year to year variability in addition to the long-term response (20-year moving average).

In the time series (a), where available, an observed time series (4) is overlaid to enable comparison between observed variability and simulated model spread. A time series of the future climate from one model is shown to illustrate what a possible future may look like (5). ACCESS1-0 was used for RCP4.5 and 8.5, and BCC-CSM-1 was used for RCP2.6, as ACCESS1-0 was not available.

In both (a) and (b), different RCPs are shown in different colours (6). Throughout this document, green is used for RCP2.6, blue for RCP4.5 and purple for RCP8.5, with grey bars used in bar plots (b) to illustrate the expected range of change due to natural internal climate variability alone (7).

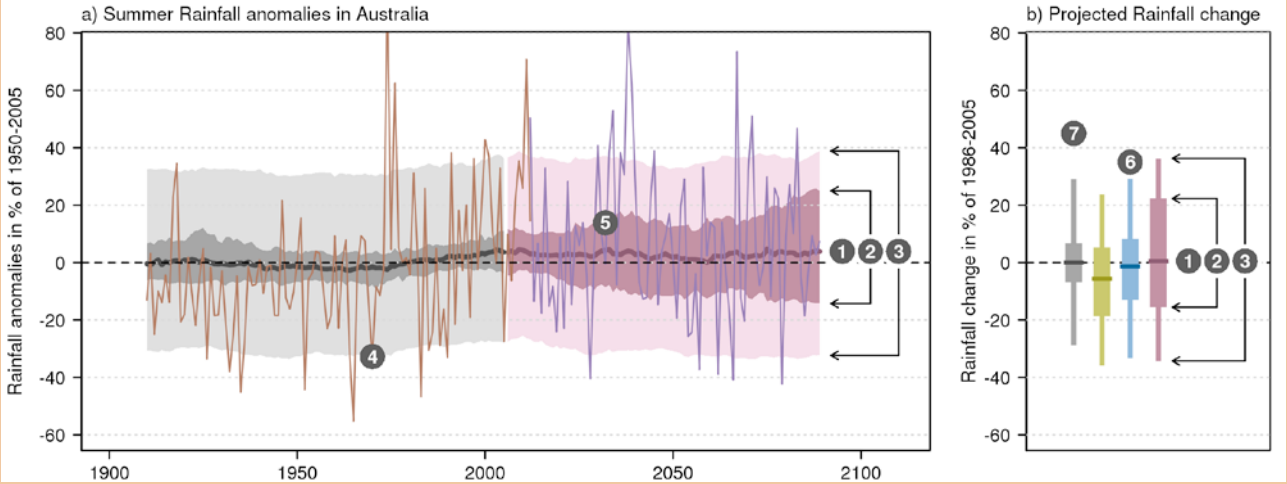

The Rangelands cluster is projected to continue to warm throughout the 21st century, with a rate that strongly follows the increase in global greenhouse gases (Figure 4.2.4). Tabulated warming for various time slices and RCPs is given in Table 1 (Appendix). For 2030, the projected warming is 0.6 to 1.5 °C (North), 0.6 to 1.3 °C (South), and 0.6 to 1.4 °C (all) for the 10th and 90th percentile, with only minor differences between the emission scenarios. The projected temperature range for 2090 shows larger differences with 1.5 to 3.1 °C (North), 1.3 to 2.6 °C (South) and 1.5 to 2.9 °C (all) for RCP4.5; and 3.1 to 5.6 °C (North), 2.8 to 5.1 °C (South), and 2.9 to 5.3 °C (all), for RCP8.5.

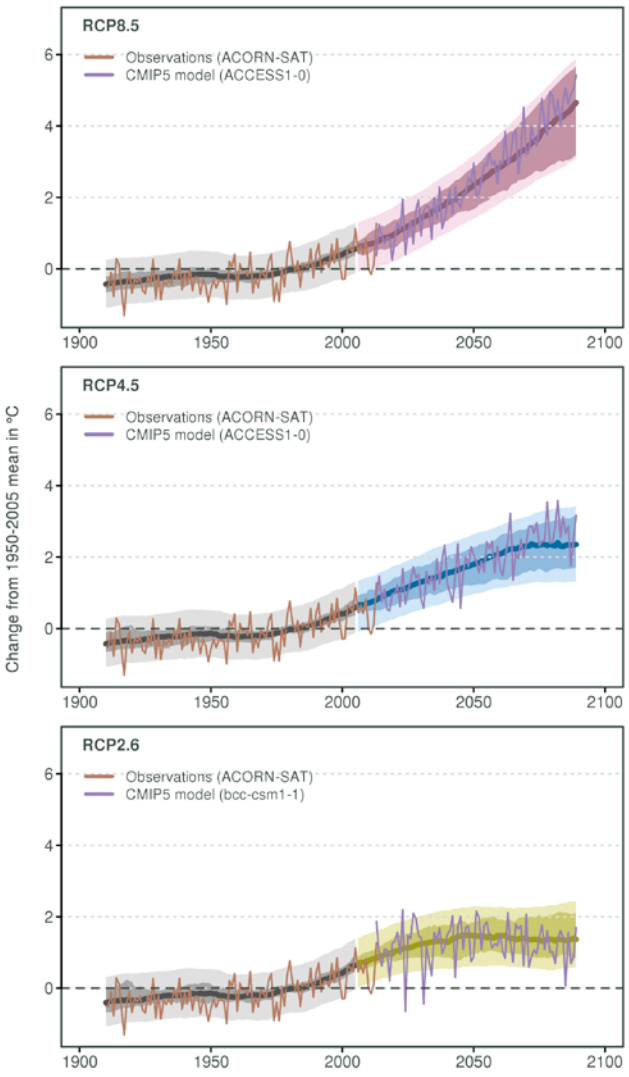

FIGURE 4.2.4: TIME SERIES FOR RANGELANDS MEAN ANNUAL AVERAGE SURFACE AIR TEMPERATURE (°C) FOR 1910–2090, AS SIMULATED IN CMIP5 RELATIVE TO THE 1950–2005 MEAN. THE CENTRAL LINE IS THE MEDIAN VALUE, AND THE SHADING IS THE 10TH AND 90TH PERCENTILE RANGE OF 20-YEAR MEANS (INNER) AND SINGLE YEAR VALUES (OUTER). THE GREY SHADING INDICATES THE PERIOD OF THE HISTORICAL SIMULATION, WHILE THREE FUTURE SCENARIOS ARE SHOWN WITH COLOUR-CODED SHADING: RCP8.5 (PURPLE), RCP4.5 (BLUE) AND RCP2.6 (GREEN). ACORN-SAT OBSERVATIONS AND PROJECTED VALUES FROM A TYPICAL MODEL ARE SHOWN. TIME SERIES PLOTS ARE EXPLAINED IN BOX 4.2.

These warmings are large compared to natural year to year variability in the cluster. For example, cold years become warmer than current warm years by 2050 under RCP8.5, and warmer than most current warm years under RCP4.5 (relative to 1986-2005). This is illustrated in Figure 4.2.4 by overlaying the simulated year to year variability in one simulation and comparing this to the historical variability. This comparison also illustrates that individual model runs produce temporal variability similar to that of observed temperature, as well as a warming trend (*i.e.* the overlaid observational time series stays largely within the lightly shadowed band representing the 10th and 90th year to year variability of the model ensemble). Overall there is good agreement between model and observed data on decadal scales.

Maps of warming (Technical Report, Figure 7.1.4) show that on average the north-western Rangelands has the largest change over the continent, while the southern coast warms less. Changes to the spatial pattern of temperature in the cluster can be illustrated by applying the projected change in annual mean temperature to the observed climatology. Figure 4.2.5 gives an example of this for the 2090 period following the high emission scenario RCP8.5 and the median warming. Contours of temperature move southwards, with the 27 °C contour moving from the far north to pass through the centre, while the 21 °C contour moves close to the south coast.

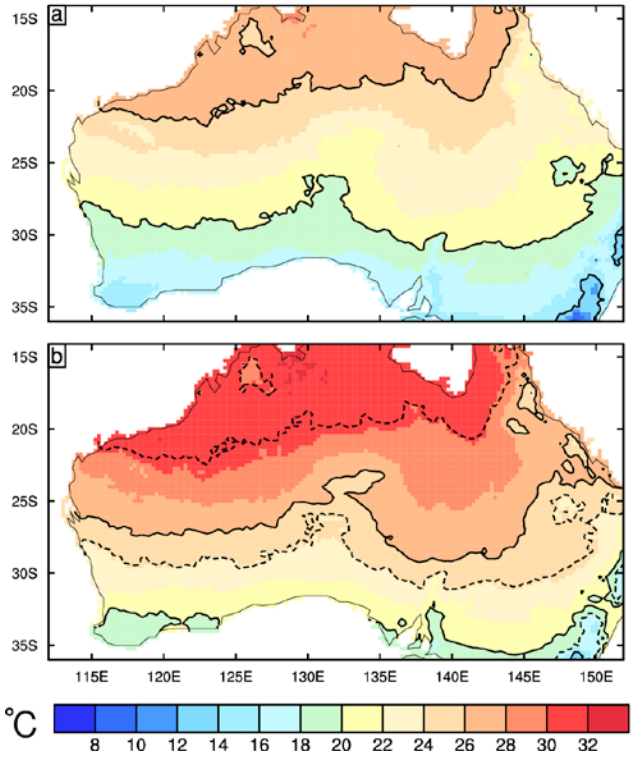

FIGURE 4.2.5: ANNUAL MEAN SURFACE AIR TEMPERATURE (°C), FOR THE PRESENT CLIMATE (A), AND FOR MEDIAN WARMING UNDER RCP8.5 2090 (B). THE PRESENT IS USING THE AWAP DATA SET FOR 1986–2005 (BASED ON A 0.25 DEGREE GRID). FOR CLARITY, THE 14, 20, AND 26 °C CONTOURS ARE SHOWN WITH SOLID BLACK LINES. IN (B) THE SAME CONTOURS FROM THE ORIGINAL CLIMATE ARE PLOTTED AS DOTTED LINES.

Projected warming in the CMIP5 models is similar across the four seasons in Rangelands, and is also broadly similar if daily maximum or minimum temperatures are considered rather than mean temperatures (Figure 4.2.6 and Table 1 in the Appendix). In winter and spring the median warming in daily maximum temperature tends to be larger than the warming in daily minimum temperature, which may be linked to the rainfall and cloudiness changes discussed in Section 4.3.

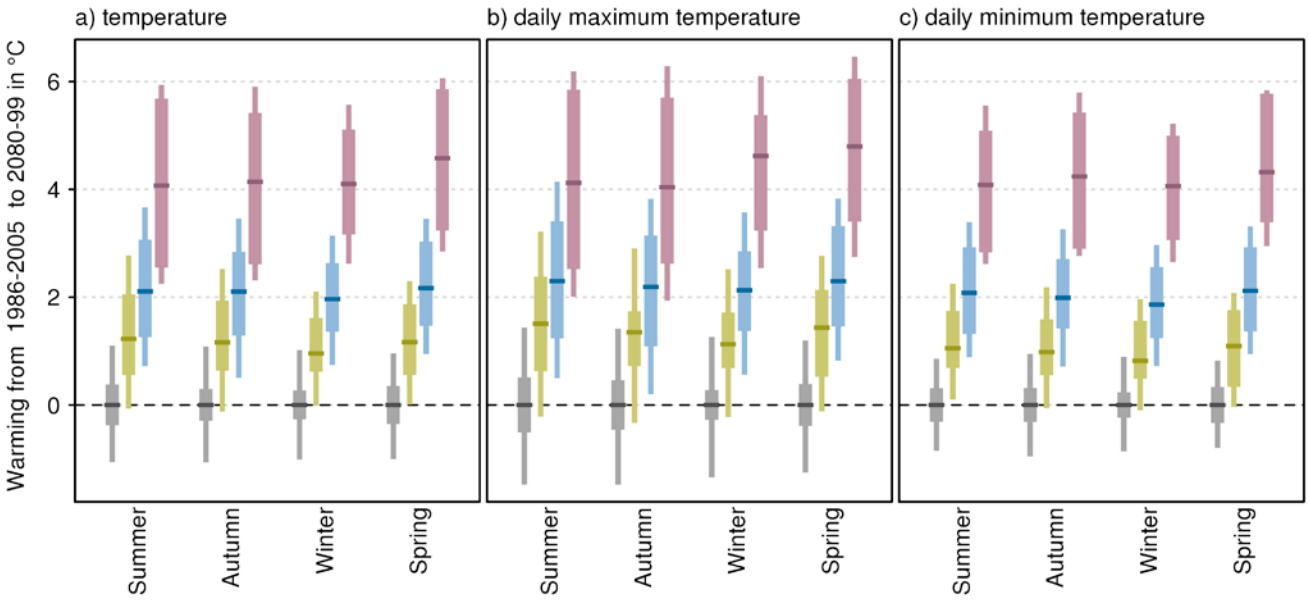

FIGURE 4.2.6: PROJECTED SEASONAL SURFACE AIR TEMPERATURE CHANGES FOR 2090. GRAPHS SHOW CHANGES TO THE: (A) MEAN, (B) DAILY MAXIMUM AND (C) DAILY MINIMUM TEMPERATURE. TEMPERATURE ANOMALIES ARE GIVEN IN °C RELATIVE TO THE 1986–2005 MEAN UNDER RCP2.6 (GREEN), RCP4.5 (BLUE) AND RCP8.5 (PURPLE). NATURAL CLIMATE VARIABILITY IS REPRESENTED BY THE GREY BAR. BAR PLOTS ARE EXPLAINED IN BOX 4.2.

Looking at downscaling results for the cluster, no significantly different trends are seen for either the dynamical or statistical downscaling method, with a strong overlap in model ensemble spread for each season.

Taking into consideration the strong agreement on direction and magnitude of change amongst GCMs and downscaling results, and the robust understanding of the driving mechanisms of warming and its seasonal variation, there is *very high confidence* in a substantial warming for the Rangelands cluster.

4.2.1 EXTREMES

Changes to temperature extremes often lead to greater impacts than changes to the mean climate. To assess these, researchers examine CMIP5 projected changes in measures such as the warmest day of the year, warm spell duration and frost risk days (see definitions below).

Heat related extremes are projected to increase at the same rate as projected mean temperature with a substantial increase in the number of warm spell days. Figure 4.2.8 gives the CMIP5 model simulated warming on the hottest day of the year averaged across the cluster for 2090, and the corresponding warming for the hottest day in 20 years (20-year return value, equal to a 5 % chance of occurrence within any one year). The rate of warming for these hot days is similar to that for all days (*i.e.* the average warming in the previous section). There is a marked increase in the warm spell index, which is defined as the annual count of days for events with at least six consecutive days with a cluster average temperature maximum above the 90th percentile (*e.g.* the 90th percentile for daily temperature maximum in Alice Springs is 37.3 °C based on historical records for January 1910 to June 2014).

Given the similarity in projected warming for the mean and hottest maximum temperature, an indication of the change in frequency of hot days locally can be obtained by applying the projected changes for maxima for selected time slices and RCPs to the historical daily record at selected sites. This is illustrated in Box 4.3 for Alice Springs, where it can be seen that by 2090 the number of days above 35 °C could increase by around 50 % under RCP4.5 and median model warming, and the number of days over 40 °C triples.

Changes in the frequency of surface frost (defined here as days when the two metre minimum temperature is less than 2 °C) are also of importance to the environment, agriculture, energy demand and other sectors. Assessing frost occurrence directly from global model output is not reliable, in part because of varying biases in land surface temperatures. However, it is possible to evaluate what CMIP5 models project about changes to frost occurrences by superimposing the projected change in temperature onto the minimal daily temperature record. Statistical downscaling may also be used, with similar results (see Technical Report section 7.1).

Box 4.3 illustrates the change in frost days using this simple approach (as was done for hot days). Note that the actual occurrence of frost will depend on many local factors not represented by this method. Results show that for Alice Springs by 2030 under RCP2.6, there is only a minor reduction in frost days. For 2090, however, substantial reductions occur in frost days under RCP4.5 and RCP8.5.

Strong model agreement and understanding of physical mechanisms of warming lead to *very high confidence* in a substantial increase in temperature of the hottest days, the frequency of hot days, and warm spell duration; and to *high confidence* in a substantial decrease in the frequency of frost.

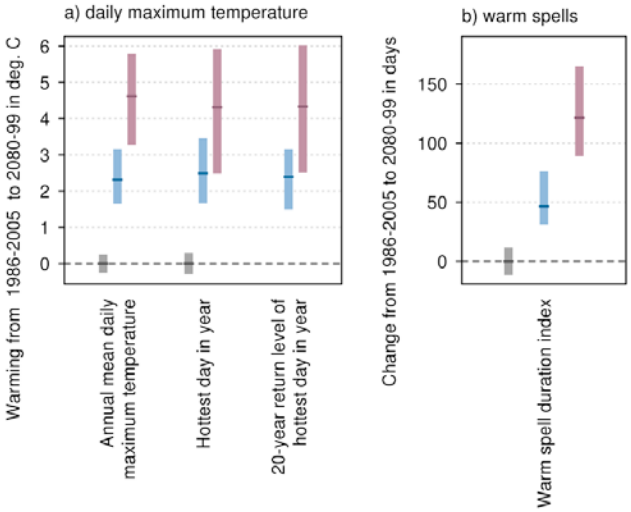

FIGURE 4.2.7: PROJECTED CHANGES IN SURFACE AIR TEMPERATURE EXTREMES BY 2090 IN (A) MEAN DAILY MAXIMUM TEMPERATURE, HOTTEST DAY OF THE YEAR AND THE 20-YEAR RETURN VALUE OF THE HOTTEST DAY OF THE YEAR (°C); AND (B) CHANGE IN THE NUMBER OF DAYS IN WARM SPELLS FOR RANGELANDS (SEE TEXT FOR DEFINITION OF VARIABLES). RESULTS ARE SHOWN FOR RCP4.5 (BLUE) AND RCP8.5 (PURPLE) RELATIVE TO THE 1986–2005 MEAN. NATURAL VARIABILITY IS REPRESENTED BY THE GREY BAR. BAR PLOTS ARE EXPLAINED IN BOX 4.2.

BOX 4.3: HOW WILL THE FREQUENCY OF HOT DAYS AND FROST RISK DAYS CHANGE IN ALICE SPRINGS?

To illustrate what CMIP5 projected warming implies for change to the occurrence of hot days and frost days at a station in Rangelands, we have conducted a simple downscaling example, whereby we add the projected change in temperature to an observed time series for Alice Springs.

The type of downscaling used here is commonly referred to as the 'change factor approach' (see Section 6.3.1. in the Technical Report), whereby a change (calculated from the simulated model change) is applied to an observed time series. In doing so, it is possible to estimate the frequency of extreme days under different emission scenarios.

In Table B4.3, days with maximum temperature above 35 and 40 °C, and frost risk days (minimum temperature less than 2 °C) are provided for a number of locations for a 30-year period (1981–2010), and for downscaled data using seasonal change factors for maximum or minimum temperature for 2030 and 2090 under different RCPs.

TABLE B4.3: CURRENT AVERAGE ANNUAL NUMBER OF DAYS (FOR THE 30-YEAR PERIOD 1981–2010) ABOVE 35 AND 40 °C AND BELOW 2 °C (FROSTS) FOR ALICE SPRINGS AIRPORT (NT) BASED ON ACORN-SAT. ESTIMATES FOR THE FUTURE ARE CALCULATED USING THE MEDIAN CMIP5 WARMING FOR 2030 AND 2090, AND WITHIN BRACKETS THE 10TH AND 90TH PERCENTILE CMIP5 WARMING FOR THESE PERIODS, APPLIED TO THE 30-YEAR ACORN-SAT STATION SERIES. NUMBERS ARE TAKEN FROM TABLE 7.1.2 AND TABLE 7.1.3 IN THE TECHNICAL REPORT.

THRESHOLD (°C)	1995	2030 RCP4.5	2090 RCP2.6	2090 RCP4.5	2090 RCP8.5
Over 35 °C	94	113 (104 to 122)	119 (104 to 132)	133 (115 to 152)	168 (145 to 193)
Over 40 °C	17	31 (24 to 40)	37 (24 to 51)	49 (33 to 70)	83 (58 to 114)
Below 2 °C	33	24 (28 to 19)	24 (30 to 17)	13 (20 to 8.4)	2.1 (6.0 to 0.8)

4.3 RAINFALL

Historical rainfall anomalies (relative to a 1986–2005 baseline average) show a slight increasing trend in averages over both North and South Rangelands (Figure 4.3.1), although with intermittent periods of wetter and drier conditions throughout the 20th century. 2011 was the wettest on record in the South sub-cluster. Naturally, variations for locations within the sub-clusters may be very different.

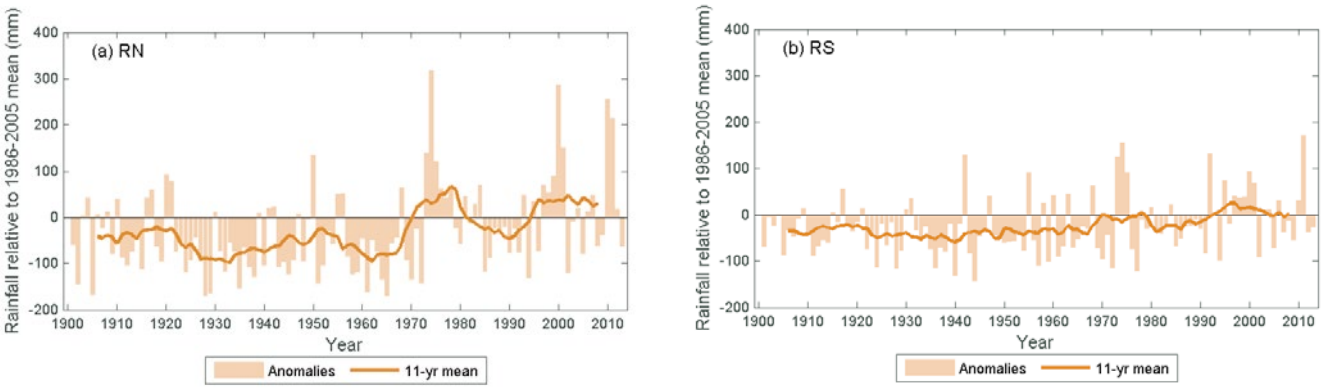

FIGURE 4.3.1: OBSERVED ANNUAL RAINFALL ANOMALIES (MM) FOR 1901–2013 COMPARED TO THE BASELINE1986–2005 FOR RANGELANDS (A) NORTH, (B) SOUTH. DATA IS FROM AWAP.

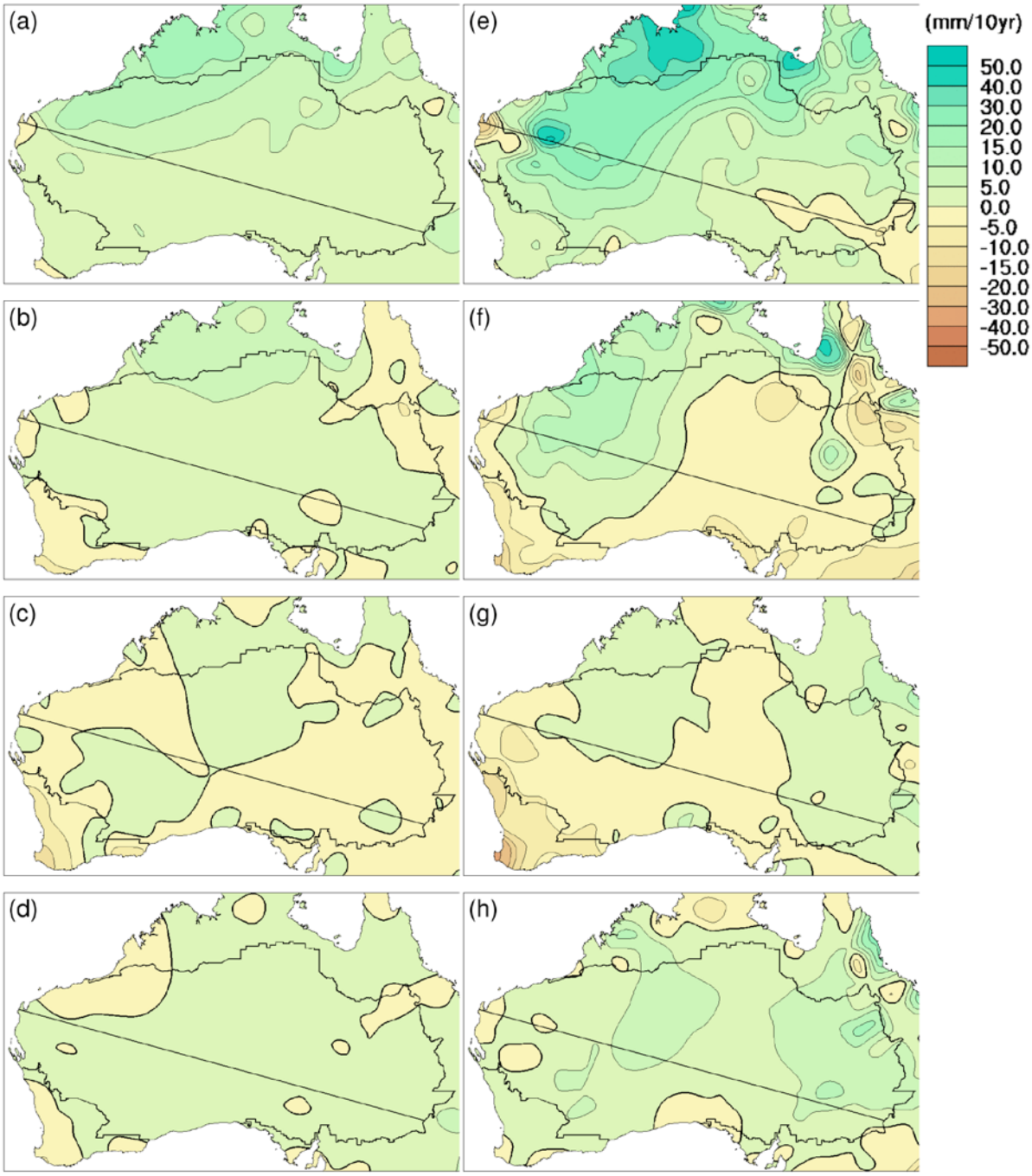

FIGURE 4.3.2: MAPS OF SEASONAL RAINFALL TRENDS (MM/DECADE). THE LEFT COLUMN OF MAPS SHOWS TRENDS FOR (A) SUMMER, (B) AUTUMN, (C) WINTER AND (D) SPRING FOR 1901–2013. THE RIGHT COLUMN SHOWS TRENDS FOR (E) SUMMER, (F) AUTUMN, (G) WINTER AND (H) SPRING FOR 1960–2012.

The increase has been largest in magnitude in the north-west and in summer, as seen in Figure 4.3.2. Most of the south experienced small decreases in autumn and winter. On average, the CMIP5 ensemble produced smaller changes for past decades. The summer increase in the north is not matched by most models.

The projected rainfall changes are unclear (Figure 4.3.3). The median change for both North and South by 2090, under high emissions, is a decrease of 4 % (Table 1 in the Appendix).

Overall, the inter-model range appears similar to the natural decadal variability of the past century. As an example of inter-annual variability in the climate models, for the coming century an individual model simulation is overlaid on the multi-model envelope.

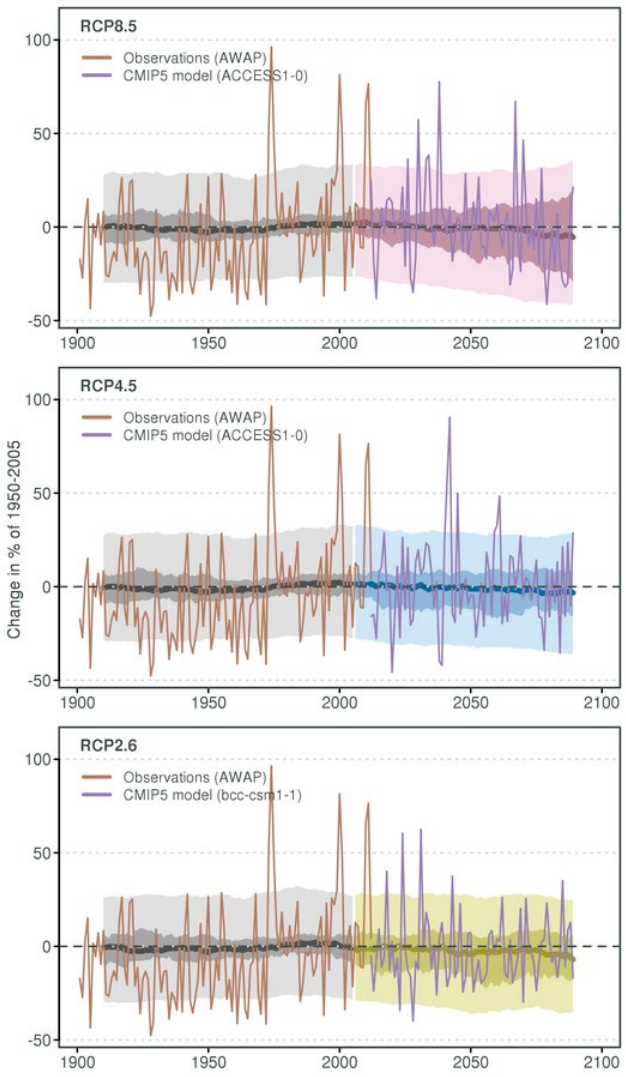

FIGURE 4.3.3: TIME SERIES FOR RANGELANDS ANNUAL RAINFALL FOR 1910–2090, AS SIMULATED IN CMIP5 EXPRESSED AS A PERCENTAGE RELATIVE TO THE 1950–2005 MEAN. THE CENTRAL LINE IS THE MEDIAN VALUE, AND THE SHADING IS THE 10TH AND 90TH PERCENTILE RANGE OF 20-YEAR MEANS (INNER) AND SINGLE YEAR VALUES (OUTER). THE GREY SHADING INDICATES THE PERIOD OF THE HISTORICAL SIMULATION, WHILE THREE FUTURE SCENARIOS ARE SHOWN WITH COLOUR-CODED SHADING: RCP8.5 (PURPLE), RCP4.5 (BLUE) AND RCP2.6 (GREEN). AWAP OBSERVATIONS (BEGINNING 1901) AND PROJECTED VALUES FROM A TYPICAL MODEL ARE SHOWN. TIME SERIES PLOTS ARE EXPLAINED IN BOX 4.2.

The mixed response from models in the direction of annual projections is also evident when looking at seasonal projections (Figure 4.3.4). Decreases in winter rainfall are projected for the South with *high confidence* by 2090. There is strong model agreement and good understanding of the physical mechanisms driving this change, namely a southward shift of winter storm systems and rising mean pressure over the region. The magnitude of the change in winter for South from the climate of 1986–2005 ranges from around −20 to +10 % for 2030 and −45 to 0 % for 2090 under RCP8.5. Decreases are also projected for spring, but with *medium confidence* only. The range by 2090 under RCP8.5 is −55 to +25 % for the North, and −55 to +20 % for the South.

Changes in summer and autumn have been more strongly linked to the large-scale pattern of tropical sea surface temperature, which varies considerably among the models. The median changes in these seasons are small in percentage terms (Table 1, Appendix), as are the annual changes. Such contrasts highlight the need to consider the risk of both a drier and wetter climate in regional impact assessments. These projections are not greatly modified by the available downscaling, although the changes in summer simulated by the dynamical downscaling tend to wetter conditions.

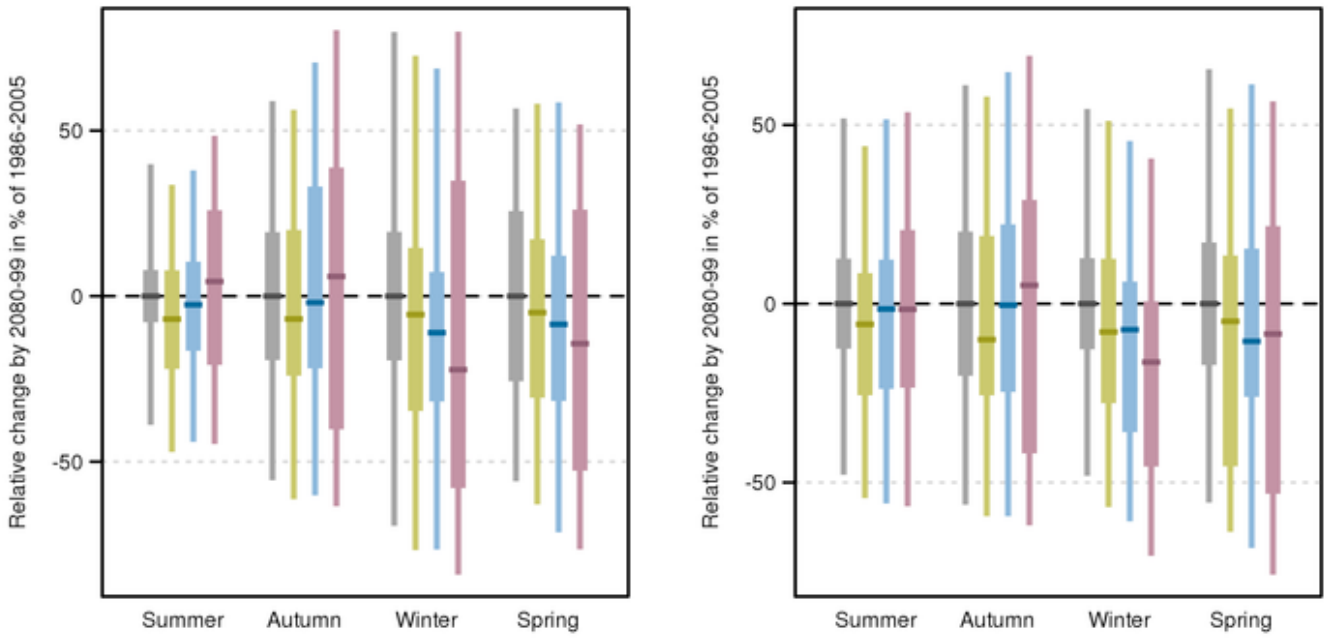

FIGURE 4.3.4: PROJECTED SEASONAL RAINFALL CHANGES FOR THE RANGELANDS SUB-CLUSTERS (A) NORTH AND (B) SOUTH FOR 2090. RAINFALL ANOMALIES ARE GIVEN IN PER CENT WITH RESPECT TO THE 1986–2005 MEAN UNDER RCP2.6 (GREEN), RCP4.5 (BLUE) AND RCP8.5 (PURPLE). NATURAL VARIABILITY IS REPRESENTED BY THE GREY BAR. BAR PLOTS ARE EXPLAINED IN BOX 4.2.

Changes to the spatial distribution of rainfall in the cluster can be illustrated by applying the CMIP5 projected change in annual mean rainfall onto the observed climatology. Figure 4.3.5 gives an example of this for 2090 following the high emission scenario RCP8.5 and the rainfall change from the CMIP5 models. The figure displays the dry (10th percentile) and wet (90th percentile) case of the simulated model range relative to the observed climatology. The drier case can be seen as an expansion of the more arid region centred on the Lake Eyre basin, while the wetter case features a contraction, with the 0.5 mm/day contour disappearing. However, depending on the strength of the individual drivers, the actual change pattern may be less coherent. The comparison of contours in Figures 4.2.5 and 4.3.5 provides some indication of analogues of future climate from the present for a single variable.

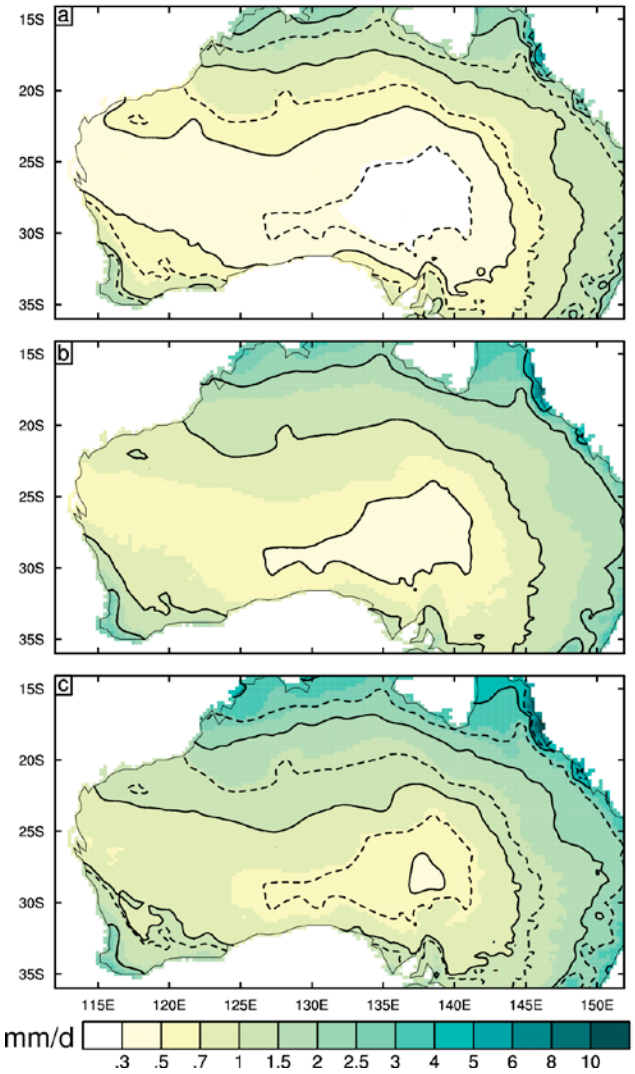

Figure 2.3(c) (in Section 2) shows the percentage projected change in rainfall in the warmer six months (November to April) by 2090 for RCP8.5. The tendency for a decline in cooler season rainfall leads to an increase in this percentage, and hence a southward shift in the contour lines. The larger increases, in the far south, east and west of the Rangelands, are seen where typically 80 % of models simulate an increase.

In summary, there is *high confidence* that natural climate variability will remain the major driver of rainfall changes by 2030 in this cluster (annual mean changes of about ± 10 %, and seasonal mean changes of ±20 % relative to the climate of 1986–2005). Decreases in winter rainfall in the South are projected to become evident by 2090 with *high confidence*. There is strong model agreement and good understanding of the contributing underlying physical mechanisms driving this change. Decreases are also indicated for spring rainfall with *medium confidence* in both North and South. Changes to rainfall in other seasons by 2090 are possible, but the direction of change cannot be reliably projected.

FIGURE 4.3.5: ANNUAL MEAN RAINFALL (MM/DAY), FOR THE PRESENT CLIMATE (B), AND DRIER END OF THE PROJECTED MODEL RANGE (A) AND WETTER END OF THE PROJECTED RANGE (C). THE PRESENT IS USING THE AWAP DATA SET FOR 1986–2005 (BASED ON A 0.25 DEGREE LONGITUDE-LATITUDE GRID). THE DRIER AND WETTER CASES USE THE 10TH AND 90TH PERCENTILE CHANGES AT 2090 UNDER RCP8.5. FOR CLARITY THE 0.5, 1, 2 AND 4 MM/DAY CONTOURS ARE PLOTTED WITH SOLID BLACK LINES. IN (A) AND (C) THE SAME CONTOURS FROM THE ORIGINAL CLIMATE (B) ARE PLOTTED AS DOTTED LINES.

4.3.1 HEAVY RAINFALL EVENTS

In a warming climate, heavy rainfall extremes are expected to increase in magnitude mainly due to a warmer atmosphere being able to hold more moisture (Sherwood *et al*., 2010).

Daily rainfall amounts from the CMIP5 simulations have been analysed and the maximum values determined in each year and within 20-year periods. For both Rangelands North and South, the models simulate an increase in the magnitude of the annual maximum 1-day rainfall and the magnitude of the 20-year return value of maximum 1-day rainfall by 2090 (Figure 4.3.6 for RCP8.5); where a 20-year return value is equivalent to a 5 % chance of occurrence within any one year. Comparing the trend in these two extreme indices with that of the annual mean rainfall (Figure 4.3.6) shows that while the projection for mean rainfall is tending towards a decrease in each sub-cluster, the extremes are projected to increase. For example, based on this median change for RCP8.5, the extreme daily rainfall amount at a location within a 20-year period by 2090 can be expected to be around 20 % larger than the extreme from a recent 20-year period. Actual values at individual locations may vary, of course. This pattern (change in mean relative to extremes) is found in all other NRM clusters, and is also supported by results from other studies (see Technical Report, section 7.2.2).

The magnitudes of the simulated changes in extreme rainfall indices are strongly dependent on emission scenario and time period. Furthermore, how changes simulated by GCMs manifest in terms of magnitude is less certain because smaller scale systems that generate extreme rainfall are not well resolved by GCMs (Fowler and Ekstroem, 2009). In summary, there is *high confidence* that the intensity of heavy rainfall extremes will increase in the cluster, but there is *low confidence* in the magnitude of change, and thus the time when any change may be evident against natural fluctuations cannot be reliably projected.

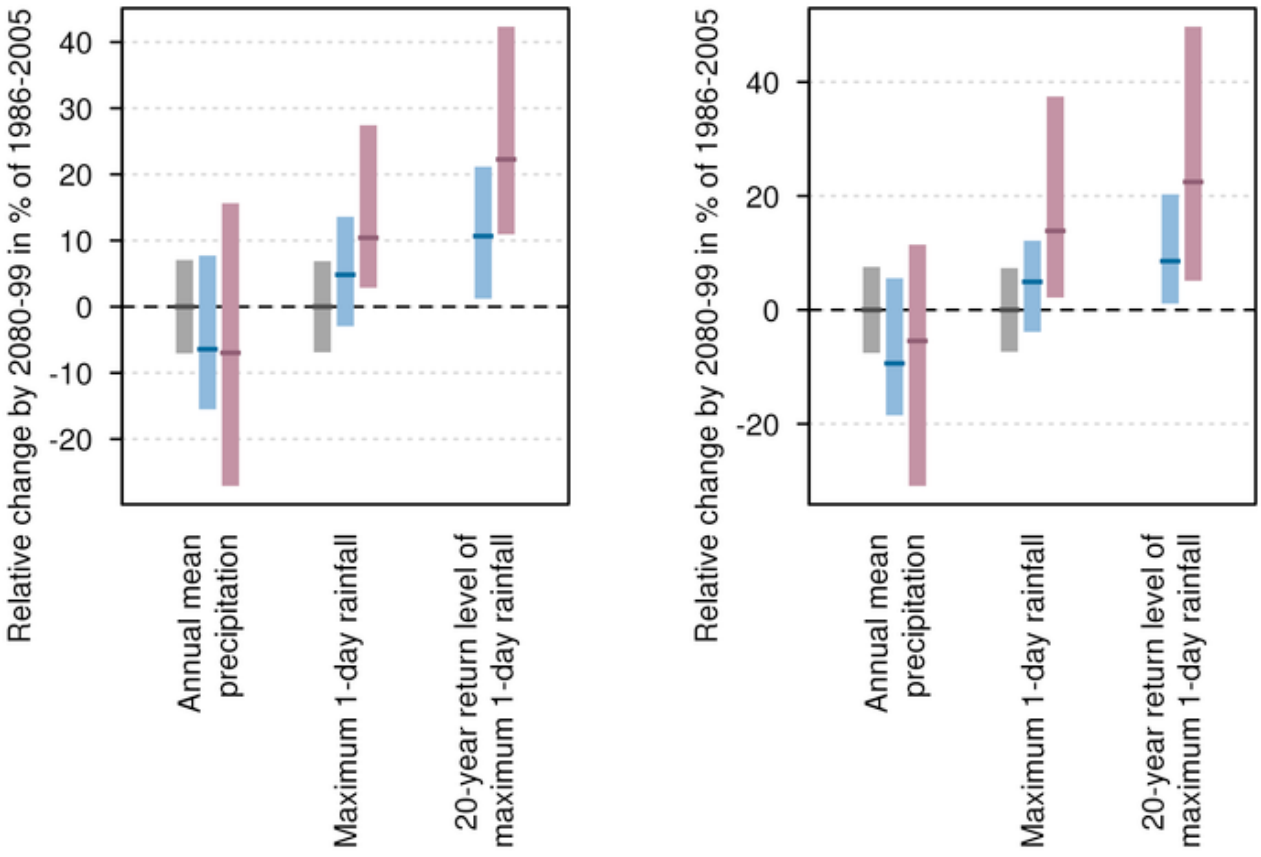

FIGURE 4.3.6: PROJECTED CHANGES IN MEAN RAINFALL, MAGNITUDE OF ANNUAL MAXIMUM 1-DAY RAINFALL AND MAGNITUDE OF THE 20-YEAR RETURN VALUE FOR THE 1-DAY RAINFALL FOR 2090 FOR RANGELANDS NORTH (LEFT) AND RANGELANDS SOUTH (RIGHT) (SEE TEXT FOR DEFINITION OF VARIABLES). CHANGES ARE GIVEN IN % WITH RESPECT TO THE 1986–2005 MEAN FOR RCP4.5 (BLUE) AND RCP8.5 (PURPLE). NATURAL CLIMATE VARIABILITY IS REPRESENTED BY THE GREY BAR. BAR PLOTS ARE EXPLAINED IN BOX 4.2.

4.3.2 DROUGHT

To assess the implications of projected climate change for drought occurrence, the Standardised Precipitation Index (SPI) was selected as a measure of meteorological drought. Duration of time spent in drought (events during which SPI falls below –1 at some time) and changes to the duration and frequency of droughts (by the number of distinct events during a 20-year period) were calculated for different levels of severity (mild, moderate, severe, and extreme). Section 7.2.3 in the Technical Report presents details on the calculation of the SPI, and further information on drought.

Projected changes to drought share much of the uncertainty of mean rainfall change, plus additional uncertainty regarding changes in rainfall variability (Figure 4.3.7). Under RCP8.5, there is an increase in the proportion of time spent in drought through the century. However the picture is less clear for RCP4.5. The 90th percentiles of the model range under RCP8.5 suggest that extreme drought will become more frequent in some models and the duration could increase. But other models (see 10th percentile) show change in the opposite direction.

Meteorological drought will continue to be a regular feature of regional climate. It may change its characteristics as the climate warms, but there is *low confidence* in projecting how the frequency and duration of extreme drought may change, although there is *medium confidence* that the time spent in drought will increase over the course of the century under RCP8.5.

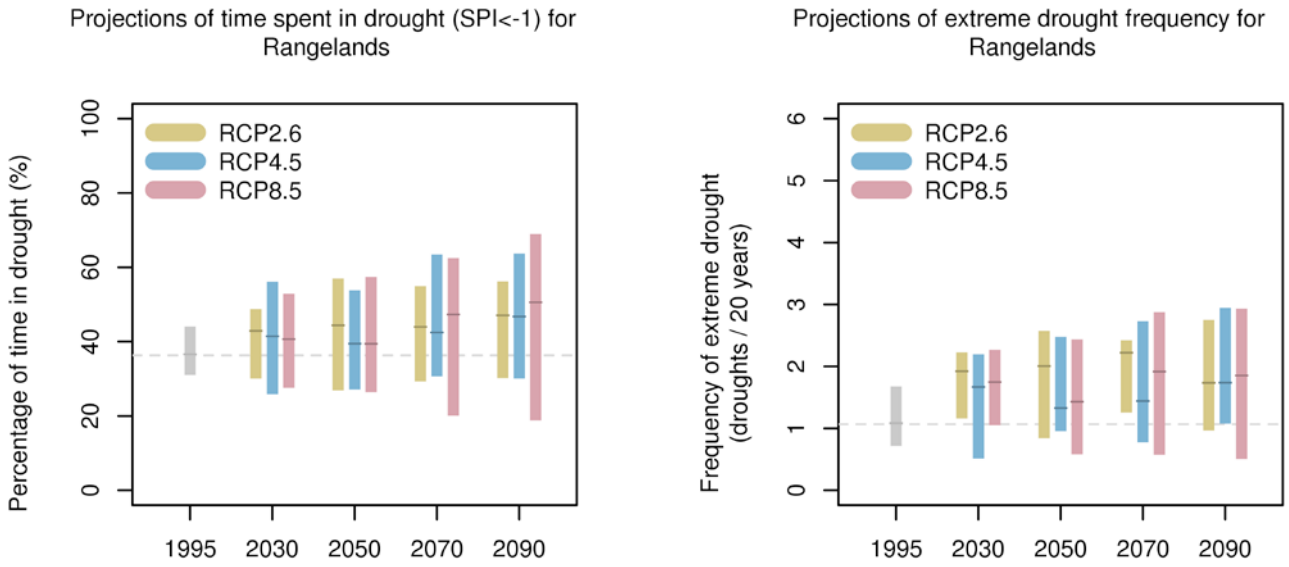

FIGURE 4.3.7: SIMULATED CHANGES IN DROUGHT BASED ON THE STANDARDISED PRECIPITATION INDEX (SPI). THE MULTI-MODEL ENSEMBLE RESULTS FOR RANGELANDS SHOW THE PERCENTAGE OF TIME IN DROUGHT (SPI LESS THAN -1) (LEFT) AND FREQUENCY OF EXTREME DROUGHT (RIGHT) FOR EACH 20-YEAR PERIOD CENTRED ON 1995, 2030, 2050, 2070 AND 2090 UNDER RCP2.6 (GREEN), RCP4.5 (BLUE) AND RCP8.5 (PURPLE). NATURAL CLIMATE VARIABILITY IS REPRESENTED BY THE GREY BAR. SEE TECHNICAL REPORT CHAPTER 7.2.3 FOR DEFINITION OF DROUGHT INDICES. BAR PLOTS ARE EXPLAINED IN BOX 4.2.

4.4 WINDS, STORMS AND WEATHER SYSTEMS

4.4.1 MEAN WINDS

The surface wind climate is driven by the large-scale circulation pattern of the atmosphere: when pressure gradients are strong, winds are strong. Just south of the tropics, where there is a high pressure belt to the south and low pressure near the equator, south-easterly 'trade winds' predominate. Over the Rangelands cluster, average surface winds are mostly south-easterly, being stronger in the South in summer, the North in winter, and the centre in the other seasons. In summer, monsoon winds can reach the northern part of the cluster, while westerlies encroach on the southern coast in winter (see Technical Report Section 7.3). Any trends in observed winds are difficult to establish due to sparse coverage of wind observations and difficulties with instruments and the changing circumstances of measurement sites (Jakob, 2010). McVicar *et al.*, (2012) and Troccoli *et al.*, (2012) have reported weak and conflicting trends across Australia (although they considered winds at different levels).

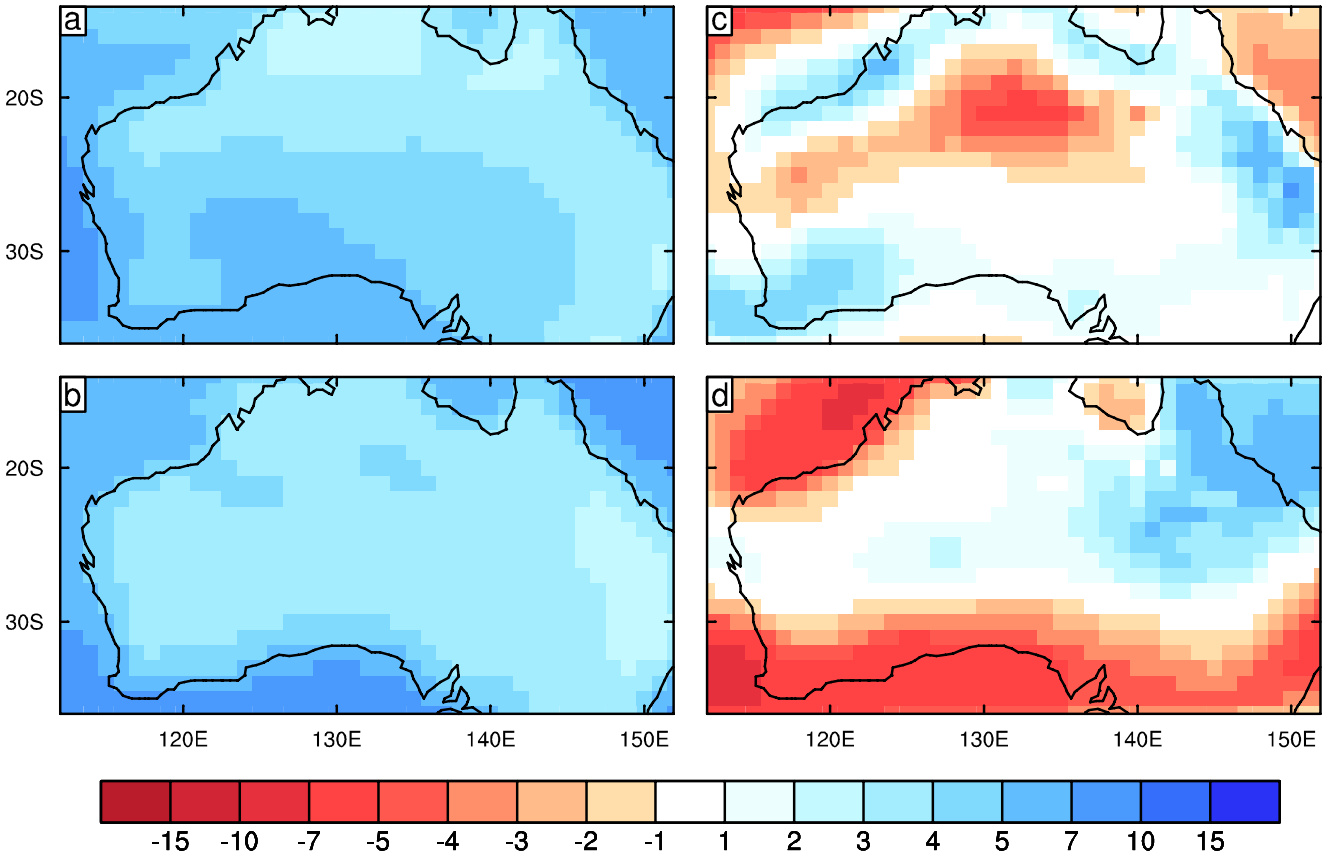

FIGURE 4.4.1: SEASONAL AVERAGES OF NEAR-SURFACE WIND SPEED FROM CMIP5 GCMS. MODEL ENSEMBLE MEAN OF SEASONAL AVERAGE WIND SPEED FOR 1986–2005 IN M/S FOR (A) SUMMER AND (B) WINTER. MEDIAN ESTIMATES OF CHANGE IN WIND SPEED FOR 2090 UNDER RCP8.5 ARE GIVEN AS A PERCENTAGE FOR (C) SUMMER, AND (D) WINTER.

The mean wind speed for summer and winter in the 1986–2005 climate simulated by the GCM ensemble (19 models) over Rangelands is shown in Figure 4.4.1. Mean speeds are between 3 m/s and 5 m/s, except for larger speeds in the far south (especially in summer). The changes for 2090 under high emissions are also shown. There are decreases of up to 10 % in the north in summer, and the far south in winter, associated with the southward shift of westerlies (Section 4.2). The Pilbara coast exhibits considerable spatial variation in the wind trends.

Changes averaged over Rangelands North and South are given in Figure 4.4.2 and Table 1 (in the Appendix). These indicate mostly small changes, in relative terms. However, larger changes (both increases and decreases) occur in some models. By 2090 under RCP8.5, the more consistent changes are decreases in the North in summer, and increases in the South in spring.

Taking into consideration the low model agreement, there is generally *low confidence* on direction of change for much of Rangelands, and generally *medium confidence* in change being small. Along the south coast, there is *medium confidence* in a decrease in winter. Due to limited understanding of physical mechanisms, we have *low confidence* in the increase in wind speeds in spring despite strong model agreement.

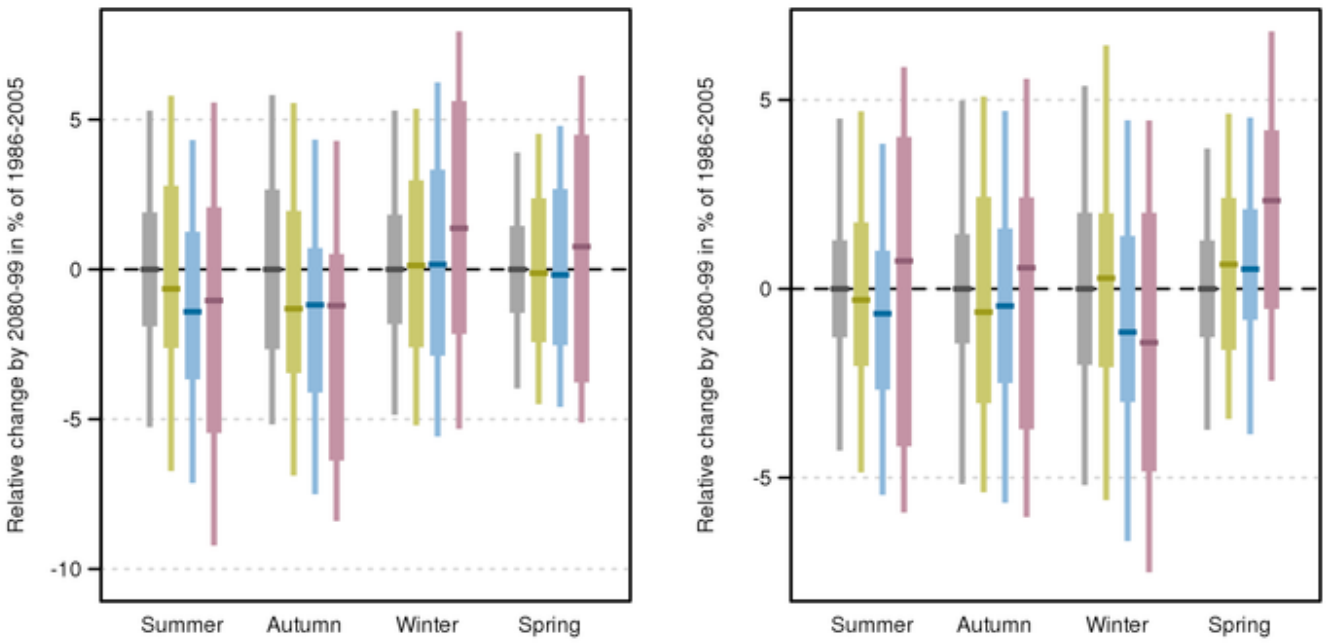

FIGURE 4.4.2: PROJECTED NEAR-SURFACE WIND SPEED CHANGES FOR 2090 FOR RANGELANDS NORTH (LEFT) AND RANGELANDS SOUTH (RIGHT). ANOMALIES ARE GIVEN IN % WITH RESPECT TO THE 1986–2005 MEAN FOR RCP2.6 (GREEN), RCP4.5 (BLUE) AND RCP8.5 (PURPLE) WITH GREY BARS SHOWING THE EXTENT OF NATURAL CLIMATE VARIABILITY. BAR PLOTS ARE EXPLAINED IN BOX 4.2.

An evaluation of maximum daily wind speeds has been made from available CMIP5 models, similar to that for temperature presented in Figure 4.2.7. Averaged over both South and North, changes are comparable to those for seasonal means of wind speed, with small changes of either direction, but median changes that are near-zero. However, global models do not resolve the more intense winds on smaller scales, in particular from tornados. There is *low confidence* in the projection of small change in extreme winds over Rangelands.

4.4.2 TROPICAL AND EXTRA-TROPICAL CYCLONES

Tropical cyclones in the eastern Indian Ocean can directly impact the Pilbara coast of the Rangelands cluster and bring rain to central Western Australia. Cyclones crossing the northern Australian and Queensland coast can lead to heavy rain events that impact most of subtropical Rangelands, in particular the Lake Eyre basin. Projected changes of tropical cyclone frequency have been assessed in the CMIP5 GCMs over the Australian north-east and north-west regions, from both the large-scale environmental conditions that promote cyclones and from direct simulation of cyclone-like synoptic features (see Section 7.4.3 of the Technical Report). Results in both the northeast and northwest regions generally indicate a decrease in the formation of tropical cyclones. These results are broadly consistent with current projections of cyclones over the globe (IPCC, 2013; Section 14.6.1), which indicate little change through to substantial decrease in frequency. It is also anticipated that the proportion of the most intense storms will increase over the century while the intensity of associated rainfall may increase further, as can be anticipated from section 4.3.1 here. In summary, based on global and regional studies, tropical cyclones are projected with *medium confidence* to become less frequent, with increases in the proportion of the most intense storms.

With regard to extra-tropical cyclones along the southern coast, studies in the literature suggest a continuation of the observed decreasing trend of storm systems and fronts and associated rainfall in winter. This relates to the southward shifts in the westerlies noted above.

4.5 SOLAR RADIATION

Changes in incoming solar radiation are caused foremost by changes to cloud cover or changes to the presence of suspended particles (aerosols) in the atmosphere. Solar radiation may also decrease due to thermally driven increases of water vapour in the atmosphere. Thus the changes vary spatially, and with scenario and GCM, although they are mostly small relative to the large baseline for radiation over Rangelands.

Projected changes to solar radiation relative to the 1986–2005 base period are summarised for two time periods and two emission levels and both North and South Rangelands in Table 1 (in the Appendix). Changes for Rangelands by 2090 are shown in Figure 4.7.1a. The most consistent trend is found in winter, with an increase in radiation projected in each scenario, particularly in the South, with a median value for 2090 under RCP8.5 of 6.5 % (Table 1, Appendix). There are similar decreases in summer and autumn – stronger in the North – but these emerge only under high emissions. The projected increase in winter may be explained by an overall decrease in cloud cover associated with declining rainfall. However, in all cases there is considerable uncertainty, as expected from the range of rainfall changes across the GCMs.

Some models are unable to adequately reproduce the climatology of solar radiation (Watterson *et al.*, 2013). Globally, CMIP3 and CMIP5 models appear to underestimate the observed trends in some regions due to underestimation of aerosol direct radiative forcing and/or deficient aerosol emission inventories (Allen *et al.*, 2013). Taking this into account, there is *high confidence* in little change for 2030. By 2090, there is *medium confidence* in increased winter radiation in South, and *low confidence* in little change in the other seasons.

4.6 RELATIVE HUMIDITY

Projected changes in relative humidity are summarised in Table 1 in the Appendix and results for 2090 are shown in Figure 4.7.1b. These are expressed in the usual unit of percentage of saturation. A decrease in relative humidity away from the coasts is expected because an increase in moisture holding capacity of a warming atmosphere, and the greater warming of land compared to sea, leads to increases in relative humidity over ocean and decreases over continents. This general tendency to decrease relative humidity over land can be counteracted by a strong rainfall increase. CMIP5 models indeed project a decrease in relative humidity, with similar changes in both Rangelands North and South. Projected reductions are more marked in winter and spring (about –5 to 0 % under RCP4.5 and –10 to 0 % under RCP8.5 for 2090, Table 1 in the Appendix). There are, however, models that simulate increases in relative humidity, as demonstrated by some positive 90th percentile values, particularly in autumn. In summary, there is *medium confidence* in little change in relative humidity for 2030. By 2090, for summer and autumn, there is *medium confidence* in a decrease, while for winter and spring there is *high confidence* in a decrease.

4.7 POTENTIAL EVAPOTRANSPIRATION

Projected changes for potential evapotranspiration using Morton's wet-environmental potential evapotranspiration (McMahon *et al.*, 2013) and Technical Report section 7.6 suggest increases for all seasons in the Rangelands (Figure 4.7.1c). There is not much difference in the increase amongst the four seasons. In absolute terms, changes are largest in summer, particularly for RCP8.5 (values given in Table 1 in the Appendix).

Overall, models generally show high agreement by 2030 or very high agreement by 2090 on substantial increase in evapotranspiration. Despite having *high confidence* in an increase, there is only *medium confidence* in the magnitude of the increase. The method is able to reproduce the spatial pattern and the annual cycle of the observed climatology and there is theoretical understanding around increases as a response to increasing temperatures and an intensified hydrological cycle (Huntington, 2006), which adds to confidence. However, there has been no clear increase in observed Pan Evaporation across Australia in data available since 1970 (see Technical Report, Chapter 4). Also, earlier GCMs were not able to reproduce the historical linear trends found in Morton's potential evapotranspiration (Kirono and Kent 2011).

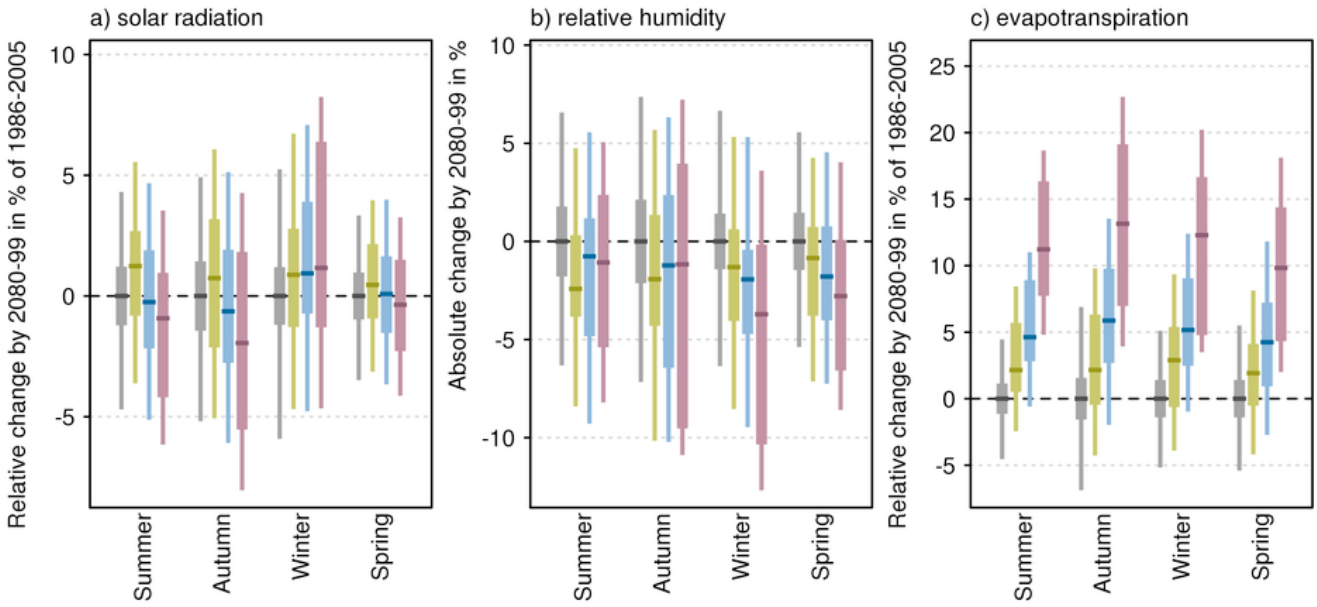

FIGURE 4.7.1: PROJECTED CHANGES IN (A) SOLAR RADIATION (%), (B) RELATIVE HUMIDITY (%, ABSOLUTE CHANGE) AND (C) WET-ENVIRONMENTAL POTENTIAL EVAPOTRANSPIRATION (%) FOR RANGELANDS IN 2090. THE BAR PLOTS SHOW SEASONAL PROJECTIONS WITH RESPECT TO THE 1986–2005 MEAN FOR RCP2.6 (GREEN), RCP4.5 (BLUE) AND RCP8.5 (PURPLE), AND THE EXTENT OF NATURAL CLIMATE VARIABILITY IS SHOWN IN GREY. BAR CHARTS ARE EXPLAINED IN BOX 4.2.

4.8 SOIL MOISTURE AND RUNOFF

Increases in potential evapotranspiration rates (Figure 4.7.1c) combined with (less certain) changes in rainfall (Figure 4.3.4) will have implications for soil moisture and runoff. However, soil moisture and runoff are difficult to simulate. This is particularly true in GCMs where, due to their relatively coarse resolution, the models cannot simulate much of the rainfall detail that is important to many hydrological processes, such as the intensity of rainfall. For these reasons, and in line with many previous studies, we do not present runoff and soil moisture as directly-simulated by the GCMs. Instead, the results of hydrological models forced by CMIP5 simulated rainfall and potential evapotranspiration are presented. Soil moisture is estimated using a dynamic hydrological model based on an extension of the Budyko framework (Zhang *et al.*, 2008), and runoff is estimated by the long-term annual water and energy balance using the Budyko framework (Teng *et al.*, 2012). Runoff is presented as change in 20-year averages, derived from output of a water balance model. The latter uses input from CMIP5 models as smoothed time series (30-year running means), the reason being that 30 years is the minimum required for dynamic water balance to attain equilibrium using the Budyko framework. For further details on methods (including limitations) see Section 7.7 of the Technical Report.

Decreases in soil moisture are projected, particularly in winter (Figure 4.8.1), when changes for RCP8.5 by 2090 range from –7 to +1 % in North, and –11 to –1 % in the South with medium model agreement on substantial decrease (Table 1 in the Appendix). The percentage changes in soil moisture are strongly influenced by those in rainfall, but tend to be more negative due to the strong increase in potential evapotranspiration. However, these estimates are based only on large-scale considerations. Given the potential limitations of this method, there is only *medium confidence* that soil moisture will decline in winter.

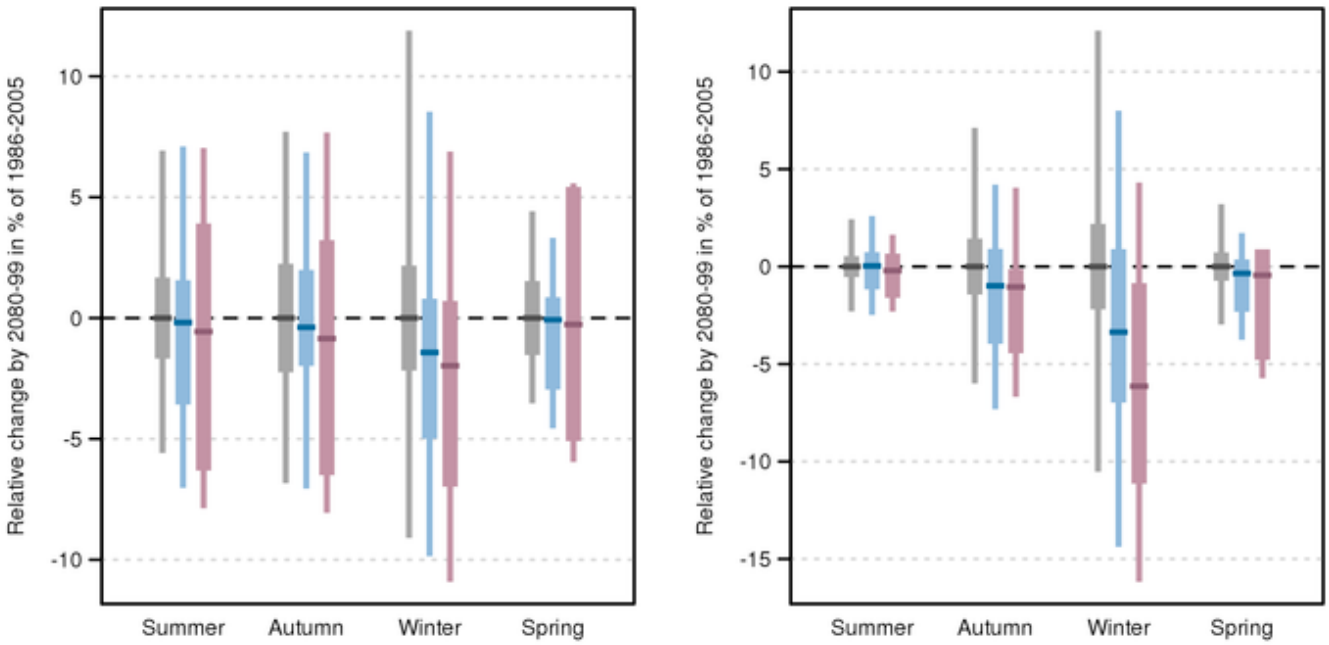

FIGURE 4.8.1: PROJECTED CHANGE IN SEASONAL SOIL MOISTURE (BUDYKO METHOD – SEE TEXT) IN RANGELANDS NORTH (LEFT) AND RANGELANDS SOUTH (RIGHT) FOR 2090. ANOMALIES ARE GIVEN IN % WITH RESPECT TO THE 1986–2005 MEAN FOR RCP4.5 (BLUE) AND RCP8.5 (PURPLE) WITH GREY BARS SHOWING THE EXTENT OF NATURAL VARIABILITY. BAR CHARTS ARE EXPLAINED IN BOX 4.2.

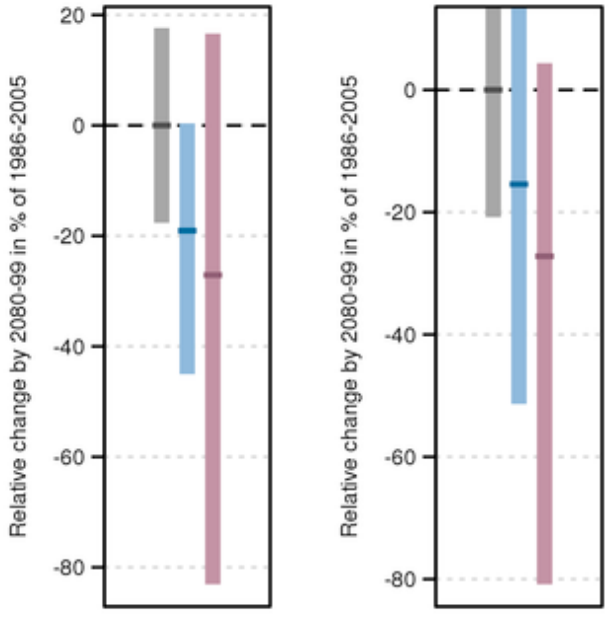

FIGURE 4.8.2: PROJECTED CHANGE IN RUNOFF (BUDYKO METHOD – SEE TEXT) IN RANGELANDS NORTH (LEFT) AND RANGELANDS SOUTH (RIGHT) FOR 2090. ANOMALIES ARE GIVEN IN % WITH RESPECT TO THE 1986–2005 MEAN FOR RCP4.5 (BLUE) AND RCP8.5 (PURPLE) WITH GREY BARS SHOWING THE EXTENT OF NATURAL VARIABILITY. BAR CHARTS ARE EXPLAINED IN BOX 4.2.

For the Rangelands, the runoff estimates following RCP4.5 and RCP8.5 for 2080–2099 relative to 1986–2005 suggest decrease in both North and South (Figure 4.8.2). The confidence in these projections is *low,* however, as the method used is not able to consider changes to rainfall intensity, seasonality and changes in vegetation characteristics, factors that each could impact future runoff, particularly at smaller scales.

Further hydrological and environmental modelling with appropriate climate scenarios (*e.g.* Chiew *et al.*, 2009) could provide further insights into impacts on future runoff and soil moisture characteristics that may be needed for detailed climate change impact assessment studies.

4.9 FIRE WEATHER

Bushfire occurrence at a given place depends on four 'switches': 1) ignition, either human-caused or from natural sources such as lightning; 2) fuel abundance or load (a sufficient amount of fuel must be present); 3) fuel dryness, where lower moisture contents are required for fire, and; 4) suitable weather conditions for fire spread, generally hot, dry and windy (Bradstock, 2010). The settings of the switches depend on meteorological conditions across a variety of time scales, particularly the fuel conditions. Given this strong dependency on the weather, climate change will have a significant impact on future fire weather (*e.g.* Hennessy *et al.*, 2005; Lucas *et al.*, 2007; Williams *et al.*, 2009; Clarke *et al.*, 2011; Grose *et al.*, 2014). The study of Clarke *et al.* (2013) show large increasing trends for the period 1973 to 2010 in observed fire weather across much of the Rangelands, although these are not always statistically significant. The most significant trends are found in southern and eastern parts of the cluster.

Fire weather is estimated here using the McArthur Forest Fire Danger Index (FFDI; McArthur, 1967), which captures two of the four switches (note that it excludes ignition). The fuel dryness is summarised by the drought factor (DF) component of FFDI, which depends on both long-term and short-term rainfall. The FFDI also estimates the ability of a fire to spread, as the temperature, relative humidity and wind speed are direct inputs into the calculation. Fuel abundance is not measured by FFDI, but does depend largely on rainfall. Higher rainfall generally results in a larger fuel load, particularly in regions dominated by grasslands. However, the relationship between fuel abundance and climate change in Australia is complex and only poorly understood. Fire weather is considered 'severe' when FFDI exceeds 50; bushfires have potentially greater human impacts at this level (Blanchi *et al.*, 2010).

Here, estimates of future fire weather using FFDI are derived from three CMIP5 models (GFDL-ESM2M, MIROC5 and CESM-CAM5), chosen to provide a spread of results across all clusters. Using a method similar to that of Hennessy *et al.* (2005), monthly mean changes to maximum temperature, rainfall, relative humidity and wind speed from these models are applied to observation-based high quality historical fire weather records (Lucas, 2010). A period centred on 1995 (*i.e.* 1981–2010) serves as the baseline. These records are modified using the changes from the three models for four 30-year time slices (centred on 2030, 2050, 2070 and 2090) and the RCP4.5 and RCP8.5 emission scenarios. In the Rangelands cluster, the weather conditions are often conducive to fire activity, and the limiting switch in these regions is fuel availability. Following wet periods, fuel is abundant and fires are more frequent. Dry periods see less fuel and fire activity. Nine stations are used in the analysis for this cluster: Cobar, Woomera, Kalgoorlie, Meekatharra, Carnarvon, Port Hedland, Alice Springs, Tennant Creek and Charleville.

Focusing on the 2030 and 2090 time slices, the results indicate a tendency towards increased fire weather risk in the future (Table 4.9.1). Increased temperature combined with lower rainfall results in a higher drought factor (DF). Across the cluster, the sum of all daily FFDI values over a year (July to June), or cumulative FFDI, is broadly indicative of general fire weather risk. This index increases from 8 % under RCP8.5 to 12 % under RCP4.5 by 2030, and from 12 % under RCP4.5 to 25 % under RCP8.5 by 2090. The increase in the number of days with a 'severe' fire danger rating increases from 35 % (RCP8.5) to 50 % (RCP4.5) by 2030, and from 50 % (RCP4.5) to 120 % (RCP 8.5) by 2090.

Bushfire activity is very episodic in most of the Rangelands. During extended dry periods, little bushfire activity is observed regardless of the level of fire weather danger. Extended wet periods allow for greater vegetation growth. Once this fuel dries (cures), and until it is consumed, fire weather (including ignition from lightning) becomes more relevant in determining bushfire occurrence and behaviour. Hence, the generally drier conditions for the models considered here (Table 4.9.1) suggest, on average, less fuel and hence less fire activity, although fire behaviour may be more extreme after episodic wet periods.

Table 2 of the Appendix shows results for individual stations and models. Rainfall varies considerably across both the chosen stations and the different models. In the current climate, 6 of the 9 stations have on average less than 320 mm/year annual rainfall, while the remaining three have in excess of 400 mm/year. This variation in rainfall is a result of the different climatological factors affecting the different stations. Some of these factors include (but are not limited to) frequency of tropical cyclones, the position and strength of the Australian monsoon and the state of the El Niño Southern Oscillation. These factors vary on inter-annual timescales and significantly impact fuel availability and bushfire frequency.

Table 2 (Appendix) also depicts large differences in future rainfall projections between the three models. The GFDL-ESM2M model suggests a sharply drying climate, with rainfall reductions of up to 40 to 50 % in some scenarios. The MIROC5 model shows an increasingly wet future, with changes of up to 10 to 20 % by 2090. The CESM projection lies between these two extremes, with relatively little change in rainfall in the South and a slightly wetter climate in the North.

As noted in the Technical Summary, a limitation of the methodology used to make the projections of fire weather in this evaluation is the inability to incorporate any possible changes in the inter-annual variability of the relevant weather drivers. No consensus exists on how variability may change in the future. Given this limitation and the broad range in rainfall projections, there is only *low confidence* in the projections of future fire weather risk for the Rangelands. If and when bushfire does occur in future climates, it can be expected to exhibit more extreme fire behaviour as a result of the changed climate. Additionally, changes to the vegetation type from the introduction of exotic species and/or the higher carbon dioxide background should also be considered. More detailed modelling efforts encompassing these effects are required to address future fire activity in the Rangelands.

TABLE 4.9.1: CLUSTER-MEAN ANNUAL VALUES OF MAXIMUM TEMPERATURE (T; °C), RAINFALL (R; MM), DROUGHT FACTOR (DF; NO UNITS), THE NUMBER OF SEVERE FIRE DANGER DAYS (SEV; FFDI GREATER THAN 50 DAYS PER YEAR) AND CUMULATIVE FFDI (Σ FFDI; NO UNITS) FOR THE 1995 BASELINE AND PROJECTIONS FOR 2030 AND 2090 UNDER RCP4.5 AND RCP8.5. AVERAGES ARE COMPUTED ACROSS ALL STATIONS AND MODELS IN EACH SCENARIO. NINE STATIONS ARE USED IN THE AVERAGING: COBAR, WOOMERA, KALGOORLIE, MEEKATHARRA, CARNARVON, PORT HEDLAND, ALICE SPRINGS, TENNANT CREEK AND CHARLEVILLE.

VARIABLE	1995 BASELINE	2030 RCP4.5	2030 RCP8.5	2090 RCP4.5	2090 RCP8.5
Temperature	28.4	29.8	29.9	30.8	32.7
Rainfall	318	273	293	293	285
Drought Fac.	8.6	8.8	8.7	8.8	8.9
Severe	12.7	18.6	17.1	18.8	27.6
Σ FFDI	6949	7784	7530	7763	8709

4.10 MARINE PROJECTIONS

Changes in mean sea levels and their extremes, as well as sea surface temperatures (SSTs) and ocean pH (acidity) have the potential to affect both the coastal terrestrial and marine environments. This is discussed at length in Chapter 8 of the Technical Report. Impacts of sea level rise and changes to the frequency of extreme sea levels will be felt through coastal flooding and erosion. For the adjacent marine environment, increases in ocean temperatures and acidity may alter the distribution and composition of marine ecosystems and affect vegetation and coastal fisheries.

4.10.1 SEA LEVEL

Changes in sea level are caused primarily by changes in ocean density ('thermal expansion') and changes in ocean mass due to the exchange of water with the terrestrial environment, including from glaciers and ice sheets (*e.g.* Church *et al.*, 2014; also see Technical Report, Section 8.1 for details). From 1966–2009, the average of the relative tide gauge trends around Australia shows a rise of 1.4 ± 0.2 mm/yr. After the influence of the El Niño Southern Oscillation (ENSO) on sea level is removed, the average trend is 1.6 ± 0.2 mm/yr. After accounting for and removing the effects of vertical land movements due to glacial rebound and the effects of natural climate variability and changes in atmospheric pressure, sea levels have risen around the Australian coastline at an average rate of 2.1 mm/yr over 1966–2009 and 3.1 mm/yr over 1993–2009. These observed rates of rise for Australia are consistent with global average values (White *et al.*, 2014).

Projections of future sea level changes are shown for Port Hedland (Figure 4.10.1). Values for this and other west coast locations are given for 2030 and 2090 periods relative to the 1986–2005 baseline in Table 3 in the Appendix.

Continued increase in sea level for both the west and south coasts of the Rangelands are projected with *very high confidence*. The rate of sea level rise during the 21st century will be larger than the average rate during the 20th century as greenhouse gas emissions grow (Figure 4.10.1). For the first decades of the 21st century the projections are almost independent of the emission scenario, but they begin to separate significantly from about 2050. For higher greenhouse gas emissions, particularly for RCP8.5, the rate of rise continues to increase through the 21st century and results in a sea level rise about 30 % higher than the RCP4.5 level by 2100. Significant inter-annual variability will continue through the 21st century. An indication of its expected magnitude is given by the dashed lines in Figure 4.10.1. In the near future (2030), the projected range of sea level rise at Port Hedland is 0.07 to 0.17 m above 1986–2005, with only minor differences between RCPs. For late in the century (2090) it is in the range 0.28 to 0.64 m for RCP4.5 and 0.40 to 0.84 m for RCP8.5. Rises elsewhere are similar to within 0.03 m. These ranges of sea level rise are considered *likely* (at least 66 % probability), however, if a collapse in the marine based sectors of the Antarctic ice sheet were initiated, these projections could be several tenths of a metre higher by late in the century (Church *et al.*, 2014).

Extreme coastal sea levels are caused by a combination of factors including astronomical tides, storm surges and wind-waves, exacerbated by rising sea levels. Along the north-west coast storm surges can occur in conjunction with tropical cyclones, while along the south coast, the majority occur with the passage of cold fronts during the winter months (*e.g.* McInnes and Hubbert, 2003; Haigh *et al.*, 2014).

Using the method of Hunter (2012), an allowance has been calculated based on the mean sea level rise, the uncertainty around the rise, and taking into account the nature of extreme sea levels along the Rangelands coastline (Haigh *et al.*, 2014). The allowance is the minimum distance required to raise an asset to maintain current frequency of breaches under projected sea level rise. When uncertainty in mean sea level rise is high (*e.g.* in 2090), this allowance approaches the upper end of the range of projected mean sea level rise. For the Rangelands in 2030 the vertical allowances along the cluster coastline are in the range of 0.12 to 0.14 m for all RCPs, and from 0.52 to 0.63 m for RCP4.5 by 2090, and from 0.70 to 0.86 m for RCP8.5 by 2090 (see Table 3 in the Appendix).

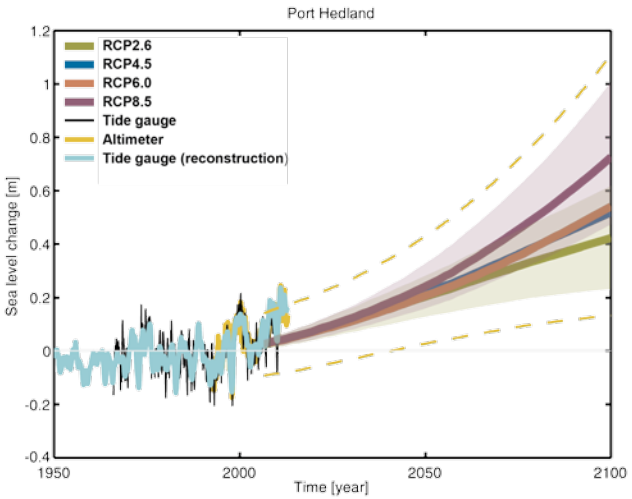

FIGURE 4.10.1: OBSERVED AND PROJECTED RELATIVE SEA LEVEL CHANGE (METRES) AT PORT HEDLAND (WHICH HAS CONTINUOUS RECORDS AVAILABLE FOR THE PERIOD 1966–2010). THE OBSERVED TIDE GAUGE RELATIVE SEA LEVEL RECORDS ARE INDICATED IN BLACK, WITH THE SATELLITE RECORD (SINCE 1993) IN MUSTARD AND TIDE GAUGE RECONSTRUCTION (WHICH HAS LOWER VARIABILITY) IN CYAN. MULTI-MODEL MEAN PROJECTIONS (THICK PURPLE AND OLIVE LINES) FOR THE RCP8.5 AND RCP2.6 SCENARIOS WITH UNCERTAINTY RANGES ARE SHOWN BY THE PURPLE AND OLIVE SHADED REGIONS FROM 2006–2100. THE MUSTARD AND CYAN DASHED LINES ARE AN ESTIMATE OF INTER-ANNUAL VARIABILITY IN SEA LEVEL (UNCERTAINTY RANGE ABOUT THE PROJECTIONS) AND INDICATE THAT INDIVIDUAL MONTHLY AVERAGES OF SEA LEVEL CAN BE ABOVE OR BELOW LONGER TERM AVERAGES. NOTE THAT THE RANGES OF SEA LEVEL RISE SHOULD BE CONSIDERED *LIKELY* (AT LEAST 66 % PROBABILITY) AND THAT IF A COLLAPSE IN THE MARINE BASED SECTORS OF THE ANTARCTIC ICE SHEET WERE INITIATED, THESE PROJECTIONS COULD BE SEVERAL TENTHS OF A METRE HIGHER BY LATE IN THE CENTURY.

4.10.2 SEA SURFACE TEMPERATURE, SALINITY AND ACIDIFICATION

Sea surface temperature (SST) has increased significantly across the globe over recent decades (IPCC, 2013). Along the Western Australian coast temperatures of up to 5 °C above average were recorded during the 2010/2011 summer. These record temperatures are associated with a warming of the Leeuwin Current over recent decades. Increases in SST pose a significant threat to the marine environment through biological changes in marine species, including in local abundance, community structure, and enhanced coral bleaching risk. For 2030, the range of projected SST increase for Port Hedland is 0.6 to 0.8 °C under RCP2.6 and 0.7 to 1.0 °C for RCP8.5 (see Table 3 in the Appendix). For 2090, there is a much larger range of warming between the different emissions scenarios. For Port Hedland the range of increase is projected to be 0.4 to 1.1 °C for RCP2.6 and 2.4 to 3.5 °C for RCP8.5.

Ocean salinity in coastal waters will be affected by changes to rainfall and evaporation and this in turn can affect stratification and mixing, and potentially nutrient supply. Changes to salinity across the coastal waters of the Rangelands cluster span a large range that includes possible increases and decreases, particularly over the longer term and higher emission scenarios as indicated in Table 3 (in the Appendix). Locally, salinity can also be affected by riverine input.

About 30 % of the anthropogenic carbon dioxide emitted into the atmosphere over the past 200 years has been absorbed by the oceans (Ciais *et al.*, 2013) and this has led to a 0.1 unit decrease in the ocean's surface water pH, which represents a 26 % increase in the concentration of hydrogen ions in seawater (Raven *et al.*, 2005). As the carbon dioxide enters the ocean it reacts with the seawater to cause a decrease in pH and carbonate concentration, collectively known as ocean acidification. Carbonate is used in conjunction with calcium as aragonite by many marine organisms such as corals, oysters, clams and some plankton such as foraminifera and pteropods, to form their hard skeletons or shells. A reduction in shell mass has already been detected in foraminifera and pteropods in the Southern Ocean (Moy *et al.*, 2009; Bednaršek *et al.*, 2012). Ocean acidification lowers the temperature at which corals bleach, reducing resilience to natural variability. Ocean acidification can affect fin and shellfish fisheries, aquaculture, tourism and coastal protection. In the cluster by 2030, pH change is projected to be another 0.07 units lower. By 2090 under RCP4.5, it is projected to be up to 0.14 units lower and up to 0.31 units lower for RCP8.5. This represents an additional increase in hydrogen ion concentration of 40 % and 100 % respectively. These changes are also accompanied by reductions in aragonite saturation state (see Table 3 in the Appendix) and together with SST changes will affect all levels of the marine food web, and make it harder for calcifying marine organisms to build their hard shells, potentially affecting resilience and viability of marine ecosystems.

In summary, there is *very high confidence* that sea surface temperatures will continue to rise along the Rangelands coastline, with the magnitude of the warming dependent on emission scenarios. Changes in salinity are related to changes in the hydrological cycle and are of *low confidence*. There is very *high confidence* that the ocean around Australia will become more acidic, showing a net reduction in pH. There is also *high confidence* that the rate of ocean acidification will be proportional to carbon dioxide emissions.

4.11 OTHER PROJECTION MATERIAL FOR THE CLUSTER

For the Rangelands area, previous projection data includes the nationwide Climate Change in Australia projections, produced by the CSIRO and BOM in 2007 (CSIRO and BOM, 2007); and regional projections produced by the state governments. These include projections by SARDI South Australia (2010) and the New South Wales Government's department for Environment and Heritage. Projections were presented in the *Climate Q* document[2], delivered as part of the Queensland state Government's Climate Smart Strategy, and by the Indian Ocean Climate Initiative, of the government of Western Australia. In some cases, these previous projections build on climate change information derived from the previous generation of GCMs included in the CMIP3 archive. Despite the use of previous generation models, these other projections remain relevant, particularly if placed in the context of the latest modelling results. Relative to the 2007 projections (based on the CMIP3 model archive) the new projections appear to give a somewhat less dry projection for Australia as a whole and for Rangelands. Please see Appendix A in the Technical Report for a comparison of CMIP3 and CMIP5 model-based projections.

2 http://www.agdf.org.au/information/sustainable-development/climate-q

5 APPLYING THE REGIONAL PROJECTIONS IN ADAPTATION PLANNING

The fundamental role of adaptation is to reduce the adverse impacts of climate change on vulnerable systems, using a wide range of actions directed by the needs of the vulnerable system. Adaptation also identifies and incorporates new opportunities that become feasible under climate change. For adaptation actions to be effective, all stakeholders need to be engaged, resources must be available and planners must have information on 'what to adapt to' and 'how to adapt' (Füssel and Klein, 2006).

This report presents information about 'what to adapt to' by describing how future climates may respond to increasing greenhouse gas concentrations. This Section gives guidance on how climate projections can be framed in the context of climate scenarios (Section 5.1) using tools such as the Climate Futures web tool, available on the Climate Change in Australia website (Box 5.1). The examples of its use presented here are not exhaustive, but rather an illustration of what can be done.

BOX 5.1: USER RESOURCES ON THE CLIMATE CHANGE IN AUSTRALIA WEBSITE

The Climate Change in Australia website provides information on the science of climate change in a global and Australian context with material supporting regional planning activities. For example, whilst this report focuses on a selected set of emission scenarios, time horizons and variables, the website enables generation of graphs tailored to specific needs, such as a different time period or emission scenario.

The website includes a decision tree yielding application-relevant information, report-ready projected change information and the web tool Climate Futures (Whetton *et al.*, 2012). The web tool facilitates the visualisation and categorisation of model results and selection of data sets that are representative of futures that are of interest to the user. These products are described in detail in Chapter 9 of the Technical Report.

www.climatechangeinaustralia.gov.au

5.1 IDENTIFYING FUTURE CLIMATE SCENARIOS

In Chapter 4 of this report, projected changes are expressed as a range of plausible change for individual variables as simulated by CMIP5 models or derived from their outputs. However, many practitioners are interested in information on how the climate may change, not just changes in one climate variable. To consider how several climate variables may change in the future, data from individual models should be considered because each model simulates changes that are internally consistent across many variables. For example, one should not combine the projected rainfall from one model with projected temperature from another, as these would represent the climate responses of unrelated simulations.

The challenge for practitioners lies in selecting which models to look at, since models can vary in their simulated response to increasing greenhouse gas emissions. Climate models can be organised according to their simulated climate response to assist with this selection. For example, sorting according to rainfall and temperature responses would give an immediate feel for how models fall into a set of discrete climate scenarios framed in terms such as: *much drier and slightly warmer, much wetter and slightly warmer, much drier and much hotter,* and *much wetter and much hotter.*

The Climate Futures web tool described in Box 9.1 of the Technical Report presents a scenario approach to investigating the range of climate model simulations for projected future periods. The following Section describes how this tool can be used to facilitate the use of model output in impact and adaptation assessment.

5.2 DEVELOPING CLIMATE SCENARIOS USING THE CLIMATE FUTURES TOOL

The example presented in Figure 5.1 represents the changes, as simulated by CMIP5 models, in temperature and rainfall in the Rangelands cluster for 2060 (years 2050–2069) under the RCP4.5 scenario. The table organises the models into groupings according to their simulated changes in rainfall (rows) and temperatures (columns). Regarding rainfall, models simulate increases and decreases from *much drier* (less than –15 %) to *much wetter* (greater than 15 %), with 14 of 27 models showing drying conditions (less than –5 %) compared to four models showing rainfall increases (greater than 5 %) and nine models showing little change (–5 to 5 % change). With regard to temperature, models show results ranging from *warmer* (0.5 to 1.5 °C warmer) to *hotter* (1.5 to 3.0 °C warming), with no models falling into the lowest category *slightly warmer* (0 to 0.5 °C warmer) nor the highest category *much hotter* (greater than 3.0 °C warming). Clearly the largest number of models falls in the *hotter* category (22 of 27 models). When considering the two variables together, we see that the most commonly simulated climate for the 2060 under RCP4.5 is a *hotter and drier* climate (8 of 27 models).

In viewing the projection data in this way, the user can gain an overview of what responses are possible when considering the CMIP5 model archive for a given set of constraints. In a risk assessment context, a user may want to consider not only the maximum consensus climate (simulated by most models), but also the best case and worst case scenarios. Their nature will depend on the application. A water-supply manager, for example, is likely to determine from Figure 5.1 that the best case scenario would be a *much wetter and warmer* climate and the worst case the *hotter and much drier* scenario.

Assuming that the user has identified what futures are likely to be of most relevance to the system of interest, Climate Futures allows exploration of the numerical values for each of the models that populate the scenarios. Further, it provides a tool for choosing a single model that most closely represents the particular future climate of interest, but also taking into account models that have been identified as sub-optimal for particular regions based on model evaluation information (described in Chapter 5 of the Technical Report). Through this approach users can select a small set of models to provide scenarios for their application, taking into consideration model spread and the sensitivity of their application to climate change.

CONSENSUS	PROPORTION OF MODELS
Not projected	No models
Very low	< 10 %
Low	10 to 33 %
Moderate	33 to 66 %
High	66 - 90 %
Very high	> 90 %

		Annual surface temperature (°C)			
		Slightly warmer 0 to +0.5	Warmer +0.5 to 1.5	Hotter +1.5 to +3.0	Much hotter > +3.0
Annual rainfall (%)	Much wetter > +15.0		1 of 27 models		
	Wetter +5.0 to +15.0			3 of 27 models	
	Little change -5.0 to +5.0		3 of 27 models	6 of 27 models	
	Drier -15.0 to -5.0		1 of 27 models	8 of 27 models	
	Much drier < -15.0			5 of 27 models	

FIGURE 5.1: AN EXAMPLE TABLE BASED ON OUTPUT FROM THE CLIMATE FUTURES WEB TOOL SHOWING RESULTS FOR RANGELANDS WHEN ASSESSING PLAUSIBLE CLIMATE FUTURES FOR 2060 UNDER RCP4.5, AS DEFINED BY GCM SIMULATED ANNUAL RAINFALL (% CHANGE) AND TEMPERATURE (°C WARMING).

Alternatively, the user may wish to consider a small set of scenarios defined irrespective of emission scenario or date (but with their likelihood of occurrence being time and emission scenario sensitive). This may be in circumstances where the focus is on critical climate change thresholds. An example of using this strategy for the Rangelands cluster is illustrated in Box 5.2 where results are produced in Climate Futures by comparing model simulations from separate time slices and emission scenarios. This box also illustrates each of these scenarios with current climate analogues (comparable climates) for selected sites.

Another user case could be the desire to compare simulations from different climate model ensembles (such as the earlier CMIP3 ensemble, or ensembles of downscaled results). Comparing model spread simulated by different generations of GCMs in Climate Futures allows an assessment of the ongoing relevance of existing impact studies based on selected CMIP3 models, as well as comparison of scenarios developed using downscaled and GCM results.

BOX 5.2: INDICATIVE CLIMATE SCENARIOS FOR THE RANGELANDS AND ANALOGUE FOR FUTURE CLIMATES

Users may wish to consider the future climate of their region in terms of a small set of scenarios defined irrespective of emission scenario or date (but with their likelihood of occurrence being time and emission scenario sensitive). An example of using this strategy for the Rangelands cluster is illustrated here. Combining the results in Climate Futures for 2030, 2050, and 2090, under RCP2.6, RCP4.5, and RCP8.5 gives a set of future climate scenarios (see Figure B5.2). From these, five highlighted scenarios are considered representative of the spread of results (with other potential scenarios excluded as less likely than the selected cases or lying within the range of climates specified by the selected cases). For each case, when available, the current climate analogue for the future climate of Alice Springs is given as an example. These were generated using the method described in Chapter 9.3.5 of the Technical Report and are based on matching annual average rainfall (within +/- 5 %) and maximum temperature (within +/- 1° C). Note that other potentially important aspects of local climate are not matched, such as rainfall seasonality, and thus the analogues should not be used directly in adaptation planning without considering more detailed information.

- *Warmer* (0.5 to 1.5 °C) with *little change in rainfall* (−5 to +5 %). This would occur by 2030 under any emission scenario, but may persist through to late in the 21st century under RCP2.6. In this case, Alice Springs' future climate would be more like the current climate of Windorah (Qld).
- *Hotter* (1.5 to 3.0 °C warmer), and *drier* (5 to 15 % reduction). This is possible by mid-century under all emission scenarios. In this case, Alice Springs' future climate would be more like Boulia (Qld).
- *Much hotter* (greater than 3.0 °C warmer) and *much drier* (greater than 15 % reduction). This may occur by 2090 under RCP4.5 or RCP8.5. In this case, Alice Springs' future climate would be more like the current climate of Karratha (WA).
- *Hotter* (1.5 to 3.0 °C warmer) with *little change in rainfall* (−5 to +5 %). This may occur by 2050 under RCP4.5 or RCP8.5. In this case, Alice Springs' future climate would be more like the current climate of Yuendumu (NT).
- *Warmer* (0.5 to 1.5 °C warmer) and *wetter* (5 to 15 % increase). This is possible early in the century under any emission scenario. In this case, the Alice Springs' future climate would be more like that of Quilpie (Qld).

FIGURE B5.2: A TABLE BASED ON OUTPUT FROM CLIMATE FUTURES SHOWING CATEGORIES OF FUTURE CLIMATE PROJECTIONS FOR THE RANGELANDS CLUSTER, AS DEFINED BY CHANGE IN ANNUAL TEMPERATURE (COLUMN) AND CHANGE IN RAINFALL (ROWS). WITHIN EACH FUTURE CLIMATE CATEGORY, MODEL SIMULATIONS ARE SORTED ACCORDING TO TIME (2030, 2050 AND 2090) AND CONCENTRATION PATHWAY (RCP2.6, RCP4.5, AND RCP8.5); THE NUMBER INDICATING HOW MANY MODEL SIMULATIONS OF THAT PARTICULAR SUB-CATEGORY FALL INTO THE CLIMATE CATEGORY OF THE TABLE (THE NUMBER OF MODELS USED IN THIS EXAMPLE VARIES FOR DIFFERENT CONCENTRATION PATHWAYS). A COLOUR CODE INDICATES HOW OFTEN A PARTICULAR CLIMATE IS SIMULATED AMONGST THE CONSIDERED MODELS (% OCCURRENCE). THE SCENARIOS DESCRIBED ABOVE ARE HIGHLIGHTED IN BOLD.

Future Realisations for the Rangelands cluster

Annual Rainfall (%)	RCP	Annual Surface Temperature (°C): Slightly Warmer 0 to +0.5			Warmer +0.5 to +1.5			Hotter +1.5 to +3.0			Much Hotter > +3.0		
		2030	2050	2090	2030	2050	2090	2030	2050	2090	2030	2050	2090
Much Wetter > +15.0	2.6												
	4.5				1								
	8.5				1					1			2
Wetter +5.0 to +15.0	2.6				2	3	1						
	4.5				3	2			1	4			
	8.5				4	1			4				3
Little Change −5.0 to +5.0	2.6				8	5	3			2			
	4.5				3	3			10	8			
	8.5				14			1	10				7
Drier −15.0 to −5.0	2.6				3	2	4	1	3	3			
	4.5				10	1	1	2	6	10			1
	8.5				4	1		3	7				8
Much Drier < −15.0	2.6				3	1	2	1	4	3			
	4.5				1			1	4				3
	8.5							2	5			1	8

By when and under what greenhouse gas pathway could this occur (colour code=% of models for that period/RCP)?

Not projected | <10% | 10-33% | 33-66%

RCP2.6-18 models
RCP4.5-27 models
RCP8.5-29 models

REFERENCES

ALLEN, R. J., NORRIS, J. R. & WILD, M. 2013. Evaluation of multidecadal variability in CMIP5 surface solar radiation and inferred underestimation of aerosol direct effects over Europe, China, Japan, and India. Journal of Geophysical Research-Atmospheres, 118**,** 6311-6336.

BEDNARŠEK, N., TARLING, G., BAKKER, D., FIELDING, S., JONES, E., VENABLES, H., WARD, P., KUZIRIAN, A., LEZE, B. & FEELY, R. 2012. Extensive dissolution of live pteropods in the Southern Ocean. Nature Geoscience, 5**,** 881-885.

BLANCHI, R., LUCAS, C., LEONARD, J. & FINKELE, K. 2010. Meteorological conditions and wildfire-related house loss in Australia. International Journal of Wildland Fire, 19**,** 914-926.

BRADSTOCK, R. A. 2010. A biogeographic model of fire regimes in Australia: current and future implications. Global Ecology and Biogeography, 19**,** 145-158.

BROHAN, P., KENNEDY, J. J., HARRIS, I., TETT, S. F. & JONES, P. D. 2006. Uncertainty estimates in regional and global observed temperature changes: A new data set from 1850. Journal of Geophysical Research: Atmospheres (1984–2012), 111**,** D12, 1-21.

CHIEW, F., KIRONO, D., KENT, D. & VAZE, J. 2009. Assessment of rainfall simulations from global climate models and implications for climate change impact on runoff studies. *18th World Imacs Congress and Modsim09 International Congress on Modelling and Simulation: Interfacing Modelling and Simulation with Mathematical and Computational Sciences*. 3907-3913

CHURCH, J. A., CLARK, P. U., CAZENAVE, A., GREGORY, J. M., JEVREJEVA, S., LEVERMANN, A., MERRIFIELD, M. A., MILNE, G. A., NEREM, R. S., NUNN, P. D., PAYNE, A. J., PFEFFER, W. T., STAMMER, D. & UNNIKRISHNAN, A. S. 2014. Sea Level Change. *In:* STOCKER, T. F., D. QIN, G.-K. PLATTNER, M. TIGNOR, S. K. ALLEN, J. BOSCHUNG, A. NAUELS, Y. XIA, V. BEX AND P. M. MIDGLEY (ed.) *Climate Change 2013: The Physical Science Basis. Contribution of Working Group I to the Fifth Assessment Report of the Intergovernmental Panel on Climate Change*.

CIAIS, P., SABINE, C., BALA, G., BOPP, L., BROVKIN, V., CANADELL, J., CHHABRA, A., DEFRIES, R., GALLOWAY, J., HEIMANN, M., JONES, C., LE QUÉRÉ, C., MYNENI, R. B., PIAO, S. & THORNTON, P. 2013. Carbon and Other Biogeochemical Cycles. Contribution of Working Group I to the Fifth Assessment Report of the Intergovernmental Panel on Climate Change. *In:* STOCKER, T. F., D. QIN, G.-K. PLATTNER, M. TIGNOR, S.K. ALLEN, J. BOSCHUNG, A. NAUELS, Y. XIA, BEX, V. & MIDGLEY, P. M. (eds.) *Climate Change 2013: The Physical Science Basis*. Cambridge, United Kingdom and New York, NY, USA: Cambridge University Press.

CLARKE, H., LUCAS, C. & SMITH, P. 2013. Changes in Australian fire weather between 1973 and 2010. International Journal of Climatology, 33**,** 931-944.

CLARKE, H. G., SMITH, P. L. & PITMAN, A. J. 2011. Regional signatures of future fire weather over eastern Australia from global climate models. International Journal of Wildland Fire, 20**,** 550-562.

CSIRO AND BOM 2007. Climate change in Australia: Technical Report. Aspendale, Australia: CSIRO Marine and Atmospheric Research. URL http://www.climatechangeinaustralia.gov.au/technical_report.php Accessed 19/8/2014

FAWCETT, R., DAY, K. A., TREWIN, B., BRAGANZA, K., SMALLEY, R., JOVANOVIC, B. & JONES, D. 2012. On the sensitivity of Australian temperature trends and variability to analysis methods and observation networks, Centre for Australian Weather and Climate Research Technical Report No.050.

FOWLER, H. & EKSTRÖM, M. 2009. Multi-model ensemble estimates of climate change impacts on UK seasonal precipitation extremes. International Journal of Climatology, 29**,** 385-416.

FÜSSEL, H.-M. & KLEIN, R. J. 2006. Climate change vulnerability assessments: an evolution of conceptual thinking. Climatic Change, 75**,** 301-329.

GROSE, M. R., FOX-HUGHES, P., HARRIS, R. M. & BINDOFF, N. L. 2014. Changes to the drivers of fire weather with a warming climate–a case study of south-east Tasmania. Climatic Change, 124**,** 255-269.

HAIGH, I. D., WIJERATNE, E., MACPHERSON, L. R., PATTIARATCHI, C. B., MASON, M. S., CROMPTON, R. P. & GEORGE, S. 2014. Estimating present day extreme water level exceedance probabilities around the coastline of Australia: tides, extra-tropical storm surges and mean sea level. Climate Dynamics, 42**,** 121-138.

HENNESSY, K., LUCAS, C., NICHOLLS, N., BATHOLS, J., SUPPIAH, R. & RICKETTS, J. 2005. Climate change impacts on fire-weather in south-east Australia. Melbourne, Australia: Consultancy report for the New South Wales Greenhouse Office, Victorian Department of Sustainability and Environment, Tasmanian Department of Primary Industries, Water and Environment, and the Australian Greenhouse Office. CSIRO Atmospheric Research and Australian Government Bureau of Meteorology 78pp. URL http://laptop.deh.gov.au/soe/2006/publications/drs/pubs/334/lnd/ld_24_climate_change_impacts_on_fire_weather.pdf Accessed 18/8/2014

HOPE, P. K., NICHOLLS, N. & MCGREGOR, J. L. 2004. The rainfall response to permanent inland water in Australia. Australian Meteorological Magazine, 53**,** 251-262.

HUNTER, J. 2012. A simple technique for estimating an allowance for uncertain sea-level rise. Climatic Change, 113**,** 239-252.

HUNTINGTON, T. G. 2006. Evidence for intensification of the global water cycle: Review and synthesis. Journal of Hydrology, 319**,** 83-95.

IPCC 2013. Climate Change 2013: The Physical Science Basis. *In:* STOCKER, T. F., D. QIN, G.-K. PLATTNER, M. TIGNOR, S. K. ALLEN, J. BOSCHUNG, A. NAUELS, Y. XIA, V. BEX & P. M. MIDGLEY (eds.) *Contribution of Working Group I to the Fifth Assessment Report of the Intergovernmental Panel on Climate Change*. Cambridge, UK, and New York, NY, USA: Cambridge University Press.

JAKOB, D. 2010. Challenges in developing a high-quality surface wind-speed data-set for Australia. Australian Meteorological Magazine, 60**,** 227-236.

JONES, D. A., WANG, W. & FAWCETT, R. 2009. High-quality spatial climate data-sets for Australia. Australian Meteorological and Oceanographic Journal, 58**,** 233-248.

KIRONO, D. G. & KENT, D. M. 2011. Assessment of rainfall and potential evaporation from global climate models and its implications for Australian regional drought projection. International Journal of Climatology, 31**,** 1295-1308.

KULESHOV, Y., DE HOEDT, G., WRIGHT, W. & BREWSTER, A. 2002. Thunderstorm distribution and frequency in Australia. Australian Meteorological Magazine, 51**,** 145-154.

LEVITUS, S., ANTONOV, J. I., BOYER, T. P. & STEPHENS, C. 2000. Warming of the world ocean. Science, 287**,** 2225-2229.

LUCAS, C. 2010. On developing a historical fire weather data-set for Australia. Australian Meteorological Magazine, 60**,** 1-13.

LUCAS, C., HENNESSY, K., MILLS, G. & BATHOLS, J. 2007. Bushfire Weather in Southeast Australia: Recent Trends and Projected Climate Change Impacts. Consultancy Report prepared for The Climate Institute of Australia. Bushfire CRC and Australian Bureau of Meteorology CSIRO Marine and Atmospheric Research. URL http://www.royalcommission.vic.gov.au/getdoc/c71b6858-c387-41c0-8a89-b351460eba68/TEN.056.001.0001.pdf Accessed 18/8/2014

MASTRANDREA, M. D., FIELD, C. B., STOCKER, T. F., EDENHOFER, O., EBI, K. L., FRAME, D. J., HELD, H., KRIEGLER, E., MACH, K. J. & MATSCHOSS, P. R. 2010. Guidance note for lead authors of the IPCC fifth assessment report on consistent treatment of uncertainties. *Intergovernmental Panel on Climate Change (IPCC)*. URL http://www.ipcc.ch/pdf/supporting-material/uncertainty-guidance-note.pdf Accessed 18/8/2014

MCARTHUR, A. G. 1967. Fire behaviour in Eucalypt forests. Leaflet. Forestry Timber Bureau Australia**,** 35-35.

MCGREGOR, J. & DIX, M. 2008. An updated description of the conformal-cubic atmospheric model. *In:* HAMILTON, K. & OHFUCHI, W. (eds.) *High Resolution Numerical Modelling of the Atmosphere and Ocean*. Springer New York.

MCINNES, K. L. & HUBBERT, G. D. 2003. A numerical modeling study of storm surges in Bass Strait. Aust. Meterological Magazine, 52**,** 143-156.

MCMAHON, T. A., PEEL, M. C., LOWE, L., SRIKANTHAN, R. & MCVICAR, T. R. 2013. Estimating actual, potential, reference crop and pan evaporation using standard meteorological data: a pragmatic synthesis. Hydrology and Earth System Sciences, 17**,** 1331-1363.

MCVICAR, T. R., RODERICK, M. L., DONOHUE, R. J., LI, L. T., VAN NIEL, T. G., THOMAS, A., GRIESER, J., JHAJHARIA, D., HIMRI, Y. & MAHOWALD, N. M. 2012. Global review and synthesis of trends in observed terrestrial near-surface wind speeds: Implications for evaporation. Journal of Hydrology, 416**,** 182-205.

MOSS, R. H., EDMONDS, J. A., HIBBARD, K. A., MANNING, M. R., ROSE, S. K., VAN VUUREN, D. P., CARTER, T. R., EMORI, S., KAINUMA, M., KRAM, T., MEEHL, G. A., MITCHELL, J. F. B., NAKICENOVIC, N., RIAHI, K., SMITH, S. J., STOUFFER, R. J., THOMSON, A. M., WEYANT, J. P. & WILBANKS, T. J. 2010. The next generation of scenarios for climate change research and assessment. Nature, 463**,** 747-756.

MOY, A. D., HOWARD, W. R., BRAY, S. G. & TRULL, T. W. 2009. Reduced calcification in modern Southern Ocean planktonic foraminifera. Nature Geoscience, 2**,** 276-280.

NAKIĆENOVIĆ, N. & SWART, R. (eds.) 2000. *Special Report on Emissions Scenarios. A Special Report of Working Group III of the Intergovernmental Panel on Climate Change*, Cambridge, United Kingdom and New York, NY, USA: Cambridge University Press.

RAVEN, J., CALDEIRA, K., ELDERFIELD, H., HOEGH-GULDBERG, O., LISS, P., RIEBESELL, U., SHEPHERD, J., TURLEY, C. & WATSON, A. 2005. Ocean acidification due to increasing atmospheric carbon dioxide. The Royal Society 68pp.

RISBEY, J. S., POOK, M. J., MCINTOSH, P. C., WHEELER, M. C. & HENDON, H. H. 2009. On the remote drivers of rainfall variability in Australia. Monthly Weather Review, 137**,** 3233-3253.

SHERWOOD, S. C., ROCA, R., WECKWERTH, T. M. & ANDRONOVA, N. G. 2010. Tropospheric water vapor, convection, and climate. Reviews of Geophysics, 48**,** RG2001.

TAYLOR, K. E., STOUFFER, R. J. & MEEHL, G. A. 2012. An overview of CMIP5 and the experiment design. Bulletin of the American Meteorological Society, 93**,** 485-498.

TENG, J., CHIEW, F., VAZE, J., MARVANEK, S. & KIRONO, D. 2012. Estimation of climate change impact on mean annual runoff across continental Australia using Budyko and Fu equations and hydrological models. Journal of Hydrometeorology, 13**,** 1094-1106.

TIMBAL, B. & MCAVANEY, B. J. 2001. An analogue-based method to downscale surface air temperature: Application for Australia. Climate Dynamics, 17**,** 947-963.

TROCCOLI, A., MULLER, K., COPPIN, P., DAVY, R., RUSSELL, C. & HIRSCH, A. L. 2012. Long-term wind speed trends over Australia. Journal of Climate, 25**,** 170-183.

VAN VUUREN, D. P., EDMONDS, J., KAINUMA, M., RIAHI, K., THOMSON, A., HIBBARD, K., HURTT, G. C., KRAM, T., KREY, V. & LAMARQUE, J.-F. 2011. The representative concentration pathways: an overview. Climatic Change, 109**,** 5-31.

WATTERSON, I. G., HIRST, A. C. & ROTSTAYN, L. D. 2013. A skill score based evaluation of simulated Australian climate. Australian Meteorological and Oceanographic Journal, 63, 181- 190.

WHETTON, P., HENNESSY, K., CLARKE, J., MCINNES, K. & KENT, D. 2012. Use of Representative Climate Futures in impact and adaptation assessment. Climatic Change, 115**,** 433-442.

WHITE, N. J., HAIGH, I. D., CHURCH, J. A., KEON, T., WATSON, C. S., PRITCHARD, T., WATSON, P. J., BURGETTE, R. J., ELIOT, M., MCINNES, K. L., YOU, B., ZHANG, X. & TREGONING, P. 2014. Australian Sea Levels - Trends, regional variability and Influencing factors. Earth-Science Reviews, 136**,** 155-174.

WILLIAMS, R. J., BRADSTOCK, R. A., CARY, G. J., ENRIGHT, N., GILL, A., LIEDLOFF, A., LUCAS, C., WHELAN, R., ANDERSEN, A. & BOWMAN, D. 2009. Interactions between climate change, fire regimes and biodiversity in Australia- A preliminary assessment. Canberra: Department of Climate Change and Department of the Environment, Water, Heritage and the Arts. URL http://climatechange.gov.au/sites/climatechange/files/documents/04_2013/20100630-climate-fire-biodiversity-PDF.pdf Accessed 18/8/2014

ZHANG, L., POTTER, N., HICKEL, K., ZHANG, Y. & SHAO, Q. 2008. Water balance modeling over variable time scales based on the Budyko framework – Model development and testing. Journal of Hydrology 360**,** 117-131.

APPENDIX

TABLE 1: GCM SIMULATED CHANGES IN A RANGE OF CLIMATE VARIABLES FOR THE 2020–2039 (2030) AND 2080–2099 (2090) PERIODS RELATIVE TO THE 1986–2005 PERIOD FOR THE RANGELANDS CLUSTER AND THE NORTH AND SOUTH SUB-CLUSTERS. THE TABLE GIVES THE MEDIAN (50TH PERCENTILE) CHANGE, AS PROJECTED BY THE CMIP5 MODEL ARCHIVE, WITH 10TH TO 90TH PERCENTILE RANGE GIVEN WITHIN BRACKETS. RESULTS ARE GIVEN FOR RCP2.6, RCP4.5, AND RCP8.5 FOR ANNUAL AND SEASONAL AVERAGES. 'DJF' REFERS TO SUMMER (DECEMBER TO FEBRUARY), 'MAM' TO AUTUMN (MARCH TO MAY), 'JJA' TO WINTER (JUNE TO AUGUST) AND 'SON' TO SPRING (SEPTEMBER TO NOVEMBER). THE PROJECTIONS ARE PRESENTED AS EITHER PERCENTAGE OR ABSOLUTE CHANGES. THE COLOURING (SEE LEGEND) INDICATES CMIP5 MODEL AGREEMENT, WITH 'MEDIUM' BEING MORE THAN 60 % OF MODELS, 'HIGH' MORE THAN 75 %, 'VERY HIGH' MORE THAN 90 %, AND 'SUBSTANTIAL' AGREEMENT ON A CHANGE OUTSIDE THE 10TH TO 90TH PERCENTILE RANGE OF MODEL NATURAL VARIABILITY. NOTE THAT 'VERY HIGH AGREEMENT' CATEGORIES ARE RARELY OCCUPIED EXCEPT FOR 'VERY HIGH AGREEMENT ON SUBSTANTIAL INCREASE', AND SO TO REDUCE COMPLEXITY THE OTHER CASES ARE INCLUDED WITHIN THE RELEVANT 'HIGH AGREEMENT' CATEGORY.

RANGELANDS

VARIABLE	SEASON	2030, RCP2.6	2030, RCP4.5	2030, RCP8.5	2090, RCP2.6	2090, RCP4.5	2090, RCP8.5
Temperature mean (°C)	Annual	0.9 (0.6 to 1.3)	1 (0.6 to 1.4)	1 (0.8 to 1.4)	1.1 (0.6 to 1.8)	2.1 (1.5 to 2.9)	4.3 (2.9 to 5.3)
	DJF	1 (0.6 to 1.3)	1 (0.5 to 1.5)	1.1 (0.6 to 1.5)	1.2 (0.6 to 2.1)	2.1 (1.3 to 3.1)	4.1 (2.5 to 5.7)
	MAM	0.9 (0.5 to 1.2)	1 (0.5 to 1.4)	1 (0.6 to 1.5)	1.2 (0.6 to 1.9)	2.1 (1.3 to 2.8)	4.1 (2.6 to 5.4)
	JJA	0.9 (0.5 to 1.3)	0.9 (0.6 to 1.3)	1.1 (0.7 to 1.5)	1 (0.6 to 1.6)	2 (1.4 to 2.6)	4.1 (3.2 to 5.1)
	SON	0.9 (0.5 to 1.5)	1 (0.6 to 1.5)	1.2 (0.7 to 1.6)	1.2 (0.6 to 1.9)	2.2 (1.5 to 3)	4.6 (3.2 to 5.9)
Temperature maximum (°C)	Annual	1 (0.6 to 1.4)	1.1 (0.7 to 1.5)	1.1 (0.8 to 1.6)	1.3 (0.6 to 2.2)	2.2 (1.4 to 3.1)	4.4 (2.9 to 5.6)
	DJF	1.1 (0.6 to 1.5)	1 (0.5 to 1.6)	1.1 (0.7 to 1.6)	1.5 (0.6 to 2.4)	2.3 (1.2 to 3.4)	4.1 (2.5 to 5.9)
	MAM	0.9 (0.5 to 1.4)	1 (0.4 to 1.4)	1.1 (0.5 to 1.6)	1.4 (0.7 to 1.7)	2.2 (1.1 to 3.1)	4 (2.6 to 5.7)
	JJA	0.9 (0.5 to 1.3)	1.1 (0.7 to 1.5)	1.2 (0.8 to 1.7)	1.1 (0.7 to 1.7)	2.1 (1.4 to 2.9)	4.6 (3.2 to 5.4)
	SON	1.1 (0.4 to 1.7)	1.1 (0.7 to 1.6)	1.3 (0.7 to 1.7)	1.4 (0.5 to 2.1)	2.3 (1.5 to 3.3)	4.8 (3.4 to 6.1)
Temperature minimum (°C)	Annual	0.8 (0.6 to 1.2)	0.9 (0.7 to 1.3)	1 (0.8 to 1.4)	1 (0.6 to 1.6)	2 (1.3 to 2.7)	4.1 (3.1 to 5.2)
	DJF	0.9 (0.5 to 1.3)	1 (0.6 to 1.4)	1 (0.7 to 1.5)	1.1 (0.7 to 1.7)	2.1 (1.3 to 2.9)	4.1 (2.8 to 5.1)
	MAM	0.8 (0.5 to 1.1)	0.9 (0.6 to 1.3)	1 (0.7 to 1.5)	1 (0.6 to 1.6)	2 (1.4 to 2.7)	4.2 (2.9 to 5.4)
	JJA	0.7 (0.5 to 1.2)	0.9 (0.5 to 1.3)	1 (0.6 to 1.4)	0.8 (0.5 to 1.6)	1.9 (1.2 to 2.6)	4.1 (3.1 to 5)
	SON	0.8 (0.4 to 1.5)	1 (0.5 to 1.5)	1.1 (0.7 to 1.6)	1.1 (0.3 to 1.8)	2.1 (1.4 to 2.9)	4.3 (3.4 to 5.8)
Rainfall (%)	Annual	-3 (-13 to +8)	-2 (-11 to +6)	-1 (-10 to +6)	-6 (-21 to +3)	-5 (-15 to +7)	-4 (-32 to +18)
	DJF	-5 (-14 to +11)	-1 (-16 to +7)	+1 (-10 to +15)	-6 (-22 to +8)	-2 (-16 to +10)	+3 (-22 to +25)
	MAM	0 (-20 to +18)	+0 (-23 to +20)	+2 (-26 to +19)	-6 (-26 to +18)	0 (-23 to +27)	+9 (-42 to +32)
	JJA	-2 (-19 to +15)	-6 (-20 to +14)	-7 (-24 to +12)	-4 (-31 to +12)	-11 (-34 to +7)	-20 (-50 to +18)
	SON	-3 (-23 to +22)	-3 (-21 to +19)	-3 (-17 to +12)	-5 (-32 to +15)	-10 (-26 to +11)	-11 (-50 to +23)
Solar radiation (%)	Annual	+0.4 (-0.7 to +1.5)	+0.2 (-0.8 to +1.1)	-0.1 (-1.2 to +0.8)	+0.6 (-0.5 to +2.2)	+0.1 (-1.3 to +1.5)	-0.5 (-2.5 to +1.4)
	DJF	+0.4 (-1 to +1.9)	+0 (-1.7 to +1.3)	-0.3 (-2 to +0.9)	+1.2 (-0.8 to +2.7)	-0.3 (-2.2 to +1.9)	-0.9 (-4.2 to +1)
	MAM	-0.1 (-1.4 to +2.3)	-0.3 (-2 to +1.8)	-0.5 (-2.5 to +1.5)	+0.7 (-2.1 to +3.2)	-0.6 (-2.8 to +1.9)	-1.9 (-5.5 to +1.8)
	JJA	+0.7 (-0.5 to +2.1)	+0.7 (-1.2 to +2.6)	+0.7 (-1.1 to +3.1)	+0.9 (-1.3 to +2.8)	+0.9 (-0.7 to +3.9)	+1.2 (-1.3 to +6.4)
	SON	+0.4 (-1.2 to +2)	+0.3 (-1 to +1.5)	-0.2 (-1.6 to +1.3)	+0.5 (-0.9 to +2.2)	+0.1 (-1.5 to +1.6)	-0.4 (-2.3 to +1.5)
Relative humidity (%, absolute)	Annual	-0.6 (-3.1 to +0.6)	-0.5 (-1.8 to +0.5)	-0.6 (-1.9 to +0.9)	-1.4 (-3.4 to +0)	-1.4 (-4.1 to +0.1)	-2.4 (-6.6 to +0.9)
	DJF	-1.1 (-3.5 to +1.1)	-0.4 (-2.7 to +1.4)	-0.5 (-2.4 to +1)	-2.4 (-3.8 to +0.3)	-0.8 (-4.8 to +1.2)	-1.1 (-5.4 to +2.4)
	MAM	-0.7 (-4.8 to +2.2)	-0.2 (-4 to +2.1)	-0.5 (-3 to +2.3)	-1.9 (-4.3 to +1.4)	-1.2 (-6.4 to +2.4)	-1.2 (-9.5 to +4)
	JJA	-0.6 (-3.3 to +0.5)	-0.7 (-3.4 to +1)	-1.1 (-3.1 to +0.4)	-1.3 (-4.1 to +0.6)	-1.9 (-4.7 to -0.4)	-3.7 (-10.3 to -0.2)
	SON	-0.5 (-4.4 to +1.3)	-0.6 (-3.2 to +0.8)	-0.8 (-3.1 to +1.2)	-0.8 (-3.8 to +0.7)	-1.8 (-4 to +0.8)	-2.8 (-6.6 to +0.1)

Potential evapotranspiration (%)	Annual	2.5 (0.8 to 4.4)	2.4 (1 to 3.9)	3 (1.2 to 4.2)	2.8 (0 to 4)	5 (2.8 to 7.8)	11 (6.2 to 16.4)
	DJF	2.3 (1.5 to 4.1)	2.6 (0.8 to 4.1)	2.6 (1.5 to 4.9)	2.2 (0.5 to 5.7)	4.6 (2.8 to 8.9)	11.2 (7.7 to 16.3)
	MAM	3.3 (0.8 to 6.2)	+3 (-0.1 to +5.3)	2.9 (0.8 to 5.8)	+2.2 (-0.5 to +6.3)	5.9 (2.7 to 9.8)	13.1 (7 to 19.1)
	JJA	2.4 (0.5 to 4.2)	+2.6 (-0.3 to +5.6)	+2.8 (-0.1 to +5.1)	+2.9 (-0.6 to +5.4)	5.2 (2.5 to 9.1)	12.3 (4.8 to 16.7)
	SON	+2.5 (-1.1 to +5.6)	2.6 (0 to 4.8)	2.6 (0.3 to 4.8)	+1.9 (-0.5 to +4.1)	4.2 (0.9 to 7.2)	9.8 (4.3 to 14.4)
Soil moisture (Budyko) %	Annual	NA	-0.3 (-1.8 to +0.4)	-0.4 (-1.6 to +0.1)	NA	-0.4 (-3.6 to +0.4)	-1 (-4.8 to +1.8)
	DJF		-0.1 (-1.3 to +0.9)	-0.3 (-1.1 to +0.9)		0 (-2.8 to +1.2)	-0.4 (-4.7 to +3)
	MAM		-0.8 (-2.3 to +1.7)	-0.2 (-1.8 to +1.3)		-0.6 (-2.8 to +0.9)	-1 (-5.7 to +1.3)
	JJA		-0.9 (-3.6 to +0.2)	-1.5 (-3.6 to -0.2)		-1.8 (-5.7 to +1)	-2.6 (-7.8 to +0.3)
	SON		-0.3 (-1.6 to +0.4)	-0.4 (-1.4 to 0)		-0.2 (-2.8 to +0.5)	-0.3 (-5 to +3.8)
Wind speed (%)	Annual	-0.2 (-1.2 to +1)	-0.2 (-1.6 to +0.9)	+0 (-1.4 to +0.9)	-0.3 (-1.8 to +2)	-0.5 (-2.2 to +1)	+0.1 (-3.3 to +2.2)
	DJF	+0.1 (-2.1 to +1.7)	-0.8 (-2.2 to +1.1)	-0.4 (-2.9 to +1.8)	-0.4 (-2.4 to +2.4)	-0.9 (-3 to +0.7)	-0.5 (-4.2 to +2.9)
	MAM	-0.3 (-1.4 to +0.9)	-0.5 (-2.1 to +1.6)	-0.6 (-2 to +0.9)	-0.8 (-3.1 to +1.5)	-1 (-3.4 to +0.6)	-0.8 (-4.6 to +1)
	JJA	+0.1 (-2 to +2.3)	-0.2 (-2 to +1.1)	+0.1 (-1.5 to +1.6)	-0.4 (-1.2 to +2)	+0 (-2.6 to +1.5)	+0.8 (-2.9 to +2.8)
	SON	+0.1 (-1.7 to +2.4)	+0.4 (-1.4 to +1.5)	+0.2 (-1 to +1.6)	+0.2 (-2.1 to +2.5)	+0.3 (-1.6 to +1.9)	+1.5 (-2.8 to +4.9)

RANGELANDS NORTH

VARIABLE	SEASON	2030, RCP2.6	2030, RCP4.5	2030, RCP8.5	2090, RCP2.6	2090, RCP4.5	2090, RCP8.5
Temperature (°C)	Annual	1 (0.6 to 1.4)	1 (0.6 to 1.5)	1.1 (0.8 to 1.5)	1.1 (0.6 to 1.9)	2.1 (1.5 to 3.1)	4.4 (3.1 to 5.6)
	DJF	0.9 (0.6 to 1.4)	1 (0.5 to 1.7)	1 (0.7 to 1.6)	1.1 (0.5 to 2.1)	2.2 (1.2 to 3.3)	4.1 (2.6 to 5.9)
	MAM	1 (0.5 to 1.3)	1.1 (0.5 to 1.5)	1.1 (0.6 to 1.6)	1.2 (0.7 to 2)	2.1 (1.4 to 3)	4.3 (2.5 to 5.8)
	JJA	0.9 (0.5 to 1.4)	1 (0.7 to 1.5)	1.1 (0.8 to 1.6)	1 (0.6 to 1.8)	2.1 (1.5 to 2.9)	4.4 (3.3 to 5.4)
	SON	0.9 (0.5 to 1.5)	1.1 (0.6 to 1.6)	1.2 (0.7 to 1.6)	1.2 (0.5 to 1.9)	2.2 (1.5 to 3.2)	4.7 (3.3 to 6.2)
Daily maximum temperature (°C)	Annual	1 (0.6 to 1.5)	1.1 (0.7 to 1.6)	1.2 (0.8 to 1.6)	1.3 (0.7 to 2.1)	2.3 (1.4 to 3.3)	4.5 (3.1 to 5.8)
	DJF	1 (0.6 to 1.6)	1.1 (0.5 to 1.7)	1.1 (0.7 to 1.7)	1.6 (0.5 to 2.6)	2.3 (1.2 to 3.7)	4.1 (2.6 to 6.1)
	MAM	1 (0.4 to 1.4)	1.1 (0.5 to 1.5)	1.2 (0.5 to 1.7)	1.3 (0.8 to 1.8)	2.2 (1.1 to 3.3)	4.2 (2.8 to 6)
	JJA	1 (0.5 to 1.4)	1.1 (0.7 to 1.5)	1.3 (0.8 to 1.7)	1.2 (0.7 to 1.9)	2.2 (1.3 to 3)	4.8 (3.3 to 5.6)
	SON	1.1 (0.4 to 1.7)	1.1 (0.6 to 1.7)	1.3 (0.7 to 1.8)	1.3 (0.5 to 2.1)	2.4 (1.3 to 3.4)	4.7 (3.3 to 6.2)
Daily minimum temperature (°C)	Annual	0.8 (0.6 to 1.2)	1 (0.6 to 1.4)	1.1 (0.8 to 1.5)	1 (0.4 to 1.7)	2 (1.4 to 2.9)	4.3 (3.3 to 5.6)
	DJF	0.9 (0.6 to 1.2)	1 (0.6 to 1.5)	1.1 (0.8 to 1.7)	1 (0.5 to 1.8)	2 (1.3 to 3.1)	4.1 (2.7 to 5.5)
	MAM	0.9 (0.5 to 1.1)	1 (0.6 to 1.3)	1.1 (0.7 to 1.6)	1.1 (0.4 to 1.7)	2.1 (1.5 to 2.9)	4.5 (3 to 5.8)
	JJA	0.7 (0.4 to 1.3)	1 (0.6 to 1.4)	1.1 (0.7 to 1.5)	0.9 (0.3 to 1.7)	2 (1.3 to 2.9)	4.2 (3.3 to 5.3)
	SON	0.9 (0.3 to 1.5)	1.1 (0.4 to 1.6)	1.2 (0.6 to 1.7)	1.2 (0.3 to 1.9)	2.2 (1.3 to 3.3)	4.5 (3.4 to 6)
Rainfall (%)	Annual	-2 (-12 to +7)	-2 (-11 to +7)	-1 (-11 to +8)	-7 (-19 to +3)	-5 (-16 to +9)	-4 (-31 to +19)
	DJF	-4 (-13 to +8)	0 (-12 to +8)	0 (-11 to +17)	-7 (-22 to +8)	-3 (-17 to +10)	+4 (-21 to +26)
	MAM	-2 (-18 to +25)	-1 (-24 to +22)	+0 (-24 to +20)	-7 (-24 to +20)	-2 (-22 to +33)	+6 (-40 to +39)
	JJA	-3 (-22 to +11)	-7 (-27 to +19)	-10 (-31 to +18)	-6 (-35 to +15)	-11 (-32 to +7)	-22 (-58 to +35)
	SON	-3 (-22 to +21)	-1 (-25 to +22)	-3 (-20 to +13)	-5 (-31 to +17)	-9 (-32 to +12)	-14 (-53 to +26)
Wind speed (%)	Annual	-0.1 (-1.6 to 0.9)	-0.3 (-2.5 to 0.8)	-0.1 (-1.3 to 0.8)	-0.4 (-2.2 to 2.1)	-0.5 (-2.6 to 1.6)	0.2 (-4.8 to 2.4)
	DJF	-0.4 (-2.2 to 2.7)	-1.2 (-2.8 to 1.5)	-0.6 (-2.8 to 1.6)	-0.6 (-2.6 to 2.8)	-1.4 (-3.7 to 1.3)	-1 (-5.5 to 2.1)
	MAM	-0.8 (-2 to 1.1)	-0.8 (-2.2 to 1.9)	-0.6 (-2.7 to 1.1)	-1.3 (-3.5 to 2)	-1.2 (-4.1 to 0.7)	-1.2 (-6.4 to 0.5)
	JJA	0.2 (-1.9 to 2.3)	0.3 (-2.2 to 1.7)	0.7 (-1.5 to 2.3)	0.1 (-2.6 to 3)	0.2 (-2.9 to 3.3)	1.4 (-2.2 to 5.6)
	SON	0.1 (-2 to 2.7)	0.4 (-1.7 to 1.6)	0.3 (-1.8 to 1.6)	-0.1 (-2.4 to 2.4)	-0.2 (-2.5 to 2.7)	0.8 (-3.8 to 4.5)
Solar radiation (%)	Annual	0.3 (-0.8 to 1.6)	0 (-0.9 to 1)	-0.1 (-1.4 to 0.9)	0.5 (-0.5 to 2.3)	0 (-1.4 to 1.5)	-0.8 (-3.3 to 1.2)
	DJF	0.4 (-0.8 to 1.8)	0.1 (-1.7 to 1.5)	-0.3 (-2.1 to 1.1)	1.1 (-1.3 to 3)	-0.2 (-2.2 to 2.2)	-1.1 (-4.6 to 1.5)
	MAM	0 (-1.8 to 2.6)	-0.4 (-2.5 to 2.1)	-0.5 (-2.7 to 1.7)	0.5 (-2.1 to 3.2)	-0.4 (-2.9 to 2.5)	-2.2 (-6.4 to 1.7)
	JJA	0.8 (-0.6 to 1.9)	0.5 (-1.3 to 2.4)	0.4 (-1.2 to 3.1)	0.6 (-1.4 to 2.6)	0.3 (-1.3 to 3.8)	0.4 (-2.7 to 6.3)
	SON	0.5 (-1.3 to 2)	0 (-1.2 to 1.8)	-0.3 (-1.8 to 1.2)	0.4 (-1 to 2.2)	0 (-1.6 to 1.7)	-0.3 (-2.3 to 1.2)
Relative humidity (%, absolute)	Annual	-0.6 (-3.1 to +0.7)	-0.3 (-2.1 to +0.8)	-0.7 (-1.9 to +0.9)	-1.5 (-3.5 to +0.1)	-1.1 (-4.8 to +0.1)	-1.9 (-7.3 to +1.1)
	DJF	-1.2 (-3.6 to +1.3)	-0.4 (-2.7 to +1.6)	-0.3 (-2.4 to +1.4)	-2.8 (-4.6 to +1)	-0.6 (-5.2 to +1.1)	-1.2 (-6.3 to +2.4)
	MAM	-0.7 (-5.6 to +3.2)	-0.3 (-4.2 to +2.4)	-0.5 (-2.9 to +2)	-2 (-4.7 to +1.2)	-0.9 (-7.7 to +3)	-1.4 (-10.6 to +4.3)
	JJA	-0.7 (-3.3 to +1)	-0.7 (-3.1 to +0.9)	-1.1 (-3.3 to +0.5)	-1.1 (-4.3 to +1)	-1.8 (-5.1 to -0.1)	-3.7 (-10.9 to +0.3)
	SON	-0.6 (-4.5 to +1.4)	-0.5 (-3.4 to +1.3)	-0.5 (-3 to +1.1)	-0.8 (-4 to +0.9)	-1.5 (-4.1 to +1.1)	-2.7 (-7.3 to +1.5)
Evapotranspiration (%)	Annual	2.8 (1 to 4.5)	2.4 (1.1 to 4.5)	3 (1.4 to 4.2)	2.5 (-0.4 to 4.5)	5.1 (3.3 to 8.4)	11.7 (6.7 to 17.7)
	DJF	2.6 (1.5 to 4)	2.6 (0.8 to 4.5)	2.8 (1.2 to 5.1)	2.3 (0.1 to 6.4)	5.2 (3 to 9.5)	12.2 (7.8 to 17.3)
	MAM	2.4 (0.3 to 6.1)	3.1 (-0.9 to 4.9)	2.6 (0.1 to 6)	2 (-1.1 to 6.1)	5.7 (2.3 to 10.2)	13.8 (6.1 to 20.4)
	JJA	2.4 (-0.2 to 4.4)	2.4 (-0.2 to 5.5)	2.3 (-0.5 to 5.3)	2.3 (-1.8 to 6.7)	5.1 (1.7 to 8.8)	11.8 (3.8 to 18.2)
	SON	2.6 (-0.7 to 6.6)	2.8 (-0.1 to 5.4)	2.7 (0.7 to 5.7)	1.8 (-0.9 to 4.8)	5 (1.6 to 7.8)	10.7 (4.2 to 16.1)
Soil moisture (Budyko) (%)	Annual	NA	-0.2 (-1.3 to 0.4)	-0.3 (-1.3 to 1.2)	NA	-0.4 (-3.5 to 0.4)	-1 (-5.2 to 2.6)
	DJF		-0.1 (-1.3 to 1.3)	-0.2 (-1.6 to 2.2)		-0.2 (-3.6 to 1.6)	-0.6 (-6.3 to 3.9)
	MAM		-0.2 (-2.7 to 2.2)	-0.1 (-1.7 to 2.4)		-0.4 (-2 to 2)	-0.8 (-6.5 to 3.2)
	JJA		-0.7 (-2.2 to 0.8)	-0.5 (-2.3 to 0.6)		-1.4 (-5 to 0.8)	-2 (-7 to 0.7)
	SON		0 (-1.5 to 0.7)	-0.4 (-1.7 to 0.1)		-0.1 (-3 to 0.9)	-0.3 (-5.1 to 5.4)

RANGELANDS SOUTH

VARIABLE	SEASON	2030, RCP2.6	2030, RCP4.5	2030, RCP8.5	2090, RCP2.6	2090, RCP4.5	2090, RCP8.5
Temperature (°C)	Annual	0.9 (0.6 to 1.2)	0.9 (0.6 to 1.2)	1 (0.7 to 1.3)	1.1 (0.6 to 1.7)	2 (1.3 to 2.6)	4 (2.8 to 5.1)
	DJF	1 (0.6 to 1.3)	1 (0.6 to 1.5)	1 (0.6 to 1.4)	1.2 (0.8 to 1.9)	2.1 (1.4 to 2.9)	4 (2.5 to 5.2)
	MAM	0.8 (0.5 to 1.3)	0.9 (0.5 to 1.3)	0.9 (0.4 to 1.5)	1.1 (0.4 to 1.7)	1.9 (1.1 to 2.5)	4 (2.6 to 5.1)
	JJA	0.8 (0.4 to 1.1)	0.8 (0.5 to 1.2)	0.9 (0.7 to 1.3)	0.9 (0.6 to 1.4)	1.7 (1.2 to 2.3)	3.8 (2.8 to 4.7)
	SON	0.9 (0.5 to 1.3)	1 (0.6 to 1.4)	1.1 (0.6 to 1.5)	1.1 (0.6 to 1.8)	2.1 (1.5 to 2.7)	4.3 (3.2 to 5.4)
Daily maximum temperature (°C)	Annual	1 (0.6 to 1.3)	1 (0.7 to 1.4)	1.1 (0.7 to 1.4)	1.3 (0.7 to 2)	2.2 (1.2 to 2.8)	4.3 (2.8 to 5.2)
	DJF	1.1 (0.8 to 1.5)	1 (0.6 to 1.6)	1.1 (0.6 to 1.5)	1.5 (0.8 to 2.3)	2.2 (1.3 to 3.1)	4.1 (2.5 to 5.5)
	MAM	0.9 (0.6 to 1.3)	0.9 (0.4 to 1.5)	1 (0.4 to 1.5)	1.3 (0.4 to 1.8)	2.1 (1 to 2.8)	4 (2.4 to 5.2)
	JJA	0.9 (0.5 to 1.3)	1 (0.5 to 1.4)	1.1 (0.6 to 1.6)	1.1 (0.7 to 1.7)	2.1 (1.2 to 2.6)	4.3 (3 to 5.1)
	SON	1.1 (0.4 to 1.8)	1.1 (0.7 to 1.5)	1.1 (0.7 to 1.8)	1.4 (0.5 to 2.1)	2.3 (1.5 to 3.1)	4.7 (3.2 to 6)
Daily minimum temperature (°C)	Annual	0.8 (0.5 to 1)	0.8 (0.6 to 1.2)	1 (0.6 to 1.3)	1 (0.6 to 1.6)	1.8 (1.2 to 2.4)	3.8 (3 to 4.6)
	DJF	0.9 (0.4 to 1.3)	0.9 (0.5 to 1.4)	1 (0.7 to 1.4)	1.1 (0.7 to 1.8)	2 (1.3 to 2.7)	4 (2.9 to 4.8)
	MAM	0.8 (0.5 to 1.1)	0.8 (0.5 to 1.2)	0.9 (0.5 to 1.5)	1.1 (0.5 to 1.4)	1.9 (1.2 to 2.4)	4 (2.9 to 5)
	JJA	0.7 (0.3 to 1)	0.7 (0.4 to 1.1)	0.8 (0.5 to 1.3)	0.8 (0.5 to 1.3)	1.5 (1 to 2.2)	3.5 (2.7 to 4.4)
	SON	0.8 (0.4 to 1.3)	0.9 (0.5 to 1.3)	1 (0.6 to 1.4)	1.1 (0.4 to 1.6)	2 (1.2 to 2.6)	4 (3 to 5.2)
Rainfall (%)	Annual	-6 (-17 to +11)	-2 (-14 to +7)	-2 (-10 to +8)	-5 (-25 to +4)	-5 (-19 to +7)	-4 (-29 to +13)
	DJF	-6 (-23 to +18)	-1 (-22 to +10)	0 (-15 to +16)	-6 (-26 to +9)	-1 (-24 to +12)	-2 (-24 to +21)
	MAM	-4 (-24 to +12)	0 (-23 to +18)	+3 (-23 to +26)	-10 (-26 to +19)	0 (-25 to +22)	+5 (-42 to +29)
	JJA	-4 (-22 to +12)	-5 (-25 to +18)	-5 (-21 to +11)	-8 (-28 to +13)	-7 (-36 to +6)	-16 (-46 to +1)
	SON	-3 (-24 to +28)	-4 (-18 to +17)	-3 (-20 to +20)	-5 (-45 to +14)	-11 (-26 to +15)	-8 (-53 to +22)
Wind speed (%)	Annual	0.1 (-1.5 to 1.7)	0 (-1.3 to 0.9)	-0.1 (-1.2 to 1)	0.1 (-1.4 to 1.6)	-0.4 (-2 to 0.8)	0.7 (-2.4 to 2)
	DJF	-0.1 (-1.9 to 2.2)	-0.6 (-2.1 to 1.5)	-0.2 (-2.9 to 1.8)	-0.3 (-2 to 1.8)	-0.7 (-2.7 to 1)	0.7 (-4.2 to 4)
	MAM	0.1 (-2.2 to 1.7)	-0.1 (-1.5 to 2)	0 (-1.8 to 1.9)	-0.6 (-3 to 2.4)	-0.5 (-2.5 to 1.6)	0.6 (-3.7 to 2.4)
	JJA	-0.4 (-2 to 2.5)	-0.1 (-2.6 to 1.9)	-0.3 (-2.3 to 1.7)	0.3 (-2.1 to 2)	-1.1 (-3 to 1.4)	-1.4 (-4.8 to 2)
	SON	0.6 (-1.8 to 2.3)	0.7 (-1.3 to 1.7)	0.2 (-0.6 to 1.9)	0.6 (-1.6 to 2.4)	0.5 (-0.8 to 2.1)	2.3 (-0.5 to 4.2)
Solar radiation (%)	Annual	0.4 (-0.7 to 2)	0.2 (-0.9 to 1.1)	0 (-1.2 to 1.1)	0.6 (-0.3 to 2.1)	0.4 (-0.8 to 1.5)	-0.3 (-1.8 to 1.4)
	DJF	0.8 (-1.1 to 2)	0.1 (-1.4 to 1.7)	-0.1 (-1.8 to 1.2)	1.2 (-0.4 to 2.2)	-0.1 (-1.9 to 1.7)	-0.8 (-3.3 to 1.1)
	MAM	0.1 (-1.7 to 3)	-0.1 (-1.9 to 1.9)	-0.7 (-2.6 to 2)	0.8 (-2.2 to 3.9)	-0.3 (-2.6 to 1.7)	-1.4 (-4.4 to 1.6)
	JJA	1 (-0.5 to 3.1)	0.9 (-0.8 to 3.2)	1 (-0.8 to 3.5)	1.4 (-0.7 to 3.7)	2.4 (0.1 to 4.8)	3.2 (0.4 to 6.5)
	SON	0.2 (-1.3 to 2.1)	0.3 (-0.9 to 1.4)	-0.1 (-1.5 to 1)	0.4 (-0.8 to 2.4)	0.4 (-1.3 to 1.9)	-0.1 (-2.2 to 1.7)
Relative humidity (%, absolute)	Annual	-0.6 (-3.7 to +0.7)	-0.9 (-1.9 to +0.6)	-0.8 (-1.8 to +0.8)	-1.3 (-3.2 to +0)	-1.6 (-3.7 to +0.3)	-2.6 (-5.1 to +0.4)
	DJF	-1.2 (-3 to +1.1)	-0.6 (-2.7 to +1.2)	-0.6 (-3.1 to +0.9)	-1.6 (-2.7 to -0.2)	-0.9 (-3.5 to +1.4)	-1.6 (-4.2 to +2)
	MAM	-0.5 (-4.4 to +1.1)	-0.3 (-3.5 to +2)	+0.1 (-3.7 to +3.1)	-1.8 (-5.3 to +2.2)	-0.8 (-4.3 to +2.1)	-1.1 (-7.5 to +3.3)
	JJA	-0.8 (-4.3 to +1.1)	-1.3 (-4.3 to +1.6)	-1 (-3.8 to +0.8)	-1.7 (-3.9 to +0.7)	-2.1 (-4.3 to -0.6)	-3.7 (-8.9 to -2.3)
	SON	0 (-4.4 to +1.4)	-0.8 (-2.7 to +0.8)	-0.6 (-2.5 to +1)	-0.8 (-3.8 to +0.5)	-1.7 (-4.4 to +0.2)	-3.2 (-5.5 to -1.1)

Evapotrans-piration (%)	**Annual**	**2.2 (0.8 to 4.5)**	**2.5 (0.7 to 3.4)**	**2.7 (1.1 to 4.8)**	**2.8 (0.7 to 4)**	**4.7 (2.6 to 7.1)**	**10.5 (6.4 to 14.5)**
	DJF	2.1 (1 to 4.3)	2.3 (-0.2 to 3.8)	2.9 (-0.1 to 4.7)	2.2 (0.2 to 4.5)	4.4 (2.4 to 7.8)	10.4 (6.2 to 15.7)
	MAM	3.4 (1.5 to 6.6)	2.7 (0.5 to 5.2)	3.3 (0.7 to 7.2)	3.1 (0.5 to 6.7)	5.7 (3.8 to 9.6)	12.9 (9.2 to 19.4)
	JJA	3.1 (0.6 to 6.3)	2.4 (0.7 to 6.1)	3.1 (0.5 to 5.5)	3.6 (1.6 to 6.3)	5.9 (2.6 to 10.1)	11.7 (6.4 to 19.6)
	SON	2.1 (-2.1 to 4.5)	1.9 (-0.2 to 4)	2.4 (0.2 to 3.7)	2 (-0.4 to 3.7)	3.2 (0.2 to 6.2)	7.1 (4.3 to 12)
Soil moisture (Budyko) (%)	**Annual**	**NA**	**-0.8 (-3.5 to 0.2)**	**-0.7 (-3.4 to 0.2)**	**NA**	**-1.5 (-3.5 to 0.5)**	**-1.7 (-5.9 to -0.5)**
	DJF		-0.2 (-1.3 to 0.3)	-0.1 (-1.2 to 0.7)		0 (-1.2 to 0.7)	-0.2 (-1.6 to 0.7)
	MAM		-0.8 (-3.6 to 1.3)	-0.4 (-2.9 to 1.7)		-1 (-4 to 0.9)	-1 (-4.4 to -0.1)
	JJA		-1.5 (-7 to -0.1)	-2.3 (-7.1 to 0.7)		-3.4 (-7 to 0.9)	-6.1 (-11.1 to -0.8)
	SON		-0.3 (-1.9 to 0.1)	-0.4 (-2.3 to 0)		-0.3 (-2.3 to 0.4)	-0.4 (-4.8 to 0.9)

LEGEND TO TABLE 1

	Very high model agreement on substantial increase
	High model agreement on substantial increase
	Medium model agreement on substantial increase
	High model agreement on increase
	Medium model agreement on increase
	High model agreement on little change
	Medium model agreement on little change
	Low model agreement on the direction of change
	High model agreement on substantial decrease
	Medium model agreement on substantial decrease
	High model agreement on decrease
	Medium model agreement on decrease

TABLE 2: ANNUAL VALUES OF MAXIMUM TEMPERATURE (T; °C), RAINFALL (R; MM), DROUGHT FACTOR (DF; NO UNITS), THE NUMBER OF SEVERE FIRE DANGER DAYS (SEV: FFDI GREATER THAN 50 DAYS PER YEAR) AND CUMULATIVE FFDI (ΣFFDI; NO UNITS) FOR THE 1995 BASELINE AND PROJECTIONS FOR 2030 AND 2090 UNDER RCP4.5 AND RCP8.5. VALUES WERE CALCULATED FROM THREE CLIMATE MODELS AND FOR SEVEN STATIONS.

STATION	VARIABLE	1995 BASELINE	2030, RCP4.5			2030, RCP8.5			2090, RCP4.5			2090, RCP8.5		
			CESM	GFDL	MIROC	CESM	GFDL	MIROC	CESM	GFDL	MIROC	CESM	GFDL	MIROC
Cobar (RNS)	T	25.3	26.4	27.1	26.5	26.7	26.9	26.5	28.3	27.5	27.2	30.3	29.9	28.4
	R	407	400	195	408	396	283	411	361	290	416	371	186	482
	DF	8.0	8.0	9.3	8.0	8.1	8.7	8.1	8.4	8.7	8.1	8.5	9.4	7.9
	SEV	4.6	5.4	12.3	5.4	5.8	8.6	5.4	8.5	8.6	6.7	12.1	16.5	7.0
	ΣFFDI	5072	5145	7072	5208	5288	6121	5181	5921	6112	5333	6473	7760	5275
Woomera (RNS)	T	25.9	27.0	27.7	27.1	27.3	27.5	27.1	28.9	28.1	27.8	30.9	30.4	28.9
	R	188	164	81	168	163	116	167	147	118	173	149	73	200
	DF	9.3	9.3	9.8	9.3	9.3	9.5	9.3	9.4	9.5	9.2	9.4	9.8	9.1
	SEV	17.7	18.9	31.3	19.3	19.8	25.2	19.1	25.2	23.6	21.0	29.6	37.9	21.1
	ΣFFDI	7932	8046	10191	8101	8223	9153	8064	8967	9090	8259	9698	11094	8193
Kalgoorlie (RNS)	T	25.2	26.3	27.0	26.4	26.6	26.8	26.4	28.2	27.4	27.1	30.2	29.7	28.2
	R	265	276	135	279	271	191	278	245	198	286	253	125	328
	DF	8.4	8.5	9.5	8.5	8.5	9.0	8.5	8.8	9.0	8.5	8.8	9.6	8.3
	SEV	10.7	11.4	20.9	12.1	12.5	16.9	11.9	15.8	15.5	13.0	20.2	25.9	13.1
	ΣFFDI	6160	6319	8331	6347	6472	7367	6326	7163	7325	6487	7778	9102	6407
Meekatharra (RNS)	T	28.9	30.0	30.7	30.1	30.3	30.5	30.1	31.9	31.1	30.8	33.9	33.4	31.9
	R	236	251	127	252	250	180	253	226	189	258	240	125	293
	DF	8.6	8.7	9.5	8.7	8.7	9.2	8.7	9.0	9.2	8.7	9.0	9.5	8.6
	SEV	23.8	27.3	49.1	28.0	28.8	37.5	28.0	39.1	36.9	31.6	48.1	61.6	32.3
	ΣFFDI	8577	8792	11002	8850	8961	9972	8822	9826	9940	9036	10613	11979	9029
Carnarvon (RNS)	T	27.5	28.5	29.2	28.7	28.8	29.0	28.6	30.4	29.6	29.4	32.4	32.0	30.5
	R	228	194	105	213	198	139	208	185	138	215	181	83	239
	DF	8.8	8.9	9.6	8.8	8.9	9.4	8.9	9.1	9.4	8.8	9.2	9.7	8.8
	SEV	0.6	0.8	2.8	0.8	0.9	1.6	0.8	1.5	1.4	1.0	2.2	3.7	0.9
	ΣFFDI	3583	3731	5843	3716	3839	4760	3700	4380	4671	3774	4846	6420	3623
Port Hedland (RNN)	T	33.4	34.3	35.5	34.5	34.7	35.5	34.5	36.0	36.1	35.5	38.1	38.8	36.5
	R	314	318	198	292	324	222	321	317	262	303	335	192	337
	DF	8.8	8.8	9.3	8.9	8.8	9.2	8.8	8.8	9.1	8.9	8.9	9.4	8.9
	SEV	10.7	10.9	26.8	12.5	12.7	21.2	12.3	15.5	20.2	14.4	22.3	46.1	13.6
	ΣFFDI	6997	6973	9738	7119	7160	8803	7119	7615	8477	7456	8510	11489	7149

Alice Springs (RNN)	T	29.2	30.1	31.4	30.3	30.5	31.3	30.3	31.8	31.9	31.3	33.9	34.6	32.3
	R	281	294	180	300	306	231	300	295	248	295	311	169	341
	DF	8.8	8.8	9.3	8.8	8.7	9.1	8.8	8.8	9.1	8.9	8.9	9.4	8.7
	SEV	22.9	24.3	48.3	24.4	26.4	38.3	27.4	33.7	34.3	29.8	45.1	68.9	28.6
	ΣFFDI	8885	8885	11150	8948	9036	10374	9032	9580	10120	9353	10516	12753	9199
Tennant Creek (RNN)	T	32.1	33.0	34.3	33.2	33.4	34.2	33.2	34.7	34.8	34.2	36.8	37.5	35.2
	R	459	480	321	465	464	375	478	468	437	470	501	319	533
	DF	8.5	8.5	8.9	8.5	8.5	8.7	8.5	8.6	8.6	8.5	8.5	9.0	8.4
	SEV	16.1	16.5	40.6	18.6	19.3	31.8	19.6	24.8	30.9	22.3	38.8	71.8	22.0
	ΣFFDI	8915	8865	11242	8982	9094	10458	9012	9600	10232	9377	10516	12962	9225
Charleville (RNN)	T	28.4	29.4	30.6	29.5	29.7	30.6	29.6	31.0	31.1	30.5	33.2	33.8	31.6
	R	491	498	296	496	519	373	499	500	405	491	511	268	568
	DF	7.9	7.9	8.8	7.9	7.8	8.5	7.9	8.0	8.4	8.0	8.1	9.0	7.9
	SEV	7.1	8.0	18.2	7.7	8.1	13.2	8.6	10.8	12.1	9.5	16.2	30.2	9.1
	ΣFFDI	6416	6404	8661	6499	6544	7894	6532	6993	7682	6822	7788	10112	6626

TABLE 3: PROJECTED ANNUAL CHANGE IN SIMULATED MARINE CLIMATE VARIABLES FOR 2020–2039 (2030) AND 2080–2099 (2090) PERIODS RELATIVE TO 1986–2005 PERIOD FOR RANGELANDS, WHERE SEA ALLOWANCE IS THE MINIMUM DISTANCE REQUIRED TO RAISE AN ASSET TO MAINTAIN CURRENT FREQUENCY OF BREACHES UNDER PROJECTED SEA LEVEL RISE. FOR SEA LEVEL RISE, THE RANGE WITHIN THE BRACKETS REPRESENTS THE 5TH AND 95TH PERCENTILE CHANGE, AS PROJECTED BY THE CMIP5 MODEL ARCHIVE WHEREAS FOR SEA SURFACE TEMPERATURE, SALINITY, OCEAN PH AND ARAGONITE CONCENTRATION THE RANGE REPRESENTS THE 10TH TO 90TH PERCENTILE RANGE. ANNUAL RESULTS ARE GIVEN FOR RCP2.6, RCP4.5, AND RCP8.5. NOTE THAT THE RANGES OF SEA LEVEL RISE SHOULD BE CONSIDERED *LIKELY* (AT LEAST 66 % PROBABILITY), AND THAT IF A COLLAPSE IN THE MARINE BASED SECTORS OF THE ANTARCTIC ICE SHEET WERE INITIATED, THESE PROJECTIONS COULD BE SEVERAL TENTHS OF A METRE HIGHER BY LATE IN THE CENTURY.

VARIABLE	LOCATION (°E, °S)	2030, RCP2.6	2030, RCP4.5	2030, RCP8.5	2090, RCP2.6	2090, RCP4.5	2090, RCP8.5
Sea level rise (m)	Port Hedland (118.57, -20.32)	0.11 (0.07-0.16)	0.12 (0.07-0.16)	0.12 (0.08-0.17)	0.38 (0.22-0.55)	0.46 (0.28-0.64)	0.61 (0.40-0.84)
	Onslow (115.13, -21.65)	0.12 (0.07-0.17)	0.12 (0.07-0.17)	0.13 (0.08-0.17)	0.39 (0.22-0.56)	0.46 (0.28-0.65)	0.62 (0.40-0.85)
	Carnarvon (113.65, -24.90)	0.12 (0.07-0.16)	0.12 (0.07-0.16)	0.13 (0.08-0.18)	0.39 (0.22-0.57)	0.46 (0.28-0.65)	0.62 (0.40-0.85)
Sea allowance (m)	Port Hedland (118.57, -20.32)	0.12	0.12	0.13	0.43	0.52	0.70
	Onslow (115.13, -21.65)	0.12	0.13	0.13	0.49	0.59	0.80
	Carnarvon (113.65, -24.90)	0.13	0.13	0.14	0.53	0.63	0.86
Sea surface temperature (°C)	Port Hedland (118.57, -20.32)	0.7 (0.6 to 0.8)	0.7 (0.6 to 1.0)	0.9 (0.7 to 1.0)	0.7 (0.4 to 1.1)	1.3 (1.1 to 1.7)	2.6 (2.4 to 3.5)
	Onslow (115.13, -21.65)	0.7 (0.6 to 0.9)	0.8 (0.6 to 1.0)	0.8 (0.6 to 1.0)	0.8 (0.6 to 1.2)	1.4 (1.2 to 1.9)	2.9 (2.4 to 3.7)
	Carnarvon (113.65, -24.90)	0.6 (0.4 to 0.8)	0.67 (0.4 to 0.9)	0.8 (0.5 to 0.9)	0.7 (0.4 to 1.1)	1.3 (1.1 to 1.7)	2.6 (2.4 to 3.5)
Sea surface salinity	Port Hedland (118.57, -20.32)	-0.00 (-0.11 to 0.42)	-0.08 (-0.28 to 0.52)	0.01 (-0.18 to 0.24)	0.01 (-0.25 to 0.32)	-0.09 (-0.29 to 0.46)	-0.06 (-0.87 to 0.78)
	Onslow (115.13, -21.65)	-0.04 (-0.15 to 0.21)	-0.08 (-0.26 to 0.15)	-0.08 (-0.14 to 0.22)	-0.05 (-0.28 to 0.21)	-0.15 (-0.47 to -0.01)	-0.11 (-0.85 to 0.29)
	Carnarvon (113.65, -24.90)	-0.01 (-0.14 to 0.22)	-0.08 (-0.23 to 0.18)	-0.06 (-0.14 to 0.17)	-0.05 (-0.29 to 0.15)	-0.15 (-0.43 to -0.04)	-0.14 (-0.63 to 0.30)
Ocean pH	Port Hedland (118.57, -20.32)	-0.07 (-0.07 to -0.06)	-0.07 (-0.08 to -0.07)	-0.08 (-0.09 to -0.08)	-0.06 (-0.07 to -0.06)	-0.14 (-0.15 to -0.14)	-0.30 (-0.31 to -0.28)
	Onslow (115.13, -21.65)	-0.06 (-0.06 to -0.06)	-0.06 (-0.07 to -0.06)	-0.07 (-0.08 to -0.07)	-0.06 (-0.07 to -0.06)	-0.14 (-0.14 to -0.14)	-0.30 (-0.31 to -0.29)
	Carnarvon (113.65, -24.90)	-0.06 (-0.07 to -0.06)	-0.07 (-0.07 to -0.06)	-0.08 (-0.08 to -0.07)	-0.07 (-0.07 to -0.06)	-0.14 (-0.15 to -0.14)	-0.31 (-0.32 to -0.30)
Aragonite saturation	Port Hedland (118.57, -20.32)	-0.31 (-0.34 to -0.21)	-0.31 (-0.35 to -0.20)	-0.36 (-0.45 to -0.28)	-0.29 (-0.32 to -0.26)	-0.70 (-0.74 to -0.64)	-1.36 (-1.49 to -1.26)
	Onslow (115.13, -21.65)	-0.31 (-0.34 to -0.24)	-0.32 (-0.35 to -0.25)	-0.36 (-0.45 to -0.31)	-0.30 (-0.32 to -0.28)	-0.69 (-0.75 to -0.67)	-1.40 (-1.50 to -1.28)
	Carnarvon (113.65, -24.90)	-0.32 (-0.35 to -0.26)	-0.34 (-0.37 to -0.29)	-0.39 (-0.44 to -0.34)	-0.33 (-0.33 to -0.28)	-0.73 (-0.77 to -0.68)	-1.45 (-1.53 to -1.33)

ABBREVIATIONS

ACORN-SAT	Australian Climate Observations Reference Network – Surface Air Temperature
AWAP	Australian Water Availability Project
BOM	Australian Bureau of Meteorology
CCAM	Conformal Cubic Atmospheric Model
CCIA	Climate Change in Australia
CMIP5	Coupled Model Intercomparison Project (Phase 5)
CSIRO	Commonwealth Scientific and Industrial Research Organisation
ENSO	El Niño Southern Oscillation
FFDI	Forest Fire Danger Index
GCMs	General Circulation Models or Global Climate Models
IOD	Indian Ocean Dipole
IPCC	Intergovernmental Panel on Climate Change
NRM	Natural Resource Management
RCP	Representative Concentration Pathway
RN	Rangelands sub-cluster 'North'
RS	Rangelands sub-cluster 'South'
SAM	Southern Annular Mode
SPI	Standardised Precipitation Index
SRES	Special Report on Emissions Scenarios
SST	Sea Surface Temperature
STR	Sub-tropical Ridge

NRM GLOSSARY OF TERMS

Adaptation	The process of adjustment to actual or expected climate and its effects. Adaptation can be autonomous or planned. *Incremental adaptation* Adaptation actions where the central aim is to maintain the essence and integrity of a system or process at a given scale. *Transformational adaptation* Adaptation that changes the fundamental attributes of a system in response to climate and its effects.
Aerosol	A suspension of very small solid or liquid particles in the air, residing in the atmosphere for at least several hours.
Aragonite saturation state	The saturation state of seawater with respect to aragonite (Ω) is the product of the concentrations of dissolved calcium and carbonate ions in seawater divided by their product at equilibrium: ($[Ca^{2+}] \times [CO^{3}_{2-}]$) / $[CaCO^{3}]$ = Ω
Atmosphere	The gaseous envelope surrounding the Earth. The dry atmosphere consists almost entirely of nitrogen and oxygen, together with a number of trace gases (*e.g.* argon, helium) and greenhouse gases (*e.g.* carbon dioxide, methane, nitrous oxide). The atmosphere also contains aerosols and clouds.
Carbon dioxide	A naturally occurring gas, also a by-product of burning fossil fuels from fossil carbon deposits, such as oil, gas and coal, of burning biomass, of land use changes and of industrial processes (*e.g.* cement production). It is the principle anthropogenic greenhouse gas that affects the Earth's radiative balance.
Climate	The average weather experienced at a site or region over a period of many years, ranging from months to many thousands of years. The relevant measured quantities are most often surface variables such as temperature, rainfall and wind.
Climate change	A change in the state of the climate that can be identified (*e.g.* by statistical tests) by changes in the mean and/or variability of its properties, and that persists for an extended period of time, typically decades or longer.
Climate feedback	An interaction in which a perturbation in one climate quantity causes a change in a second, and that change ultimately leads to an additional (positive or negative) change in the first.
Climate projection	A climate projection is the simulated response of the climate system to a scenario of future emission or concentration of greenhouse gases and aerosols, generally derived using climate models. Climate projections are distinguished from climate predictions by their dependence on the emission/concentration/radiative forcing scenario used, which in turn is based on assumptions concerning, for example, future socioeconomic and technological developments that may or may not be realised.
Climate scenario	A plausible and often simplified representation of the future climate, based on an internally consistent set of climatological relationships that has been constructed for explicit use in investigating the potential consequences of anthropogenic climate change, often serving as input to impact models.
Climate sensitivity	The effective climate sensitivity (units; °C) is an estimate of the global mean surface temperature response to doubled carbon dioxide concentration that is evaluated from model output or observations for evolving non-equilibrium conditions.
Climate variability	Climate variability refers to variations in the mean state and other statistics (such as standard deviations, the occurrence of extremes, etc.) of the climate on all spatial and temporal scales beyond that of individual weather events. Variability may be due to natural internal processes within the climate system (internal variability), or to variations in natural or anthropogenic external forcing (external variability).
Cloud condensation nuclei	Airborne particles that serve as an initial site for the condensation of liquid water, which can lead to the formation of cloud droplets. A subset of aerosols that are of a particular size.

CMIP3 and CMIP5	Phases three and five of the Coupled Model Intercomparison Project (CMIP3 and CMIP5), which coordinated and archived climate model simulations based on shared model inputs by modelling groups from around the world. The CMIP3 multi-model dataset includes projections using SRES emission scenarios. The CMIP5 dataset includes projections using the Representative Concentration Pathways (RCPs).
Confidence	The validity of a finding based on the type, amount, quality, and consistency of evidence (*e.g.* mechanistic understanding, theory, data, models, expert judgment) and on the degree of agreement.
Decadal variability	Fluctuations, or ups-and-downs of a climate feature or variable at the scale of approximately a decade (typically taken as longer than a few years such as ENSO, but shorter than the 20–30 years of the IPO).
Detection and attribution	Detection of change is defined as the process of demonstrating that climate or a system affected by climate has changed in some defined statistical sense, without providing a reason for that change. An identified change is detected in observations if its likelihood of occurrence by chance due to internal variability alone is determined to be small, for example, less than 10 per cent. Attribution is defined as the process of evaluating the relative contributions of multiple causal factors to a change or event with an assignment of statistical confidence.
Downscaling	Downscaling is a method that derives local to regional-scale information from larger-scale models or data analyses. Different methods exist *e.g.* dynamical, statistical and empirical downscaling.
El Niño Southern Oscillation (ENSO)	A fluctuation in global scale tropical and subtropical surface pressure, wind, sea surface temperature, and rainfall, and an exchange of air between the south-east Pacific subtropical high and the Indonesian equatorial low. Often measured by the surface pressure anomaly difference between Tahiti and Darwin or the sea surface temperatures in the central and eastern equatorial Pacific. There are three phases: neutral, El Niño and La Niña. During an El Niño event the prevailing trade winds weaken, reducing upwelling and altering ocean currents such that the eastern tropical surface temperatures warm, further weakening the trade winds. The opposite occurs during a La Niña event.
Emissions scenario	A plausible representation of the future development of emissions of substances that are potentially radiatively active (*e.g.* greenhouse gases, aerosols) based on a coherent and internally consistent set of assumptions about driving forces (such as demographic and socioeconomic development, technological change) and their key relationships.
Extreme weather	An extreme weather event is an event that is rare at a particular place and time of year. Definitions of rare vary, but an extreme weather event would normally be as rare as or rarer than the 10th or 90th percentile of a probability density function estimated from observations.
Fire weather	Weather conditions conducive to triggering and sustaining wild fires, usually based on a set of indicators and combinations of indicators including temperature, soil moisture, humidity, and wind. Fire weather does not include the presence or absence of fuel load.
Global Climate Model or General Circulation Model (GCM)	A numerical representation of the climate system that is based on the physical, chemical and biological properties of its components, their interactions and feedback processes. The climate system can be represented by models of varying complexity and differ in such aspects as the spatial resolution (size of grid-cells), the extent to which physical, chemical, or biological processes are explicitly represented, or the level at which empirical parameterisations are involved.
Greenhouse gas	Greenhouse gases are those gaseous constituents of the atmosphere, both natural and anthropogenic, that absorb and emit radiation at specific wavelengths within the spectrum of terrestrial radiation emitted by the Earth's surface, the atmosphere itself, and by clouds. Water vapour (H_2O), carbon dioxide (CO_2), nitrous oxide (N_2O), methane (CH_4) and ozone (O_3) are the primary greenhouse gases in the Earth's atmosphere.

Hadley Cell/Circulation	A direct, thermally driven circulation in the atmosphere consisting of poleward flow in the upper troposphere, descending air into the subtropical high-pressure cells, return flow as part of the trade winds near the surface, and with rising air near the equator in the so-called Inter-Tropical Convergence zone.
Indian Ocean Dipole (IOD)	Large-scale mode of interannual variability of sea surface temperature in the Indian Ocean. This pattern manifests through a zonal gradient of tropical sea surface temperature, which in its positive phase in September to November shows cooling off Sumatra and warming off Somalia in the west, combined with anomalous easterlies along the equator.
Inter-decadal Pacific Oscillation	A fluctuation in the sea surface temperature (SST) and mean sea level pressure (MSLP) of both the north and south Pacific Ocean with a cycle of 15–30 years. Unlike ENSO, the IPO may not be a single physical 'mode' of variability, but be the result of a few processes with different origins. The IPO interacts with the ENSO to affect the climate variability over Australia. A related phenomena, the Pacific Decadal Oscillation (PDO), is also an oscillation of SST that primarily affects the northern Pacific.
Jet stream	A narrow and fast-moving westerly air current that circles the globe near the top of the troposphere. The jet streams are related to the global Hadley circulation. In the southern hemisphere the two main jet streams are the polar jet that circles Antarctica at around 60 °S and 7–12 km above sea level, and the subtropical jet that passes through the mid-latitudes at around 30 °S and 10–16 km above sea level.
Madden Julian Oscillation (MJO)	The largest single component of tropical atmospheric intra-seasonal variability (periods from 30 to 90 days). The MJO propagates eastwards at around 5 m s^{-1} in the form of a large-scale coupling between atmospheric circulation and deep convection. As it progresses, it is associated with large regions of both enhanced and suppressed rainfall, mainly over the Indian and western Pacific Oceans.
Monsoon	A monsoon is a tropical and subtropical seasonal reversal in both the surface winds and associated rainfall, caused by differential heating between a continental-scale land mass and the adjacent ocean. Monsoon rains occur mainly over land in summer.
Percentile	A percentile is a value on a scale of one hundred that indicates the percentage of the data set values that is equal to, or below it. The percentile is often used to estimate the extremes of a distribution. For example, the 90th (or 10th) percentile may be used to refer to the threshold for the upper (or lower) extremes.
Radiative forcing	Radiative forcing is the change in the net, downward minus upward, radiative flux (expressed in W m^{-2}) at the tropopause or top of atmosphere due to a change in an external driver of climate change, such as a change in the concentration of carbon dioxide or the output of the Sun.
Representative Concentration Pathways (RCPs)	Representative Concentration Pathways follow a set of greenhouse gas, air pollution (*e.g.* aerosols) and land-use scenarios that are consistent with certain socio-economic assumptions of how the future may evolve over time. The well mixed concentrations of greenhouse gases and aerosols in the atmosphere are affected by emissions as well as absorption through land and ocean sinks. There are four Representative Concentration Pathways (RCPs) that represent the range of plausible futures from the published literature.
Return period	An estimate of the average time interval between occurrences of an event (*e.g.* flood or extreme rainfall) of a defined size or intensity.
Risk	The potential for consequences where something of value is at stake and where the outcome is uncertain. Risk is often represented as a probability of occurrence of hazardous events or trends multiplied by the consequences if these events occur.
Risk assessment	The qualitative and/or quantitative scientific estimation of risks.
Risk management	The plans, actions, or policies implemented to reduce the likelihood and/or consequences of risks or to respond to consequences.

Sub-tropical ridge (STR)	The sub-tropical ridge runs across a belt of high pressure that encircles the globe in the middle latitudes. It is part of the global circulation of the atmosphere. The position of the sub-tropical ridge plays an important part in the way the weather in Australia varies from season to season.
Southern Annular Mode (SAM)	The leading mode of variability of Southern Hemisphere geopotential height, which is associated with shifts in the latitude of the mid-latitude jet.
SAM index	The SAM Index, otherwise known as the Antarctic Oscillation Index (AOI) is a measure of the strength of SAM. The index is based on mean sea level pressure (MSLP) around the whole hemisphere at 40 °S compared to 65 °S. A positive index means a positive or high phase of the SAM, while a negative index means a negative or low SAM. This index shows a relationship to rainfall variability in some parts of Australia in some seasons.
SRES scenarios	SRES scenarios are emissions scenarios developed by Nakićenović and Swart (2000) and used, among others, as a basis for some of the climate projections shown in Chapters 9 to 11 of IPCC (2001) and Chapters 10 and 11 of IPCC (2007).
Uncertainty	A state of incomplete knowledge that can result from a lack of information or from disagreement about what is known or even knowable. It may have many types of sources, from imprecision in the data to ambiguously defined concepts or terminology, or uncertain projections of human behaviour. Uncertainty can therefore be represented by quantitative measures (*e.g.* a probability density function) or by qualitative statements (*e.g.* reflecting the judgment of a team of experts).
Walker Circulation	An east-west circulation of the atmosphere above the tropical Pacific, with air rising above warmer ocean regions (normally in the west), and descending over the cooler ocean areas (normally in the east). Its strength fluctuates with that of the Southern Oscillation.

GLOSSARY REFERENCES

AUSTRALIAN BUREAU OF METEOROLOGY - http://www.bom.gov.au/watl/about-weather-and-climate/australian-climate-influences.shtml (cited August 2014)

INTERGOVERNMENTAL PANEL ON CLIMATE CHANGE - http://www.ipcc.ch/pdf/glossary/ar4-wg1.pdf (cited August 2014)

INTERGOVERNMENTAL PANEL ON CLIMATE CHANGE - http://ipcc-wg2.gov/AR5/images/uploads/WGIIAR5-Glossary_FGD.pdf (cited August 2014)

MUCCI, A. 1983. The solubility of calcite and aragonite in seawater at various salinities, temperatures, and one atmosphere total pressure *American Journal of Science*, 283 (7), 780-799.

NAKIĆENOVIĆ, N. & SWART, R. (eds.) 2000. *Special Report on Emissions Scenarios. A Special Report of Working Group III of the Intergovernmental Panel on Climate Change*, Cambridge, United Kingdom and New York, NY, USA: Cambridge University Press.

STURMAN, A.P. & TAPPER, N.J. 2006. *The Weather and Climate of Australia and New Zealand*, 2nd ed., Melbourne, Oxford University Press.


PHOTO: DARREN CLEMENTS PHOTOGRAPHY
−20°
−10°
0°
10°
20°
30°
40°
50°

WWW.CLIMATECHANGEINAUSTRALIA.GOV.AU

14-00140